AREA
UT south
Struc

K.L. Cook
Personal copy

Jour. Research U.S. Geol. Survey
Vol. 6, No. 2, Mar.–Apr. 1978, p. 175–192

BLUE RIBBON LINEAMENT, AN EAST-TRENDING STRUCTURAL ZONE WITHIN THE PIOCHE MINERAL BELT OF SOUTHWESTERN UTAH AND EASTERN NEVADA

By PETER D. ROWLEY; PETER W. LIPMAN; HARALD H. MEHNERT, DAVID A. LINDSEY; and JOHN J. ANDERSON,[1] Denver, Colo.; Hawaii Volcano Observatory, Hawaii; Denver, Colo.; Kent, Ohio

Abstract.—The Blue Ribbon lineament is an east-west structural zone that is about 25 kilometers wide and passes through the Pioche mineral belt at about 38°10′ N. It is best known in Utah, where it is at least 190 km long, and extends from the southern Sevier Plateau in the High Plateaus westward and across southern Mountain Home (Needle) Range in the Great Basin. It probably continues westward an additional 170 km into Nevada, where it connects with the eastern end of the 230-km Warm Springs lineament. The Blue Ribbon lineament is defined by range terminations and east-trending valleys, alinement of eruptive centers of middle Miocene (20 million years) to Pliocene(?) (5–1.8 m.y.) alkalic rhyolite, alinement of areas of middle Miocene to Pliocene mineralized rocks (mostly fluorine, uranium, tungsten) and hydrothermally altered rocks, east-trending magnetic highs and interruptions of magnetic anomalies, and east-striking basin-range faults of late Tertiary and Quaternary age. Mountains south of the lineament are topographically and structurally lower than those to the north. North-striking Quaternary basin-range faults, the Thermo hot springs area, several warm springs and former hot springs, and numerous dacitic to andesitic volcanic centers of early to middle Miocene age (26–20 m.y.) occur along the lineament. The Blue Ribbon lineament is believed to be a deep crustal fault zone dating from at least middle Miocene time and possibly much earlier. It thus developed generally coincident with northerly trending classical basin-range faults. Its fracture system was an important, long-lived conduit for mineralizing fluids, and it should be an attractive target for minerals exploration in the future. The lineament could be due to an east-trending warp in the subducting mantle plate, or it could be part of a past or present intracontinental transform fault that locally gets younger eastward and dies out eastward in the western Colorado Plateaus province.

This report is an outgrowth of various studies on the geology of southwestern Utah. One of these studies was a detailed geologic mapping of the southwestern part of the High Plateaus subprovince of the Colorado Plateaus and mapping of the nearby Black Mountains of the eastern Great Basin (Anderson and Rowley, 1975). Other studies were conducted farther west in the Great Basin and consisted of an investigation of the Staats (Monarch) mine–Blawn Mountain area in the southern Wah Wah Mountains by D. A. Lindsey (unpub. data, 1976) and reconnaissance geochemical studies in the southern parts of the Wah Wah Mountains and Mountain Home Range (formerly called Needle Range) by D. R. Shawe and D. A. Lindsey (unpub. data, 1976). During these studies it became apparent that Tertiary volcanic centers, Tertiary mineralized and hydrothermally altered rock, geophysical anomalies, topographic features, and Tertiary and Quaternary basin-range faults defined an east-trending structural belt that passed through all the previously studied areas.

In 1975 an opportunity arose to investigate the hot springs and associated rhyolite centers along this east-trending structural feature, as well as those hot springs and rhyolites north of the feature, as part of a program of reconnaissance and detailed mapping of young rhyolite centers around the rim of the Colorado Plateaus province for their geothermal potential (for example, Lipman and others, 1975; 1978; Rowley and Lipman, 1975). A major phase of this program was the determination of K-Ar ages of alkalic rhyolite (Mehnert and others, 1977). These ages indicated that the rhyolite centers were 20 million years old and younger, generally coincident with the broad episode of basin-range faulting in this part of Utah. The youngest K-Ar age of four rhyolites was from a dome at Blue Ribbon Summit, which gives its name to the structural feature described here.

This report describes the nature of the Blue Ribbon lineament, a through-going structural feature at about 38°10′ N., that crosses the Wasatch Front and the dominant trend of basin-range faults nearly at right angles. The Blue Ribbon lineament is about 25 kilometers wide

[1] Kent State University.

See page 183 for location of Blue Ribbon Summit

and extends about 190 km through the Great Basin and Colorado Pleateaus of southwestern Utah and probably an additional 170 km westward through eastern Nevada. The lineament appears to be collinear at about 116° W., in Nevada, with the 230-km east-trending Warm Springs lineament (Ekren and others, 1976) of similar characteristics, which extends to the western edge of the Great Basin. In Utah, where detailed data are available and where we are most familiar with the geology, the lineament is traced from southwest of Indian Peak in the Mountain Home Range near the Nevada border east to the Antimony mining district, which is east of the southern Sevier Plateau (fig. 14). The southern edge of the lineament is several kilometers south of the latitude of Antimony, and the northern edge is near the latitude of Beaver.

The Blue Ribbon lineament as here defined lies within the southern half of the broad Wah Wah-Tushar mineral belt (fig. 2) of Hilpert and Roberts (1964) and just north of the Pioche mineral belt of Roberts (1964). It crosses the axis of the "Pioche mineral belt" as redefined by Shawe and Stewart (1976) but, because of the overall coincidence with the Pioche mineral belt in Utah, the Blue Ribbon lineament is here considered to be a distinctive zone within the broader feature as defined by Shawe and Stewart (1976).

Acknowledgments.—Recognition and analysis of the Blue Ribbon lineament is due partly to discussions with T. A. Steven, G. P. Eaton, D. R. Shawe, and E. B. Ekren. We are grateful to E. B. Ekren, J. H. Stewart, and D. R. Shawe for making available much unpublished data on east-trending features in the Great Basin. R. K. Glanzman, G. L. Galyardt, and P. L. Williams provided information on some areas in the Great Basin with which they are familiar. J. S. Pallister assisted with collecting specimens for K-Ar study and made most mineral separations.

PREVIOUSLY DESCRIBED EAST-TRENDING BELTS IN GREAT BASIN

East-trending belts of mineral occurrences, geophysical anomalies, structural features, and patterns of Cenozoic igneous rocks in the Great Basin have been observed and described by many geologists, starting with Butler and others (1920). Various geologists and geophysicists have placed belt axes differently, as described in the following paragraphs and shown on figure 2; none of these axes are mutually exclusive because the authors used different scales and different criteria for plotting them. Most of the lineaments probably reflect in one way or another the effects of deep east-trending fault systems in the Great Basin, apparently of an age coincident with classical basin-range structure but perhaps controlled by features that are partly older than basin-range structure.

Hilpert and Roberts (1964) summarized previous work and described three broad belts of intrusive rocks and metal mining districts in western Utah (fig. 2), from north to south the Oquirrh-Uinta, Deep Creek-Tintic, and Wah Wah-Tushar belts. The mining districts on the belts account for 95 percent of Utah's copper, lead, silver, gold, and zinc. Erickson (1974) discussed the northernmost belt, which he renamed the Uinta-Gold Hill trend and which he extended farther eastward. The southern two belts continue into Nevada as the Cherry Creek belt and the Pioche belt (Roberts, 1964); Roberts (1966) later described the broad curving Cortez-Uinta axis, which connects with the Oquirrh-Uinta belt, and the Hamilton-Ely belt at about 39°10′ N. Callaghan (1973) also called attention to east-trending mineral belts. Zietz and others (1969) noted east-trending aeromagnetic patterns in the Oquirrh-Uinta, Deep Creek-Tintic, and Cortez-Uinta belts. Cook and his coworkers (for example, Cook and Montgomery, 1974) postulated three broad east-trending zones in Utah defined by gravity data. The axes of these zones are at 40°40′ N., 40° N., and 38°40′ N. within the mineral belts of Hilpert and Roberts (1964).

Shawe and Stewart (1976) discussed the three major Utah mineral belts as well as Nevada mineral belts. Their Pioche mineral belt, which extends east-northeastward from Nevada into Utah, contains the Wah Wah-Tushar belt of Hilpert and Roberts (1964) and the Pioche belt of Roberts (1964). The axes of the belts generally are defined by alined Cretaceous and Tertiary plutons, zones of faults that are transverse to the northerly basin-range faults, gross aeromagnetic patterns, and major mineral occurrences. To the three major belts they added another, smaller belt south of the Pioche belt, which they called the Delamar-Iron Springs mineral belt (fig. 2). Stewart, Moore, and Zeitz (1977) discussed the belts in terms of distribution of igneous rocks; they observed that broad east-trending zones of volcanic rocks in Nevada and western Utah decrease in age from north to south. The axes of their volcanic belts correspond to the axes of the belts of Shawe and Stewart (1976).

Eaton (1975, 1976; unpub. data, 1976) described a major east-trending crustal boundary that crosses Nevada at about 37° N. (fig. 2), thence gently swings northeasterly into southern Utah, coincident with the Intermountain Seismic Belt. This zone, which is defined largely by gravity and magnetic data, seismicity, and depth to the M-discontinuity, marks the sou

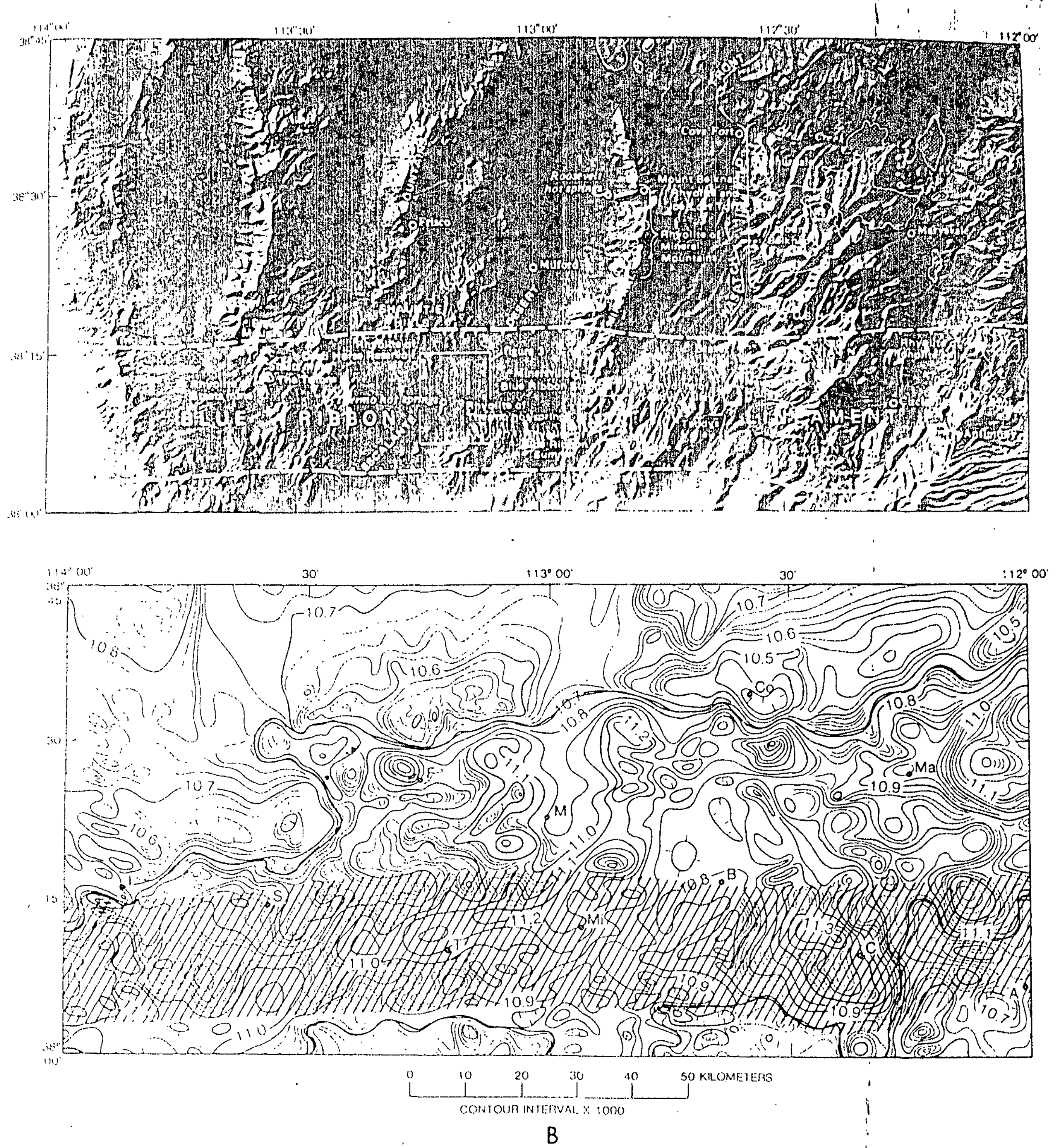

FIGURE 1.—Index maps showing topographic and aeromagnetic expression of most of the Utah part of the Blue Ribbon lineament. *A*, Raised relief map showing location of geographic and geologic features near the Blue Ribbon lineament as well as location of areas of figures 3 and 4. Approximate boundaries of Blue Ribbon lineament shown by dashed hachured lines. Wasatch Front shown by dashed line. Occurrence of alkalic rhyolite, stippled. *B*, Aeromagnetic map, from Zeitz, Shuey, and Kirby (1976). Blue Ribbon lineament shown by lined ruling. Outlines of aeromagnetic ridge of Pioche mineral belt, modified from Stewart, Moore, and Zeitz (1977, fig. 5), is shown by heavy solid line. Contour intervals are 20 and 100 gammas. I, Indian Park; S, Staats (Monarch) mine; F, Frisco; T, Thermo hot springs; M, Milford; Mi, Minersville; B, Beaver; Co, Cove Fort; C, Circleville; Ma, Marysvale; and A, Antimony.

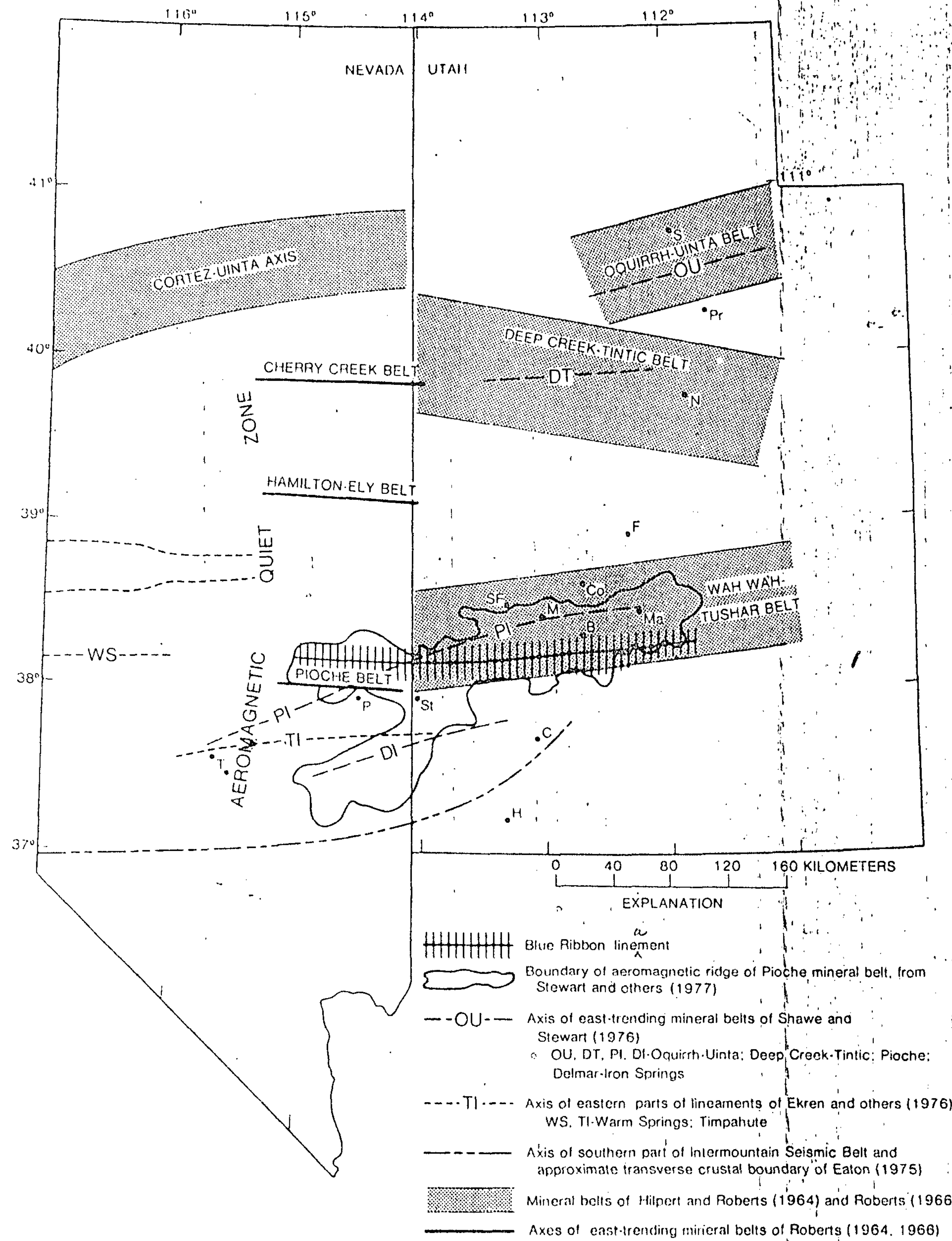

FIGURE 2.—Index map of eastern Nevada and western Utah showing location of the Blue Ribbon lineament and other east-trending structural, mineral, and geophysical belts described in the published literature. S (Salt Lake City), Pr (Provo), N (Nephi), F (Fillmore); Co (Cove Fort); B (Beaver), C (Cedar City), and H (Hurricane) mark the extreme eastern edge (Wasatch Front) of the Great Bas T (Tempiute); P (Pioche); St (Stateline mining distric SF, (San Francisco mining district), M (Milford), and (Marysvale) occur at sites of major mining activity in east-trending Pioche mineral belt of Shawe and Stew (1976).

edge of volcanic rocks and mining districts in the Great Basin. In Utah, this belt coincides with faults of the same strike and with strings of plutons and volcanic centers (Cook, 1960, maps 1–21; Blank and Mackin, 1967, pl. 1).

Ekren and others (1976) documented four lineaments between lat 37°40′ and 39° N. in south-central Nevada, each of which ranges in length from 200 to 300 km (fig. 2). Their evidence consists mostly of topographic discontinuities and disruptions, terminations and alinements of aeromagnetic anomalies, alinements of plutons and volcanic centers, and other structural features. Their northern lineament may connect with a similar lineament in west-central Nevada described by Bingler (1971). The southern two lineaments of Ekren and others (1976) were called the Warm Springs lineament and Timpahute lineament. The Warm Springs lineament probably connects with the Blue Ribbon lineament, and the Timpahute lineament extends into Utah as the northern edge of the Clover Mountains and Bull Valley Mountains and into the Iron Springs mining district, which occurs at the intersection between the Timpahute lineament and Eaton's crustal boundary (1975, 1976; unpub. data, 1976).

PIOCHE MINERAL BELT

The Pioche mineral belt, as defined by Shawe and Stewart (1976), is a broad zone more than 50 km wide that extends more than 300 km from the Tempiute mining district in Nevada east through the Marysvale volcanic pile in Utah (fig. 2). As Shawe and Stewart noted, considerable commodities have been produced along the belt, such as gold, silver, lead, zinc, tungsten, uranium, fluorine, manganese, copper, and alunite. Some mining districts in the belt are shown on figure 2. Those along the Blue Ribbon lineament are described in the following discussion.

In addition to the features enumerated by Shawe and Stewart (1976), other characteristics of the mineral belt are noteworthy. The easterly to east-northeasterly trends of occurrences of fluorine, tungsten, gold, copper, molybdenum, lead-zinc-silver, manganese, uranium, and barium minerals are apparent from published compilations (for example, Walker and Osterwald, 1963; U.S. Geological Survey, Utah Geological and Mineralogical Survey, 1964; U.S. Geological Survey, Nevada Bureau of Mines, 1964); occurrences of iron, beryllium, alunite, sulfur, and other minerals have a less well defined but nontheless general east-trending distribution. Many mineral occurrences, notably those of fluorine, beryllium, uranium, tungsten, and sulfur, are young and commonly occur near centers of alkalic rhyolites that range in age from middle Miocene (20 m.y.) to Pleistocene. At Marysvale, for example, uranium deposits (Kerr and others, 1957; Kerr, 1968) were dated at about 13 m.y. by Bassett and others (1963). Steven and others (1977) concluded that much alunite, uranium, fluorine, and molybdenite at Marysvale are 16–9 m.y. old, but that other deposits of alunite and base and precious metals are early to middle Miocene in age. Most other mineral deposits of the Pioche mineral belt are of middle to late Tertiary age, and some, as at Tempiute and Pioche (Krueger and Schilling, 1971; Johnston, 1972), may be totally Cretaceous in age. In the Pioche mineral belt, many hot spring areas occur, including known geothermal resource areas (KGRA's) that may provide geothermal energy in future years such as the Roosevelt area just west of the Mineral Mountains and the Cove Fort-Sulfurdale area just northeast of the Mineral Mountains. Clearly the overall Pioche mineral belt has been in existence at least from middle Tertiary to Holocene time and perhaps even longer.

The Pioche mineral belt of Shawe and Stewart (1976) includes the topographically highest mountains in southern Utah and is also structurally high. East-striking faults occur in the mineral belt. Callaghan and Parker (1962), Kennedy (1963), and Callaghan (1973) noted that the Tushar Mountains probably occupy part of an east-trending arch that is bounded on its northern side (in the major east-trending valley of Clear Creek near the northern edge of the mineral belt) by a parallel downwarp. The arch occurs in the same area where an east-trending highland of probable Late Cretaceous or early Tertiary age extended both east and west of the Tushar Mountains (Butler and others, 1920; Callaghan, 1973; Anderson and Rowley, 1975). Because of the highland, lacustrine and fluvial rocks of early Tertiary age in the northern High Plateaus are different in lithology from lacustrine and fluvial rocks of the same age in the southern High Plateaus, and sedimentary rocks of early Tertiary age in the Tushar Mountains are absent or are thin and of different character from beds of the same age to the north and south.

As noted by Shawe and Stewart (1976, fig. 2), the Pioche mineral belt is characterized by plutons and volcanic rocks mostly of Cenozoic age. One of these is the granitic batholith of the Mineral Mountains (Liese, 1957; Earll, 1957), which is in the first range west of the Wasatch Front (fig. 1), and is the largest pluton in Utah; published K-Ar ages of 15–9 m.y. (Park, 1968; Armstrong, 1970) have received some confirmation from Rb-Sr dating (C. E. Hedge, unpub. data, 1976). Lava and tuff fields of alkalic rhyolite are abundant in the Pioche mineral belt. The largest such field is the Mount Belknap Rhyolite, about 21–17 m.y. old (Bassett and others, 1963; Cunningham and Steven, 1977; Steven and others, 1977), and the related Joe Lott Tuff (Callaghan, 1939) in the Tushar Mountains. Alkalic rhyolite is exposed at several places south of the San Francisco Mountains (P.L. Williams, oral commun., 1976). Alkalic rhyolite of Pleistocene age overlies the Mineral Mountains batholith (Liese, 1957; Earll, 1957; Lipman and others, 1975, 1978). A large province of Quaternary basalt and minor rhyolite occurs north of the Mineral Mountains on the northern side of the Pioche mineral belt (Mehnert and others, 1977). Upper Cenozoic alkalic rhyolites are extensive in the southern parts of the Mountain Home Range and the Wah Wah Mountains (D. A. Lindsey and D. R. Shawe, oral commun., 1975).

The mineralized and hydrothermally altered rocks in the Pioche mineral belt are closely outlined by a broad aeromagnetic ridge (fig. 2; Stewart and others, 1977, fig. 5). The overall magnetic high (fig. 1B) contains numerous high-amplitude (that is, shallow crustal) hills and depressions (Zietz and others, 1976) that mostly reflect the presence of plutons (Hilpert and Roberts, 1964) and volcanic centers (Stewart and others, 1977). In contrast, the areas north and south of the ridge are magnetically low and contain few superimposed magnetic hills and depressions. The aeromagnetic ridge extends from about 115° W. east to about 111° 45′ W.; the west end is terminated by a broad north-trending "quiet" aeromagnetic belt that bisects the Great Basin (Eaton, 1976; Stewart and others, 1977; G. P. Eaton, unpub. data, 1976). In detail (fig. 1B), the aeromagnetic ridge consists of both east- and east-northeast-trending components. One effect of the two trends within the magnetic ridge is that the western half of the ridge is forked, containing a branch that continues west and a branch extending from about 113°30′ W. south-southwest to the western end of the Delamar-Iron Springs mineral belt.

The Pioche mineral belt has striking similarities to the Deep Creek-Tintic mineral belt. For example, the Deep Creek-Tintic mineral belt contains major occurrences of beryllium, fluorine, lead-zinc-silver, copper, manganese, gold, uranium, tungsten, and other minerals. Most of these mineral occurrences clearly show a general east-trending distribution (U.S. Geological Survey, Utah Geological and Mineral Survey, 1964; U.S. Geological Survey, Nevada Bureau of Mines, 1964; Cohenour, 1963; Park, 1968; Lindsey and others, 1973, 1975; Van Alstine, 1976) or a northeast-trending distribution (Shawe, 1966). The Deep Creek-Tintic belt contains numerous centers of young (10–3 m.y.) alkalic rhyolite (Lindsey and others, 1975; Armstrong, 1970; Mehnert and others, 1977), numerous pluton (Hilpert and Roberts, 1964), and numerous east-striking faults (Stokes, 1963; Loring, 1972). It is axial to a broad zone of Cenozoic volcanic rocks and is the site of a broad east-trending magnetic ridge, with superimposed highs and lows, that extends into Nevada (Zietz and others, 1969; Zietz, Shuey, and Kirby, 1976; Stewart and others, 1977). The Crater Springs hot springs area occurs along its southern edge. Like the Pioche belt, the eastern end of the Deep Creek-Tintic belt contains a base metal and precious metal mining district (Tintic) near the Wasatch Front, while just west of this district the young, 17- to 16-m.y.-old (Armstrong, 1970; Cohenour, 1970; D. A. Lindsey, unpub. data, 1976) granite of Sheeprock Mountains is exposed in a configuration similar to that of the Marysvale mining district and Mineral Mountains batholith of the Pioche belt.

BLUE RIBBON LINEAMENT IN UTAH

The Blue Ribbon lineament in Utah occupies an east-trending zone, about 25 km wide and 190 km long (fig. 1A), that is defined by magnetic highs and interruptions of magnetic anomalies, alinement of Tertiary centers of alkalic rhyolite and dacitic to andesitic rock, range terminations and valleys, Tertiary and Quaternary basin-range faults, and Tertiary mineralized (mostly fluorine, uranium, and tungsten) and hydrothermally altered rock. Several hot springs also occur along the lineament, and their presence suggests that hot water circulation along the lineament, which in Tertiary time produced altered rock and carried minerals, is remarkably long lived.

The lineament concentrates many diverse features but not exclusively so with respect to those in other parts of the Pioche mineral belt; the lineament is only one of several controls of such features within the broad mineral belt. Another such feature is a second less clearly defined east-west lineament that occurs along the northern edge of the Pioche belt, mostly between the latitudes of Cove Fort and Marysvale (centered on 38°30′ N.) and extending from at least 30 km west of Frisco to at least Marysvale. Parts of this feature were recognized by G. L. Galyardt (oral commun., 1976), who observed east-trending geophysical pattern in the Cove Fort-Sulfurdale area, and T. A. Steven (oral commun., 1977) who observed east-trending alinements of published mineral occurrences (U.S. Geological Survey, Utah Geological and Mineralogical Survey, 1964). The lineament also is defined by folds and faults (especially in the Clear Creek area west of Cove Fort topography, aeromagnetic anomalies, coincidence with hot springs, and alinement of plutons and volcanic centers.

Of the types of evidence for the presence of the Blue Ribbon lineament, the magnetic patterns are especially instructive. As the aeromagnetic map (fig. 1B) shows, the Blue Ribbon lineament contains a series of east-alined highs and lows. These are superimposed on the larger Pioche magnetic ridge. Thus the lineament forms one of several east-trending details in the Pioche magnetic high. In Utah the Blue Ribbon lineament occupies the southern edge of the Pioche magnetic ridge, but in Nevada the Blue Ribbon lineament is near the central part of the Pioche aeromagnetic ridge (fig. 2; Zietz, Shuey, and Kirby, 1976). We believe that the magnetic patern shown by the lineament results from a combination of geologic features. These features will be described from west to east.

Volcanic centers and hot springs

Volcanic centers and plutons mark the lineament throughout its length but are rare or nonexistent south of the lineament. Several hot springs occur near the volcanic centers. At the western end of the lineament in Utah, south of Indian Peak in the southern Mountain Home (Needle) Range (fig. 1A), two Tertiary porphyritic plutons, each underlying an area of 1 square kilometer, have been mapped (Hintze, 1963). These are intrusive into lower Tertiary ash-flow tuff of intermediate composition. The southern of these plutons is 1.5 km west of the Cougar Spar mine, the main producer of fluorspar in the Indian Peak mining district. Thurston and others (1954, p. 6, pl. 1) reported that rhyolite lava flows, including perlite and rhyolite dikes, occur in the vicinity of the Cougar Spar and other mines.

Farther east along the Blue Ribbon lineament, in the Staats (Monarch) mine—Blawn Mountain area of the southern Wah Wah Mountains, two alkalic rhyolite plugs or sills occupy an area of more than 1 km² near the Staats (Monarch) mine (Miller, 1966; Whelan, 1965). One of these, called by Whelan the "main intrusion," yielded a new K-Ar age of 20.2 m.y. (table 1); it is here called the rhyolite of Staats mine. Petrography of the rhyolite is summarized in table 2. Mineral separations demonstrate that considerable accessory topaz occurs in the rock, and semiquantitative spectrographic analyses show anomalously high amounts of fluorine, beryllium, niobium, lead, tin, europium, and lithium in fresh rock of the main intrusion (D. A. Lindsey, unpub. data, 1976). New mapping revealed that lava flows of similar composition underlie The Tetons, about 2 km south of the Staats (Monarch) mine. Taylor and Powers (1953) and Whelan (1965) mapped numerous other areas of rhyolite in the Staats (Monarch) mine–Blawn Mountain area, but at least some of these are of Oligocene age (Bushman, 1973).

Erickson and Dasch (1963) mapped two plugs of alkalic rhyolite in the southern Shauntie Hills. These are intrusive into volcanic rocks that they correlated with the Isom Formation, but recent mapping (fig. 3) shows that these rocks belong to a local sequence of Tertiary lava flows and volcanic mudflow breccia of intermediate composition. The southern of the two rhyolite plugs, near Dead Horse Reservoir, yielded a new K-Ar age of 11.6 m.y. (table 1). The plugs are here called the rhyolite of Dead Horse Reservoir.

A deeply eroded dome and possible lava flows of alkalic rhyolite yielded a new K-Ar age of 10.3 m.y. (table 1). It is here called the rhyolite of Thermo hot springs area. It forms two small hills about 3 km east of the hot springs, in the Escalante Desert between the Shauntie Hills and the Black Mountains (fig. 3). Most rhyolite is devitrified, the exception being a vitrophyre zone on the southwestern part of the rhyolite exposures (table 2). The Thermo hot springs area is the site of a KGRA. The hot springs occur in two en echelon north-trending silica mounds controlled by Quaternary north-striking fractures, probably faults (Petersen, 1973). East-striking faults east of the hot springs cut Quaternary surficial deposits, including Pleistocene shorelines of the Escalante arm of Lake Bonneville. Thus an

TABLE 1.—*Analytical data for K-Ar ages for alkalic rhyolites along the Blue Ribbon lineament*

[Decay constants for K^{40}: $\lambda_\epsilon = 0.581 \times 10^{-10} yr^{-1}$, $\lambda_\beta = 4.963 \times 10^{-10} yr^{-1}$; atomic abundance: $K^{40}/K = 1.167 \times 10^{-4}$; $*Ar^{40}$=radiogenic argon; mineral analyzed for all samples: sanidine; potassium determinations made with Instrumentation Laboratories flame photometer with a Li internal standard]

Location of rhyolite	Sample No.	Locality		K_2O (percent)	$*Ar^{40}$ $\times 10^{-10}$	$*Ar^{40}$ (percent)	Age (m.y. $\pm 2\sigma$)
		Lat N.	Long W.				
Staats mine----------	ST-R	38°14′45″	113°34′45″	8.86, 8.84	2.582	74.0	20.2±0.86
Dead Horse Reservoir--	75L-14A	38°14′25″	113°14′25″	10.44, 10.37	1.755	87.2	11.6±0.46
Thermo hot springs----	75L-13A	38°10′30″	113°9′50″	9.11, 9.04	1.347	82.0	10.3±0.40
Blue Ribbon Summit----	75L-12	38°10′10″	112°50′25″	8.96, 8.94	.950	50.2	7.4±0.40

TABLE 2.—*Modal data and petrographic descriptions of rhyolites along the Blue Ribbon lineament*

[1,000 points or more counted on thin sections; --- = not present]

Mineral	Modes (volume percent)						
	Staats mine[1]	Dead Horse Reservoir[2]	Thermo hot springs[3]	Muddy Hill[4]	Blue Ribbon Summit[5]	Teddys Valley[6]	Phonolite Hill[7]
Plagioclase------	2.9	5.9	0.3	---	1.1	0.1	2.9
Quartz-----------	1.3	7.6	.9	Trace	1.7	---	Trace
K-feldspar-------	7.8	5.7	.5	6.7	1.9	---	.4
Biotite----------	.1	1.0	Trace	.4	.1	---	---
Hornblende-------	---	---	.3	Trace	Trace	---	---
Pyroxene---------	---	---	---	---	---	.3	---
Sphene-----------	---	.1	---	---	---	---	---
Opaque minerals--	.1	.5	Trace	.4	.1	---	Trace
Groundmass-------	87.8	79.2	97.9	89.5	95.1	99.6	96.5
Xenoliths--------	---	---	---	2.9	---	---	.1

[1]Devitrified flow-foliated rhyolite containing vapor-phase minerals and some feldspar microlites.

[2]Devitrified resistant, locally vesicular pink rhyolite from a plug with a diameter of about 1/2 km.

[3]Average of 2 thin sections. Obsidian and mostly devitrified flow-foliated rhyolite containing feldspar microlites and vapor-phase minerals.

[4]Average of 5 thin sections. Devitrified poorly welded tuff structure. Some specimens contain vapor-phase minerals. Scattered ash-flow tuff, dikes, plugs, and volcanic mudflow breccia at and near Muddy Hill (2 km southeast of Minersville).

[5]Average of 5 thin sections. Mostly devitrified flow-foliated rhyolite. Some specimens contain bands of slightly devitrified rhyolite alternating with bands of lighter colored devitrified rhyolite. Some specimens contain feldspar microlites, and some contain vesicles and spherulites. One specimen is of slightly devitrified perlitic glass. Two specimens from dikes 3 km south of Blue Ribbon Summit, other two from dome at Blue Ribbon Summit.

[6]Mostly devitrified flow-foliated rhyolite that is somewhat vesicular and contains feldspar microlites.

[7]Average of 5 thin sections, given in Rowley (1968, p. 319-321); chemical analyses of two specimens also in Rowley (1968, p. 44-49). Mostly flow-foliated rhyolite containing bands of slightly devitrified rhyolite alternating with bands of lighter colored devitrified vesicular and amygdular spherulitic rhyolite. One sample essentially nondevitrified perlitic glass; another an intrusive breccia. Four specimens from Phonolite Hill, and one from basal glass of a lava flow on the eastern flank of the southern Sevier Plateau north of Kingston Canyon.

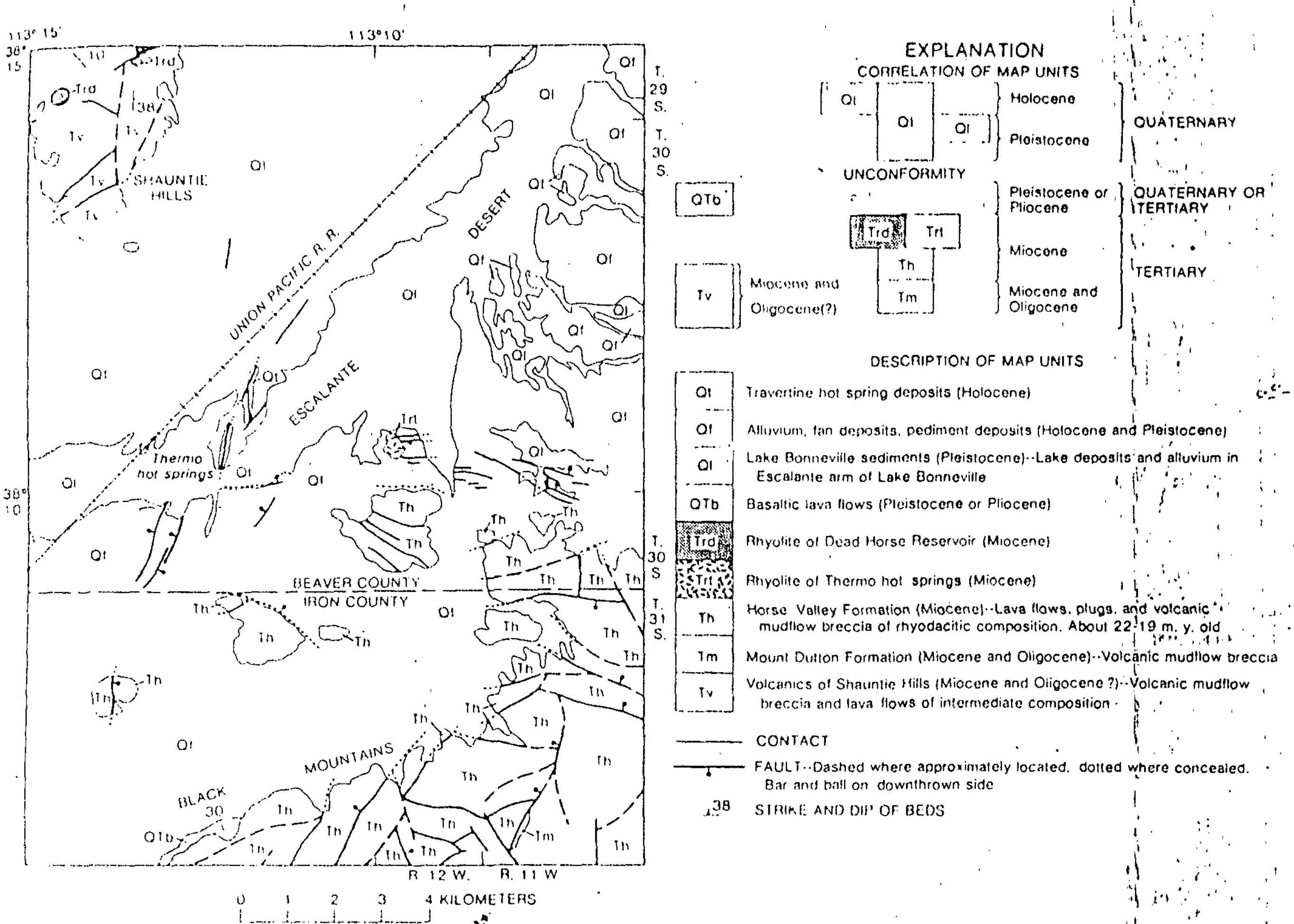

FIGURE 3.—Preliminary geologic map of Thermo hot springs area and southern Shauntie Hills (P. D. Rowley, unpub. data, 1975) showing distribution of alkalic rhyolite (Trd, Trt). Note east-trending faults at the latitude of the hot springs and of the rhyolite of Thermo hot springs. See Anderson and Rowley (1975) and Fleck, Anderson, and Rowley (1975) for additional details.

orthogonal system of faults appears to control the hot springs (Rowley and Lipman, 1975); this interpretation is supported by geophysical studies by the University of Utah (Robert Sawyer, oral commun., 1977).

About 10–15 km south and southeast of the Thermo hot springs area, in the northwestern Black Mountains (Anderson and Rowley, 1975), stratovolcano sources for rhyodacitic volcanic mudflow breccia, plugs, and lava flows of the Horse Valley Formation (22–19 m.y. old) are exposed.

Most volcanic rocks (volcanic mudflow breccia and lava flows) lying north of the canyon east of Minersville and extending south through the Black Mountains belong to the Mount Dutton Formation (26–20 m.y. old). One source for these volcanic rocks of intermediate composition is a dacitic(?) plug, the apparent core of a stratovolcano, at Black Mountain, about 4 km southeast of Minersville. A major N. 10° W.-striking fault that passes through Minersville and partly coincides with several centers of silicic tuff south and southeast of Minersville postdates the Miocene dacitic to andesitic rocks; this silicic tuff here is called the rhyolite(?) of Muddy Hill (table 2). Dotsons warm spring (Mundorff, 1970, p. 43) on the eastern outskirts of Minersville lies along a major north-trending fault zone. Lee (1908) noted silica mounds, indicative of former hot springs, near North Spring about 5.5 km north of Minersville, and Earll (1957) recorded sulfurous fumes and warm water at Oak Spring nearly 1 km northeast of North Spring.

Blue Ribbon Summit, in the northern Black Mountains about 9 km southeast of Minersville, is underlain by a dome and lava flows of alkalic rhyolite (fig. 4) that are partly covered by basalt lava flows (Anderson and Rowley, 1975, p. 37). The rhyolite yielded a new K-Ar age of 7.4 m.y. (table 1). Alkalic rhyolite also is exposed less than 3 km south-southeast of Blue Ribbon Summit. These rocks, here called the rhyolite of Blue

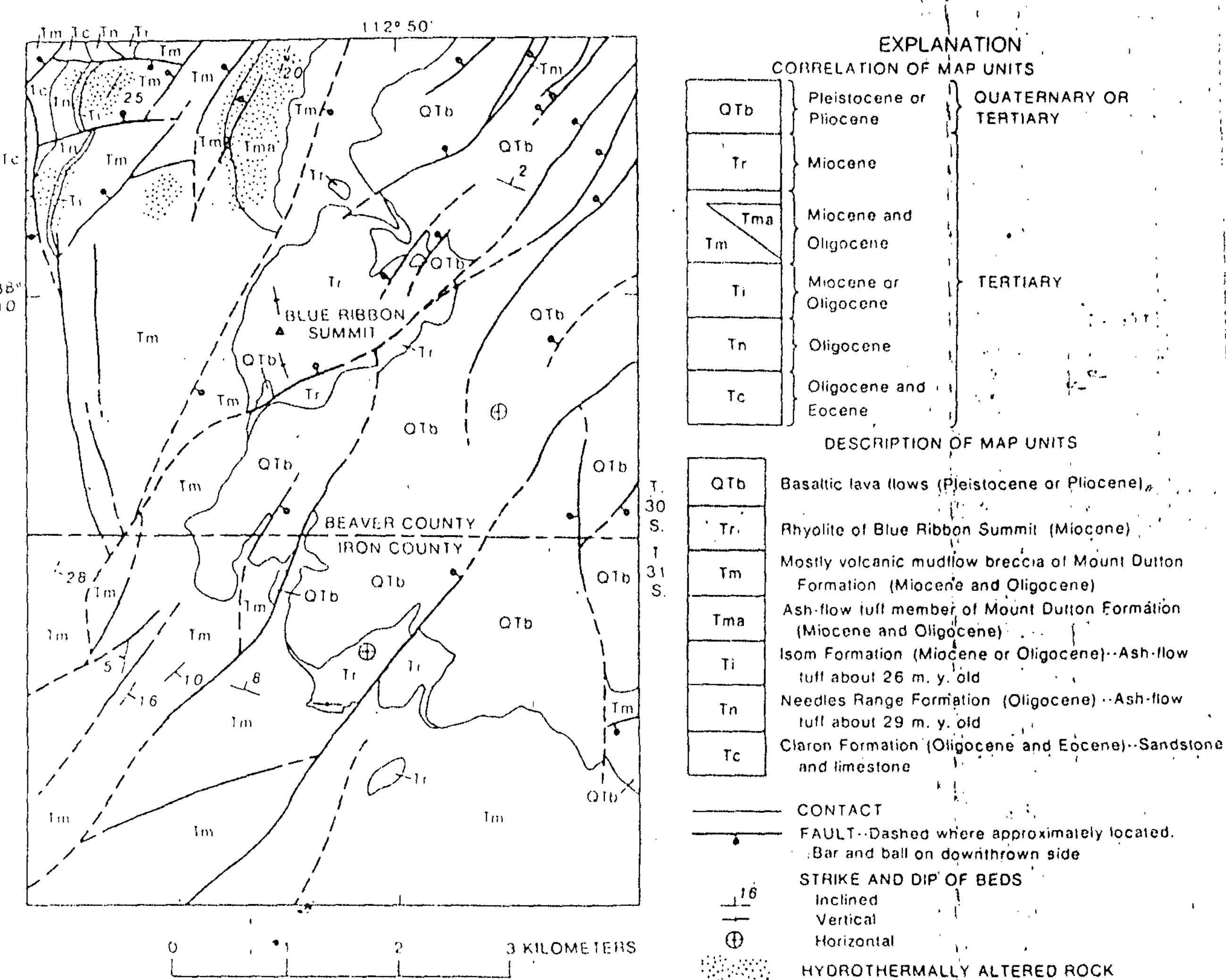

FIGURE 4.—Preliminary geologic map of the Blue Ribbon Summit area, northern Black Mountains (P. D. Rowley, unpub. data, 1975), showing distribution of alkalic rhyolite (Tr). See Anderson and Rowley (1975) and Fleck, Anderson, and Rowley (1975) for additional details.

Ribbon Summit, are mostly perlite and devitrified rhyolite; obsidian is rare (table 2). Vents of alkalic basalt lie 1-2 km east of Blue Ribbon Summit. The rhyolite and basalt are cut by north-northeast-striking faults, most with displacements of less than 50 m.

A dissected rhyolite dome, the rhyolite of Teddys Valley, occurs in a similar geologic setting, and of an assumed similar age, 10 km east of Blue Ribbon Summit (table 2). It covers an area of about 0.2 km² just north of Teddys Valley and is partly covered by basalt that is transected by north-northeast-striking faults.

Nevershine Hollow, draining north, and Fremont Wash, draining south, separate the Black Mountains on the west from the Tushar Mountains and Markagunt Plateau on the east. Dacitic, coarsely porphyritic lava flows of the Beaver Member (25 m.y. old) of the Mount Dutton Formation and their probable plutonic source were mapped by Anderson and Rowley (1975) east and west, respectively, of Nevershine Hollow. Eas of Nevershine Hollow, J. J. Anderson (unpub. data 1976) mapped a small caldera less than 3 km in longes diameter that erupted a green poorly welded to non welded silicic ash-flow tuff (Rowley and Anderson 1975, p. 12). This rock is crystal poor except fo abundant tiny hornblende crystals. The tuff, as well a caldera breccia and landslide breccia, occupies the in ner sides of the caldera and the low grassy valley in the interior of the caldera. Some tuff also occurs i Nevershine Hollow. The caldera is cut by numerou youthful basin-range faults of relatively small dis placement. The topographic expression of the calder and the presence of the tuff exhumed from Nevershin Hollow argue that the caldera and tuff are young probably Pliocene or late Miocene, and thus the tuff i roughly correlative in age with other rhyolites alon the lineament.

A very large positive magnetic anomaly (Eppich, 1973; Zietz, Shuey, and Kirby, 1976) underlies the southern Tushar Mountains, on line with the Blue Ribbon lineament. Major vents of the Mount Dutton Formation, the Dry Hollow Formation (22 m.y. old), older basalt flows (22 m.y. old), and perhaps younger (upper Cenozoic) basalt flows (Anderson and Rowley, 1975) occur on the lineament in the southern Tushar Mountains. The largest of these vent structures is identified by the presence of a large arcuate fault, convex southward, that was mapped by J. J. Anderson (unpub. data, 1974) on the southern side of Birch Creek Mountain near the southwestern side of the large positive magnetic anomaly. The fault is of major displacement that is down on the northern side and is considered to reflect collapse due to eruption of magma of the Mount Dutton Formation. The fault probably is the partial surface trace of a deeply eroded caldera, about 6 km in diameter, that is concealed on the western, northern, and eastern sides by basin-range faults and younger rocks. Locations of other nearby major vent complexes (J. J. Anderson, unpub. data, 1976) of the Mount Dutton Formation—marked by dike swarms and autoclastic flows and locally by hydrothermally altered rocks—include the following areas: Circleville Canyon (Rowley and Anderson, 1975, p. 25), two places about 4 km west and west-southwest of Circleville, two places about 12 km east of Nevershine Hollow, and several places on the southeastern flank of the Tushar Mountains (Circleville Mountain and north) between the latitudes of Junction and Circleville (Douglas Kohout, unpub. data, 1972). A dike swarm vent area for older basalt flows occurs in Little Dog Valley about 14 km south-southwest of Circleville. A large laccolith of Oligocene age, the Spry pluton, and several inferred laccoliths of Miocene age occur in the northern Markagunt Plateau along the southern side of the Blue Ribbon lineament (Anderson and Rowley, 1975, p. 16–17, 38–39); the Spry pluton, in particular, forms a large positive aeromagnetic anomaly (Eppich, 1973, p. 38–39).

At the extreme eastern end of the lineament, extensive alkalic rhyolite occurs in the eastern Kingston Canyon area of the southern Sevier Plateau. Here three plugs of alkalic rhyolite underlie an area of 1 km² near the bottom of the canyon, and lava flows of alkalic rhyolite about 300 m thick underlie an area of 36 km² on the Sevier Plateau north of the canyon and in Grass Valley east of the plateau (Rowley, 1968, pl. 1; Rowley and Anderson, 1975, p. 27). A pronounced positive anomaly, shown on the aeromagnetic map (fig. 14), under the rhyolite suggests the presence of a shallow intrusive body beneath the anomaly. The possibility of a shallow intrusive body is suggested because rhyolite lavas, in general, are magnetically benign and rarely give rise to pronounced magnetic anomalies (G. D. Bath, oral commun., 1976). The largest rhyolite plug in Kingston Canyon, probably a main vent for the lava flows, was pictured by Dutton (1880) in his classic report and the rock was named phonolite, although Dutton noted that the samples he collected were too altered for microscopic examination. Chemistry and petrography clearly show that the plugs and flows are mostly devitrified rhyolite (table 2); minor obsidian at the intrusive contacts of the plug and at the base of the flows, as well as perlite, composes some of the rock. On the basis of petrographic similarity, the rhyolite in Kingston Canyon was correlated (Rowley, 1968; Anderson and Rowley, 1975) with the Mount Belknap Rhyolite, which has a K-Ar age of about 21–17 m.y. (Bassett and others, 1963; Cunningham and Steven, 1977; Steven and others, 1977). The rhyolite in Kingston Canyon may be considerably younger than the Mount Belknap Rhyolite, however. The rhyolite of the plugs and lava flows is here called informally the rhyolite of Phonolite Hill.

Most dacitic to andesitic volcanic centers along the Blue Ribbon lineament probably are late Oligocene to middle Miocene (27–20 m.y.) in age, in keeping with the middle Tertiary volcanic sequence that characterizes this part of Utah (Anderson and Rowley, 1975). The four dated centers of alkalic rhyolite along the Blue Ribbon lineament, however, are revealed to be middle to late Miocene (20–7 m.y.) in age, generally correlative in age with the upper Tertiary and Quaternary sequence that roughly coincides with basin-range faulting (Anderson and Rowley, 1975; Rowley and others, 1977). The four rhyolite centers get progressively younger toward the east. Hamblin and Best (1975) and Best and Brimhall (1974), among other workers, observed a similar eastward progression of ages in upper Cenozoic basalt centers in extreme southwestern Utah and northwestern Arizona. They attributed the progression to an eastward migration of basin-range block faulting. V. IMP.

Topographic and structural features

The Blue Ribbon lineament is marked by gross east-trending topographic and structural patterns. The mountains are both topographically and structurally higher on the northern side of the lineament than on the southern side. In fact, the south-facing step in topography is similar in trend, amplitude, and facing direction to that of the lineament at 37° N. (G. P.

Eaton, written commun., 1976). East-striking faults, rare in this part of the Great Basin where most faults strike north-northwest to north-northeast, also characterize the lineament. South of the lineament, east-striking faults are rare or nonexistent. Topographic and structural features are discussed from west to east.

The long linear north-trending Mountain Home Range and Wah Wah Mountains and intervening Pine Valley are broken up within and south of the lineament into a series of scattered hills with no clear trend and with no major valley separating them (fig. 1*A*). However, these hills form a block of east-trending high ground that is nearly continuous with the Black Mountains and High Plateaus to the east (fig. 1*A*). Paleozoic rocks are exposed widely in the Mountain Home Range and Wah Wah Mountains north of the lineament, but are exposed only sparsely south of it; this suggests that the northern area is structurally higher than the southern area. Taylor and Powers (1953) and Hintze (1963) mapped east-striking faults in the mountains north of Indian Peak and north of the Staats (Monarch) mine-Blawn Mountain area. Landsat images clearly show large east-trending linear features, presumably faults, just south of Indian Peak and the Staats (Monarch) mine-Blawn Mountain area.

The Shauntie Hills and other hills forming the southern end of the San Francisco Mountains terminate abruptly on the northern side of the lineament (fig. 1*A*). Paleozoic rocks are widely exposed in these areas. Many east-striking faults are mapped (Hintze, 1963) through these hills, and are considered by Baer (1962) to be younger than the faults with northerly trends, even though younger(?) uplift of these hills seems to be more strongly influenced by north-striking faults.

A deep east-trending canyon along the lineament east of Minersville separates the low Black Mountains to the south from the high Mineral Mountains to the north. The northern edge of the Black Mountains has an easterly trend for over 50 km. A major north-trending fault zone, which terminates the western side of the Mineral Mountains, offsets the easterly trend of the northern Black Mountains at Minersville; the northern flank of the eastern Black Mountains is 6 km north of the northern flank of the western Black Mountains. The southern part of the Mineral Mountains has a general plunge to the south, and Paleozoic and Mesozoic rocks, abundant to the north, are exposed in only a few small areas in the northernmost Black Mountains. The southern Mineral Mountains and northern Black Mountains are broken into scores of small blocks by the intersection of northerly and easterly faults. Numerous east-striking faults occur in the southern Mineral Mountains and northern Black Mountains (Hintze, 1963; P. D. Rowley, unpub. data, 1976). They are confined to an east-trending zone that extends from about 10 km north to about 6 km south of Minersville. A major east-striking fault zone (Earll, 1957; Hintze, 1963) passes through the Mineral Mountains about 10 km north of Minersville, at the northern side of the lineament. The area north of the fault zone has been uplifted more than 350 m (Earll, 1957, p. 67) relative to the southern side. The huge, young Mineral Mountains batholith is on the northern side of the fault zone. At least some east-striking faults, as in the Escalante Desert north of the western Black Mountains, are clearly Quaternary (fig. 3). A swarm of north-striking faults, extending eastward in the valley between Minersville Reservoir and Beaver, are also Quaternary (J. J. Anderson and P. D. Rowley, unpub. data, 1976).

The lineament crosses the Wasatch Front near Beaver and passes along the southern edge of the Tushar Mountains, which range in altitude from 3000 to more than 3400 meters, and along the northern edge of the lower Markagunt Plateau, which ranges in altitude from 2100 to 2600 m. The Tushar Mountains are much higher structurally than the Markagunt Plateau; Mesozoic rocks are exposed in the former but not the latter area. The abrupt south-facing scarp between the southern Tushar Mountains and northern Markagunt Plateau (at the southern side of the lineament) probably was not caused by east-striking faults. For the Tushar Mountains, however, vertical offset along northerly striking faults certainly was much greater and the type of faulting was different; horsts and grabens characterize the northern Markagunt Plateau, but a single giant horst forms the Tushar Mountains. Intersecting north-northeast- and north-northwest-striking faults produce rhombic blocks along the south-facing mountain front; these are believed to reflect twisting due to different senses of tilting between the Markagunt Plateau and Tushar Mountains (P. D. Rowley and J. J. Anderson, unpub. data, 1976), along the Blue Ribbon lineament. On the southern side of the lineament, Anderson (1965, 1971) mapped major east-striking faults, about 24 m.y. old, that controlled part of the distribution of rocks of the lower Miocene Buckskin Breccia and Bear Valley Formation.

Near its eastern end, the lineament underlies the 1200-m-deep Kingston Canyon, where an east-flowing antecedent stream crosses the Sevier Plateau. The Sevier Plateau is slightly higher north of Kingston Canyon than it is south of the canyon. The western end of the canyon is incised in fault blocks of the Sevier fault zone. The Sevier fault zone, along which the western side of the Sevier Plateau is uplifted, consists of en echelon faults that strike north-northeast south of the Blue Ribbon lineament and north-northwest north of the lineament (Rowley, 1968). These two sets of faults intersect and produce a rhombic pattern of fault blocks in the eastern Kingston Canyon region. A similar, but mirror image, zone of intersecting faults occurs 40 km to the north (P. D. Rowley and J. J. Anderson, unpub. data, 1976) at the eastern end of the canyon of Clear Creek and the northern edge of the Pioche mineral belt and on the east-trending lineament at lat 38°30′ N. Just west of Clear Creek, Crosby (1973) and Cook and Montgomery (1974) postulated right-lateral offset of the Wasatch Front along a hypothetical east-trending transverse fault.

Mineralized and hydrothermally altered areas

Mineralized and hydrothermally altered rocks are the major features in several areas along the Blue Ribbon lineament in Utah. Fluorine, uranium, and tungsten minerals are the most important additions. Many mineral occurrences along the lineament are in the youngest rocks and commonly occur near centers of relatively young alkalic rhyolite. In contrast, mineralized and hydrothermally altered rocks are essentially unknown south of the lineament in the Black Mountains, Markagunt Plateau, and Sevier Plateau. There is a good possibility that additional deposits of these or other minerals may be present at shallow depth along the lineament. For this reason the deposits and altered rock will be described in detail.

Indian Peak mining district and vicinity.—The Indian Peak mining district (also called Washington District) in the southern Mountain Home Range (fig. 1A) was a leading producer of fluorspar in southwestern Utah (Thurston and others, 1954) but now is largely inactive; uranium has also been reported in the district. The Cougar Spar mine is the main producer (Whelan, 1973). The rocks in the district consist largely of faulted and hydrothermally altered ash-flow tuff of the Oligocene Needles Range Formation (Bullock, 1976). Most fluorspar occurs as veins in and near breccia zones (Thurston and others, 1954). The deposits may accompany or postdate rhyolite or one or more Tertiary porphyritic plutons that have been mapped in the area (Thurston and others, 1954; Hintze, 1963; Bullock, 1976).

Staats (Monarch) mine–Blawn Mountain area.—The Staats (Monarch) mine and Blawn Mountain area, also known as the Pine Grove mining district, in the southern Wah Wah Mountains (fig. 1A), has been an intermittent minor producer of fluorspar and lesser uranium and base metals for many years. Fluorspar at the Staats (Monarch) mine occurs as lenticular shoots in the faulted, brecciated, and hydrothermally altered contact between alkalic rhyolite and lower Paleozoic carbonates (Thurston and others, 1954; Whelan, 1965, 1973; Bullock, 1976). Uranium (uraninite, autunite, uranophane, and metatorbernite) occurs as impregnations and coatings on fluorite (Whelan, 1965). At Blawn Mountain, Whelan (1965) mapped intensely hydrothermally altered rock (kaolinite, alunite, silica) and minor mineralized rock (iron, uranium, fluorine) at the contact between Tertiary rhyolite and lower Paleozoic carbonates and quartzites. Alunite resources, perhaps related to ancient hot springs, recently have been discovered in and north of the Blawn Mountain area (William Walker, Earth Sciences, Inc., oral commun., 1976). Intensely hydrothermally altered rocks occur about 15 km east-southeast of the Staats (Monarch) mine (R. K. Glanzman, oral commun., 1976).

Shauntie Hills.—All rocks in the southern Shauntie Hills (fig. 3) are hydrothermally altered and silicified to some degree, and the most intensely altered rocks are adjacent to plugs of the rhyolite of Dead Horse Reservoir, prompting Erickson and Dasch (1963) to suggest that at least some alteration is due to emplacement of the plugs. No detailed work has been done on the types and amounts of mineralized and altered rocks.

Significant mineralized and altered rocks are exposed elsewhere in the Shauntie Hills and areas to the north (Hintze and Whelan, 1973). For example, 7 km north of the rhyolite of Dead Horse Reservoir, Stringham (1963) mapped an 11- by 2-km east-trending belt of mineralized rocks (sulfur related to former hot-spring activity, uranium minerals, and hematite) and hydrothermally altered rocks (mostly alunite, kaolinite, and silica). Undated rhyolite plugs occur north of the belt (Stringham, 1963, pl. 4; Erickson, 1973; P. L. Williams, oral commun., 1976) and may have produced some of the mineralized and altered rocks; mineralization postdates rock of the 24- to 21-m.y.-old Quichapa Group.

Northern Black Mountains and southern Mineral Mountains.—Local areas of intense hydrothermally altered rocks occur along the northern edge of the Black Mountains (Erickson and Dasch, 1963, 1968) but few introduced metals other than minor iron have been recorded. The Jarloose mining district (Erickson and Dasch, 1968), several kilometers southeast of Minersville, has several mines, but the type of mineral deposit is not known and apparently no ore was produced. The area is broadly hydrothermally altered at and outward from Black Mountain, which is underlain by a Tertiary dacitic plug. Probably this plug was a main vent for lava flows and volcanic mudflow breccia of the Mount Dutton Formation in this area, and the vent area likely was the source of altered and sparsely mineralized rocks.

Most rocks near Minersville are mineralized and hydrothermally altered to some degree, and, as its name suggests, the town was a mining center during its early days. Copper staining is visible in rocks exposed below a dissected pediment about 1 km northeast of Minersville. Lincoln mining district, in the southern Mineral Mountains about 5 km north of Minersville, produced mostly lead, silver, and zinc. Bradshaw district, 8 km north of Minersville, produced tungsten, gold, silver, and lead. Granite district, about 13 km northeast of Minersville and continuing farther north along the eastern side of the Mineral Mountains, produced mostly tungsten (Hobbs, 1945; Earll, 1957); the beryllium mineral helvite was discovered in this district by Sainsbury (1962). Minor fluorspar also occurs in the Bradshaw and Granite districts (Bullock, 1976). Most minerals north of Minersville are contact-metamorphic and fissure-vein deposits that formed during intrusion of the young Mineral Mountains batholith.

Southern Tushar Mountains and vicinity.—Mineralized and hydrothermally altered rocks occur in most of the Tushar Mountains, including the southern end. One of these, in the southern Birch Creek Mountain area, was mentioned by Anderson and Rowley (1975, p. 28); it consists of intense hydrothermally altered rock, including silicified sandstone, in a north-northwest-trending zone at least 4 km long, and it postdates rocks of the Mount Dutton Formation. On the southern side of the Blue Ribbon lineament, cinnabar deposits, silicified rock, argillic altered rock, fluorspar, and other minerals have been reported (Doelling, 1975, p. 139–143) on the northwestern side of the Spry pluton.

Eastern Kingston Canyon and vicinity.—Kingston Canyon, cut in the southern Sevier Plateau, contains scattered patches of intense hydrothermally altered rocks, at least some of which are associated with rhyolite plugs (Rowley, 1968). Antimony and arsenic have been mined east of the town of Antimony (Doelling, 1975).

BLUE RIBBON LINEAMENT IN NEVADA

Because of our lack of firsthand knowledge of the geology of eastern Nevada and because of the absence of a detailed aeromagnetic map of this region, the extension of the Blue Ribbon lineament into Nevada is more speculative, and the discussion brief. At 113°30′ W., in Utah, the southern branch of the Pioche magnetic ridge crosses the Blue Ribbon lineament and extends west-southwesterly into Nevada, where it terminates at the north-trending "quiet" magnetic zone (Eaton, 1976; Stewart and others, 1977; Eaton, unpu data, 1976) and at the western end of the Delama Iron Springs mineral belt of Shawe and Stewa (1976).

The northern branch of the aeromagnetic expressio of the Pioche mineral belt (fig. 1), as shown on th generalized aeromagnetic map of Stewart, Moore, an Zietz (1977, fig. 5), extends westward into Nevada far as 115° W., where it terminates at the quiet zon The Blue Ribbon lineament coincides with the crest this northern branch and is centered at about 38°10′ A large east-trending magnetic high at 38°10′ N. u derlies the White Rock Mountains and Wilson Cre Mountains. The crest of this high, in the Wilson Cre Mountains, is overlain by a large area of rhyoli (Stewart and Carlson, 1975); the area has not be mapped in detail, but Tschanz and Pampeyan (197 noted that glassy flows and significant reserves of pe lite occur there, near the Hollinger mine. The ma netic high may reflect a pluton at depth.

The lineament passes through the southern edge the next two ranges to the west, the Fairview and t Schell Creek; the area is underlain by a circular ma netic high, and rhyolites and east-striking faults a known at the surface (Tschanz and Pampeyan, 197 Stewart and Carlson, 1974). The largest exposures rhyolite are in the southern Fairview Range; here t rhyolite is described as perlitic pitchstone (Westga and Knopf, 1932, p. 32) and is the site of one Nevada's largest perlite mines (Tschanz and Pa peyan, 1970. A Tertiary granodiorite pluton is mapp in the southern Schell Creek Range (Tschanz a Pampeyan, 1970).

The north-trending magnetic quiet zone is just w of these ranges, from about 115° to 116° W. and expression of the lineament can be seen on the gr aeromagnetic maps available. Even though aeroma netic expression is not evident, the geology at surface suggests that the lineament passes through t quiet zone. Thus large rhyolitic intrusive and extrus masses underlie the Quinn Canyon Range at ab 38° N. (Stewart and Carlson, 1974), and, from to 38°25′ N., the range is dotted by numerous mi which have produced fluorine, uranium, and tu sten, and which contain occurrences of beryllium (U Geological Survey, Nevada Bureau of Mines, 19 Shawe, 1966; Sainsbury and Kleinhampl, 19 Tschanz and Pampeyan, 1970). Just west of the Qu Canyon Range, at 38°10′ N., is the eastern end of Warm Springs lineament of Ekren and others (197 here the Warm Springs lineament exhibits interr tions of aeromagnetic anomalies (U.S. Geological S vey, 1968).

CONCLUSIONS

Although the genesis of east-trending mineralized structural belts in the eastern Great Basin is poorly known, it is possible to draw a modest set of conclusions from the observations on the Blue Ribbon lineament. The lineament is a fault zone, as indicated by alinement of topographic features, alinement with aeromagnetic contours, and coincidence with major high-angle faults. Although at least some major faults of the Warm Springs lineament have strike-slip movement (Ekren and others, 1976), only dip-slip movement is known for major faults along the Utah portion of the Blue Ribbon lineament. The lower topography and structure south of the lineament indicates that cumulative throw is down to the south. Major post basin-range transcurrent movement is not indicated along the lineament in Utah because the basins and ranges and related structures are not known to be offset laterally. Strike-slip movement along the lineament might have occurred prior to about 20 m.y. ago, however. Alternately, the Blue Ribbon lineament in Utah may be an incipient strike-slip fault. This is suggested by a general similarity between the fault patterns along the Blue Ribbon lineament and those Riedel shear patterns of "peak structure" illustrated by Tchalenko (1970, fig. 9). East-striking faults of the Blue Ribbon lineament are rare east of the Wasatch Front, indicating that the fault system dies out eastward.

The age of the lineament is unknown, but igneous and (or) hydrothermal activity along the lineament started 20 m.y. ago or earlier and continued to at least as late as 7 m.y. ago, as indicated by new K-Ar ages of rhyolites, and probably to as young as Holocene, as suggested by the presence of past and present hot springs. Thus it has been a persistent geologic feature. Furthermore, it is generally coincident with extensional rifting of the eastern Great Basin. Rhyolite and basalt along the lineament, for example, are correlated with Anderson and Rowley's (1975) upper Tertiary and Quaternary sequence (20 m.y. to present), which is generally synchronous with basin-range development in this part of Utah (Rowley and others, 1977) and with young extensional tectonics in the western United States (Christiansen and Lipman, 1972). Some features on the lineament, however, belong to the middle Tertiary sequence (Anderson and Rowley, 1975), and still others may date to early Tertiary or older.

The lineament fracture system extends to a depth where partial melting and fractionation of the rhyolite magma occurred. As the magma rose along the fracture system and the pressure decreased, metal-laden hydrothermal fluids were released. Thus the lineament should serve as a guide to mineral exploration because it marks the locus of a fracture system that controlled the migration of mineralizing solutions.

The larger mechanism of control of such faults is open to question, but Stewart, Moore, and Zietz (1977) hypothesized that east-trending features may be due to east-trending warps in the subducting mantle plate, and credited one of us (Lipman) with preliminary suggestion of the idea. Another possible explanation is that the Blue lineament was or is part of an intracontinental transform fault, which extends from a zone of clear strike-slip faulting (Warm Springs lineament) eastward along strike to the forerunning fracture zone and from there to die out in the Colorado Plateaus province. The K-Ar ages of rhyolites suggest that at least some parts of the fault system are younger eastward, in keeping with recent ideas on the eastward expansion of the eastern Great Basin (Best and Hamblin, 1977) The Blue Ribbon lineament is parallel with the general worldwide pattern of transform faults (Moore, 1973). At right angles to the lineament, classical northerly trending basin-range faults of the same age as the lineament occur in the extension direction, analogous to the trend in the extension direction of spreading lines in an ocean basin and rifts on a continent where they are parallel to and above the typical (Moore, 1973) north-trending spreading ocean ridge. Both hypotheses need considerable further testing, however, and resolution of the genesis of east-trending features in the Great Basin must await new studies.

REFERENCES CITED

Anderson, J. J., 1965, Geology of northern Markagunt Plateau, Utah: Austin, Texas Univ., Ph. D. dissert., 194 p.

———1971, Geology of the southwestern High Plateaus of Utah; Bear Valley Formation, an Oligocene-Miocene volcanic arenite: Geol. Soc. America Bull., v. 82, no. 5, p. 1179–1205.

Anderson, J. J., and Rowley, P. D., 1975, Cenozoic stratigraphy of southwestern High Plateaus of Utah, *in* Anderson, J. J., Rowley, P. D., Fleck, R. J., and Nairn, A. E. M., Cenozoic geology of southwestern High Plateaus of Utah: Geol. Soc. America Spec. Paper 160, p. 1–52.

Armstrong, R. L., 1970, Geochronology of Tertiary igneous rocks, eastern Basin and Range Province, western Utah, eastern Nevada, and vicinity, U.S.A.: Geochim. et Cosmochim. Acta, v. 34, no. 2, p. 203–232.

Baer, J. L., 1962, Geology of the Star Range, Beaver County, Utah: Brigham Young Univ. Geology Studies, v. 9, pt. 2, p. 29–52.

Bassett, W. A., Kerr, P. F., Schaeffer, O. A., and Stoenner, R. W., 1963, Potassium-argon dating of the late Tertiary volcanic rocks and mineralization of Marysvale, Utah: Geol. Soc. America Bull., v. 74, p. 213–220.

Best, M. G., and Brimhall, W. H., 1974, Late Cenozoic alkalic basaltic magmas in the western Colorado Plateaus and the Basin and Range transition zone, U.S.A., and their bearing on mantle dynamics: Geol. Soc. America Bull., v. 85, no. 11, p. 1677–1690.

Best, M. G., and Hamblin, W. K., 1977, Origin of the Basin Range-implications from the geology of its eastern boundary, *in* Smith, R. B., and Eaton, G. P., eds., Cenozoic tectonics and regional geophysics of the western United States: Geol. Soc. America Mem. (In press.)

Bingler, E. C., 1971, Major east-west lineament in west-central Nevada: Geol. Soc. America Abs. with Programs, v. 3, no. 2, p. 83.

Blank, H. R., Jr., and Mackin, J. H., 1967, Geologic interpretation of an aeromagnetic survey of the Iron Springs district, Utah: U.S. Geol. Survey Prof. Paper 516-B, 14 p.

Bullock, K. C., 1976, Fluorite occurrences in Utah: Utah Geol. and Mineral Survey Bull. 110, 89 p.

Bushman, A. V., 1973, Pre-Needles Range silicic volcanism, Tunnel Spring Tuff (Oligocene), west-central Utah: Brigham Young Univ. Geol. Studies, v. 20, pt. 4, p. 159–190.

Butler, B. S., Loughlin, G. F., Heikes, V. C., and others, 1920, The ore deposits of Utah: U.S. Geol. Survey Prof. Paper 111, 672 p.

Callaghan, Eugene, 1939, Volcanic sequence in the Marysvale region in southwest-central Utah: Am. Geophys. Union Trans., 20th Ann. Mtg., Washington 1939, pt. 3, p. 438–452.

———1973, Mineral resources potential of Piute County, Utah and adjoining area: Utah Geol. and Mineralog. Survey Bull. 102, 135 p.

Callaghan, Eugene, and Parker, R. L., 1962, Geology of the Sevier quadrangle Utah: U.S. Geol. Survey Geol. Quad. Map GQ-156.

Christiansen, R. L., and Lipman, P. W., 1972, Cenozoic volcanism and paleo-tectonic evolution of the Western United States—pt. 2, Late Cenozoic: Royal Soc. London Philos. Trans. A, v. 271, p. 249–284.

Cohenour, R. E., 1963, The beryllium of western Utah, *in* Beryllium and uranium mineralization in western Jaub County, Utah: Utah Geol. Soc. Guidebook to the Geology of Utah, no. 17, p. 4–7.

———1970, Sheeprock granite, *in* Whelan, J. A., compiler, Radioactive and isotopic age determinations of Utah rocks: Utah Geol. and Mineralog. Survey Bull. 81, p. 31.

Cook, E. F., 1960, Geologic atlas of Utah—Washington County: Utah Geol. and Mineralog. Survey Bull. 70, 119 p.

Cook, K. L., and Montgomery, J. R., 1974, Crustal structure and east-west transverse structural trends in eastern Basin and Range province as indicated by gravity data: Geol. Soc. America Abs. with Programs, v. 6, no. 3, p. 158.

Crosby, G. W., 1973, Regional structure in southwestern Utah, *in* Hintze, L. F., and Whelan, J. A., eds, Geology of the Milford area, 1973: Utah Geol. Assoc. Pub. 3, 27–32.

Cunningham, C. G., and Steven, T. A., 1977, Mount Belknap and Red Hills calderas and associated rocks, Marysvale volcanic field, west-central Utah: U.S. Geol. Survey Open-File Rept. 77–568, 40 p.

Doelling, H. H., 1975, Geology and mineral resources of Garfield County, Utah: Utah. Geol. Mineral Survey Bull., 107 p.

Dutton, C. E., 1880, Report on the geology of the h plateaus of Utah: U.S. Geog. Geol. Survey, Rocky M Region (Powell), 307 p.

Earll, F. N., 1957, Geology of the central Mineral Range, Bea County, Utah: Salt Lake City, Utah Univ., Ph. D. the 112 p.

Eaton, G. P., 1975, Characteristics of a transverse crus boundary in the Basin and Range Province of south Nevada: Geol. Soc. America Abs. with Programs, v. 7, 7, p. 1062.

———1976, Fundamental bilateral symmetry of the west Basin and Range Province: Geol. Soc. America Abs. w Programs, v. 8, no. 5, p. 583.

Ekren, E. B., Bucknam, R. C., Carr, W. J., Dixon, G. L., Quinlivan, W. D., 1976 East-trending structural lin ments in central Nevada: U.S. Geol. Survey Prof. Pa 986, 16 p.

Eppich, G. K., 1973, Aeromagnetic survey of south-cent Utah: Salt Lake City, Utah Univ., M.S. thesis, 78 p.

Erickson, A. J., 1974, The Uinta-Gold Hill trend—an econ ically important lineament, *in* Hodgson, R. A., Gay, P., Jr., and Benjamins, J. Y., eds., Proceedings of the Fi International Conference on the New Basement Tecton Utah Geol. Assoc. Pub. 5, p. 126–138.

Erickson, M. P., 1973, Volcanic rocks of the Milford ar Beaver County, Utah, *in* Geology of the Milford ar Utah Geol. Assoc. Pub. 3, p. 13–21.

Erickson, M. P., and Dasch, E. J., 1963, Geology and hyd thermal alteration in northwestern Black Mountains a southern Shauntie Hills, Beaver and Iron Counties, Uta Utah Geol. and Mineralog. Survey Spec. Studies, no. 32 p.

———1968, Volcanic stratigraphy, magnetic data and alte tion, geologic map, and sections of the Jarloose mini district southeast of Minersville, Beaver County, Uta Utah Geol. Mineralog. Survey, Map 26.

Fleck, R. J., Anderson, J. J., and Rowley, P. D., 1975, Chro ology of mid-Tertiary volcanism in High Plateaus regi of Utah, *in* Anderson, J. J., Rowley, P. D., Fleck, R. J., a Nairn, A. E. M., Cenozoic geology of southwestern Hi Plateaus of Utah: Geol. Soc. America Spec. Paper 160, 53–62.

Hamblin, W. K., and Best, M. G., 1975, The geologic bounda between the Colorado Plateau and the Basin Ran Province: Geol. Soc. America Abs. with Programs, v. no. 7, p. 1097.

Hilpert, L. S., and Roberts, R. J., 1964, Geology—Econon geology, *in* U.S. Geological Survey, Mineral and water sources of Utah: U.S. 88th Cong., 2d sess., p. 28–38.

Hintze, L. F., 1963, Geologic map of southwestern Utah: Sa Lake City, Utah Geol. and Mineralog. Survey.

Hintze, L. F., and Whelan, J. A., eds., 1973, Geology of t Milford area, 1973: Utah Geol. Assoc. Pub. 3, 94 p.

Hobbs, S. W., 1945, Tungsten deposits in Beaver County, Uta U.S. Geol. Survey Bull. 945-D, p. 81–111.

Johnston, W. P., 1972, K-Ar ages of the Blind Mounta stock and Yuba dike, Lincoln County, Nevada: Isochro West, no. 3, p. 30.

Kennedy, R. R., 1963, Geology of Piute County, Utah: Tucso Arizona Univ., Ph.D. thesis, 282 p.

Kerr, P. F., 1968, The Marysvale, Utah, uranium deposits, Ore deposits of the United States, 1933–1967 (Grato

Sales Volume): Am. Inst. Mining, Metall. and Petroleum Engineers, v. 2, p. 1020-1042.

Kerr, P. F., Brophy, G. P., Dahl, H. M., Green, Jack, and Woolard, L. E., 1957, Marysvale, Utah, uranium area—Geology, volcanic relations, and hydrothermal alteration: Geol. Soc. America Spec. Paper 64, 212 p.

Krueger, H. W., and Schilling, J. H., 1971, Geochron/Nevada Bureau of Mines K/Ar age determinations—list 1: Isochron/West, no 71-1, p. 9-14.

Lee, W. T., 1908, Water resources of Beaver Valley, Utah: U.S. Geol. Survey Water Supply Paper 217, 57 p.

Liese, H. C., 1957, Geology of the northern Mineral Range, Millard and Beaver Counties, Utah: Salt Lake City, Utah Univ. M.S. thesis, 88 p.

Lindsey, D. A., Ganow, Harold, and Mountjoy, Wayne, 1973, Hydrothermal alteration associated with beryllium deposits at Spor Mountain, Utah: U.S. Geol. Survey Prof. Paper 818-A, 20 p.

Lindsey, D. A., Naeser, C. W., and Shawe, D. R., 1975, Age of volcanism, intrusion, and mineralization in the Thomas Range, Keg Mountain, and Desert Mountain, western Utah: U.S. Geol. Survey Jour. Research, v. 3, no. 5, p. 597-604.

Lipman, P. W., Rowley, P. D., and Pallister, J. S., 1975, Pleistocene rhyolite of the Mineral Range, Utah—geothermal and archeological significance: Geol. Soc. America Abs. with Programs, v. 7, no. 7, p. 1173.

Lipman, P. W., Rowley, P. D., Mehnert, H. H., Evans, S. H., Jr, Nash, W. P., and Brown, F. H., 1978, Pleistocene rhyolite of the Mineral Mountains, Utah—Geothermal and archeological significance: U.S. Geol. Survey Jour. Research, v. 6, no. 1, p. 133-147.

Loring, A. K., 1972, Temporal and spatial distribution of basin-range faulting in Nevada and Utah: Los Angeles, Southern California Univ., M.S. thesis, 163 p.

Mehnert, H. H., Rowley, P. D., and Lipman, P. W., 1977, K-Ar ages and geothermal implications of young rhyolites in west-central Utah: Isochron/West. (In press.)

Miller, G. M., 1966, Structure and stratigraphy of southern part of Wah Wah Mountains, southwest Utah: Am. Assoc. Petroleum Geol. Bull., v. 50, p. 858-900.

Moore, G. W., 1973, Westward tidal lag as the driving force of plate tectonics: Geology, v. 1, no. 3, p. 99-100.

Mundorff, J. C., 1970, Major thermal springs of Utah: Utah Geol. and Mineralog. Survey Water-Resources Bull. 13, 60 p.

Park, G. H., 1968, Some geochemical and geochronologic studies of the beryllium deposits in western Utah: Salt Lake City, Utah Univ., M. S. thesis, 91 p.

Petersen, C. A., 1973, Roosevelt and Thermo hot springs, Beaver County, Utah, *in* Hintze, L. F., and Whelan, J. A., eds., Geology of the Milford area, 1973: Utah Geol. Assoc. Pub. 3, p. 73-74.

Roberts, R. J., 1964, Economic geology, *in* Mineral and water resources of Nevada: U.S. 88th Cong., 2d sess., Senate Doc. 87, p. 39-48.

———1966, Metallogenic provinces and mineral belts in Nevada, *in* AIME Pacific Southwest Mineral Industry Conf., Sparks, Nev., 1965, Papers, pt. A: Nevada Bur Mines Rept. 13, pt. A, p. 47-72.

Rowley, P. D., 1968, Geology of the southern Sevier Plateau, Utah: Austin, Texas Univ. Ph.D. thesis, 385 p.

Rowley, P. D., and Anderson, J. J., 1975, Guidebook to the Cenozoic structural and volcanic evolution of the southern Marysvale volcanic center, Iron Springs mining district, and adjacent areas, southwestern Utah—Geol. Soc. America Ann. Mtg., Salt Lake City, Utah, 1975, Field Trip 2: Gamma Zeta Chapter, Sigma Gamma Epsilon, Kent State Univ., Kent, Ohio, 37 p.

Rowley, P. D., and Lipman, P. W., 1975, Geologic setting of the Thermo KGRA (known geothermal resource area), Beaver County, Utah: Geol. Soc. America Abs. with Programs, v. 7, no. 7, p. 1254.

Rowley, P. D., Anderson, J. J., Williams, P. L., and Fleck, R. J., 1977, Age of structural differentiation between the Colorado Plateaus and Basin and Range provinces in southwestern Utah: Geology (In press).

Sainsbury, C. L., 1962, Helvite near Beaver, Utah: Am. Mineralogist, v. 47, nos. 3-4, p. 395-398.

Sainsbury, C. L., and Kleinhampl, F. J., 1969, Fluorite deposits of the Quinn Canyon Range, Nevada: U.S. Geol. Survey Bull. 1272-C, 22 p.

Shawe, D. R., 1966, Arizona-New Mexico and Nevada-Utah beryllium belts, *in* Geological Survey research 1966: U.S. Geol. Survey Prof. Paper 550-C, p. C206-C213.

Shawe, D. R., and Stewart, J. H., 1976, Ore deposits as related to tectonics and magmatism, Nevada and Utah: Am. Inst. Mining, Metall., and Petroleum Engineers Trans., v. 260, p. 225-232.

Steven, T. A., Cunningham, C. G., Naeser, C. W., and Mehnert, H. H., 1977, Revised stratigraphy and radiometric ages of volcanic rocks and mineral deposits in the Marysvale area, west-central Utah: U. S. Geol. Survey Open-File Rept. 77-569, 45 p.

Stewart, J. H., and Carlson, J. E., 1974, Preliminary geologic map of Nevada: U.S. Geol. Survey Misc. Field Studies Map MF-609.

Stewart, J. H., Moore, W. J., and Zietz, Isidore, 1977, East-west patterns of Cenozoic igneous rocks, aeromagnetic anomalies, and mineral deposits, Nevada and Utah: Geol. Soc. America Bull., v. 88, no. 1, p. 67-77.

Stokes, W. L., 1963, *Geologic map of northwestern Utah*: Salt Lake City, Utah Geol. and Mineralog. Survey.

Stringham, Bronson, 1963, Hydrothermal alteration in the southeast part of the Frisco quadrangle, Beaver County, Utah: Utah Geol. and Mineralog. Survey Spec. Studies, no. 4, 21 p.

Taylor, A. O., and Powers, J. F., 1953, Reconnaissance geologic map of the Wah Wah Range, Beaver County, Utah: U.S. Geological Survey, open-file map.

Tchalenko, J. S., 1970, Similarities between shear zones of different magnitudes: Geol. Soc. America Bull., v. 81, no. 6, p. 1625-1640.

Thurston, W. R., Staatz, M. H., Cox, D. C., and others, 1954, Fluorspar deposits of Utah: U.S. Geol. Survey Bull. 1005, 53 p.

Tschanz, C. M., and Pampeyan, E. H., 1970, Geology and mineral deposits of Lincoln County, Nevada: Nevada Bur. Mines Bull. 73, 188 p.

U.S. Geological Survey, 1968, Aeromagnetic map of the Hot Creek Range region, south-central Nevada: U.S. Geol. Surveys Geophys. Inv. Map GP-637.

U.S. Geological Survey, Utah Geological and Mineralogical Survey, 1964, Mineral and water resources of Utah: U.S. 88th Cong., 2d sess., Comm. rept., (Utah Geol. and Mineralog. Survey Bull. 73) 275 p.

U.S. Geological Survey, Nevada Bureau of Mines, 1964, Mineral and water resources of Nevada: U.S. 88th Cong., 2d sess., Senate Doc. 87 (Nevada Bur. Mines Bull. 65), 314 p.

Van Alstine, R. E., 1976, Continental rifts and lineaments associated with major fluorspar districts: Econ. Geology, v. 71, no. 6, p. 977–987.

Walker, G. W., and Osterwald, F. W., 1963, Introduction to the geology of uranium-bearing veins in the conterminous United States, including sections on geographic distribution and classification of veins: U. S. Geol. Survey Prof. Paper 455–A, p. A1–A28.

Westgate, L. G., and Knopf, Adolph, 1932, Geology and ore deposits of the Pioche district, Nevada: U.S. Geol. Surv Prof. Paper 171, 79 p.

Whelan, J. A., 1965, Hydrothermal alteration and mineraliz tion, Staats mine and Blawn Mountain areas, central W Wah Range, Beaver County, Utah: Utah Geol. a Mineralog. Survey Spec. Studies 12, 31 p.

———1973, Mineral resources of the Milford area, Beav County, Utah, *in* Hintze, L. F., and Whelan, J. A., ed Geology of the Milford area, 1973: Utah Geol. Assoc. Pu 3, p. 1–3.

Zietz, Isidore, Bateman, P. C., Case, J. E., Crittenden, M. Jr. Grissom, Andrew, King, E. R., Roberts R. J., a Lorentzen, G. R., 1969, Aeromagnetic investigation crustal structure for a strip across the western Unit States: Geol. Soc. America Bull., v. 80, no. 9, p. 170 1714.

Zietz, Isidore, Shuey, R. T., and Kirby, J. R., 1976, Aeroma netic map of Utah: U.S. Geol. Surveys Geophys. In Map GP–907.

Oligocene and Miocene metamorphism, folding, and low-angle faulting in northwestern Utah

AREA
UT-nwest
Faults

ROBERT R. COMPTON *Department of Geology, Stanford University, Stanford, California 94305*
VICTORIA R. TODD *U.S. Geological Survey, Menlo Park, California 94025*
ROBERT E. ZARTMAN
CHARLES W. NAESER } *U.S. Geological Survey, Denver, Colorado 80225*

ABSTRACT

An area of 3,000 km² in and around the Grouse Creek Mountains and the Raft River Mountains exposes Precambrian, Paleozoic, and Triassic sedimentary rocks that were folded several times and displaced tens of kilometres on low-angle faults. Overturned folds and local imbrications indicate transport westward and northward during two episodes of metamorphic deformation and transport eastward after metamorphism. Metamorphic grade increases downward in the allochthonous sheets and autochthon and increases westward in the autochthon. Mineral grains are flattened into the horizontal plane, and shear strains increase upward, suggesting that the deformations were caused by gravity acting on a broadly heated dome. Rb-Sr dating of granitic plutons affected by the deformations indicates that (1) the area is underlain by adamellite, about 2.5 b.y. old, in which deformation decreased progressively downward; (2) the first metamorphic deformation probably ended before 38.2 ± 2.0 m.y. ago; and (3) the second metamorphic deformation was still underway 24.9 ± 0.6 m.y. ago.

High-grade allochthonous rocks that lie on low-grade parts of the autochthon indicate as much as 30 km of eastward transport after metamorphism. Parts of the dome sagged to form broad basins 12 m.y. ago, and the coarse sediments and tuffs that accumulated in them were overrun by allochthonous sheets measuring at least 11 by 19 km. Two Rb-Sr mineral isochrons and several fission-track ages indicate that some parts of the area cooled below 400 °C only 10 m.y. ago.

INTRODUCTION

The area studied is one of many in the region that expose low-angle faults of Mesozoic or Tertiary age; it is also one of about 20 localities where metamorphism and deformation were partly concurrent (Fig. 1). The map shows the great extent of these features but also presents a problem in interpreting them. The localities west of the belt of upthrusts are shown as separate dots because each is a mountain range surrounded by extensive alluvium. Folds and faults are superbly exposed in the ranges, but most are too complex to be connected reliably across the broad intervening basins. The belt of upthrusts, which is exposed more continuously, provides ample evidence of major eastward thrusting in Late Cretaceous and early Tertiary time, but contemporaneous tectonic features have been dated in only a few localities to the west (Hose and Blake, 1976; A. Snoke, 1974, oral commun.) Isotopic data from the western localities suggest a wide range of igneous rock ages, few of which have been attached firmly to tectonic events. A major problem is that K-Ar ages have been variably reset by Cenozoic heating. Nonetheless, the regional history has been interpreted by several persons (Misch, 1960; Roberts and others, 1965; Armstrong and Hansen, 1966; Armstrong, 1968b, 1972; Roberts, 1968; Hose and Danes, 1973; and Roberts and Crittenden, 1973). These histories are too varied to review here, but some events pertinent to our study have been assigned ages so consistently as to seem firmly dated: (1) the Grouse Creek–Raft River area lay in the hinterland of a broad belt of west-to-east thrusting (or sliding) during Cretaceous and possibly Late Jurassic time; (2) metamorphism in the region was concurrent with deformation during the early part of that period only; and (3) starting no later than middle Tertiary time, the entire region underwent extension and consequent high-angle faulting, so that thrusting must have ceased.

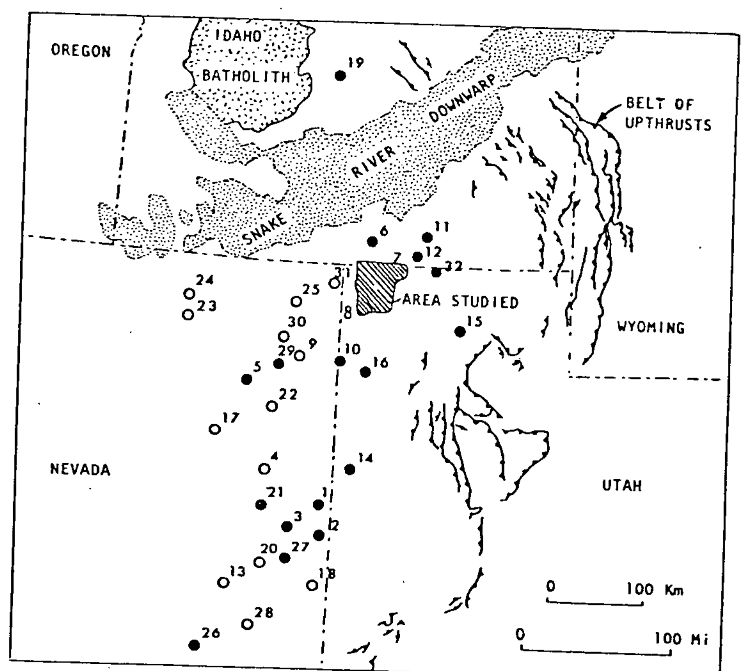

Figure 1. Tectonic features near area studied. Open circles = places where low-angle faults of Mesozoic or Tertiary age have been reported; solid circles = places where metamorphic rocks were involved in deformation. 1, Ahlborn (1973); 2, Hazzard and Turner (1957), Misch and Hazzard (1962); 3, Young (1960); 4, Misch (1960), Hazzard and Turner (1957); 5, Howard (1966), Kistler and Willden (1969); 6, Armstrong (1968a); 7, Compton (1969, 1972); 8, Todd (1973); 9, Thorman (1970); 10, Woodward (1967), O'Neill (1969); 11 and 12, Anderson (1931); 13, Moores and others (1968); 14, Nelson (1966, 1969), Nolan (1935); 15, Olson (1956); 16, Schaeffer and Anderson (1960); 17, Willden and others (1967); 18, Whitebread (1966), Lee and others (1970); 19, Dover (1969); 20, Misch (1960); 21, Woodward (1964); 22, Misch (1960); 23, Kerr (1962); 24, Fagan (1962); 25, Riva (1970); 26, Cebull (1970); 27, Drewes (1967); 28, Tchanz and Pampeyan (1970); 29, Thorman (1970); 30, Oversby (1972); 31, Slack (1974); 32, Peace (1956). Thrust faults are from King (1969).

Geological Society of America Bulletin, v. 88, p. 1237–1250, 13 figs., September 1977, Doc. no. 70903.

The dates determined in this study therefore seemed surprising, as did the directions of tectonic transport during metamorphism. In brief, our data indicate that metamorphism and folding in the Grouse Creek–Raft River area were going on as recently as 20 m.y. ago, that metamorphic flow and low-angle faulting were mainly northward and westward rather than eastward, that some allochthonous sheets traveled 30 km eastward after metamorphism, and that allochthonous sheets were emplaced locally onto 11-m.y.-old sedimentary and volcaniclastic rocks. We present our age data here and briefly describe structural relations. Geologic

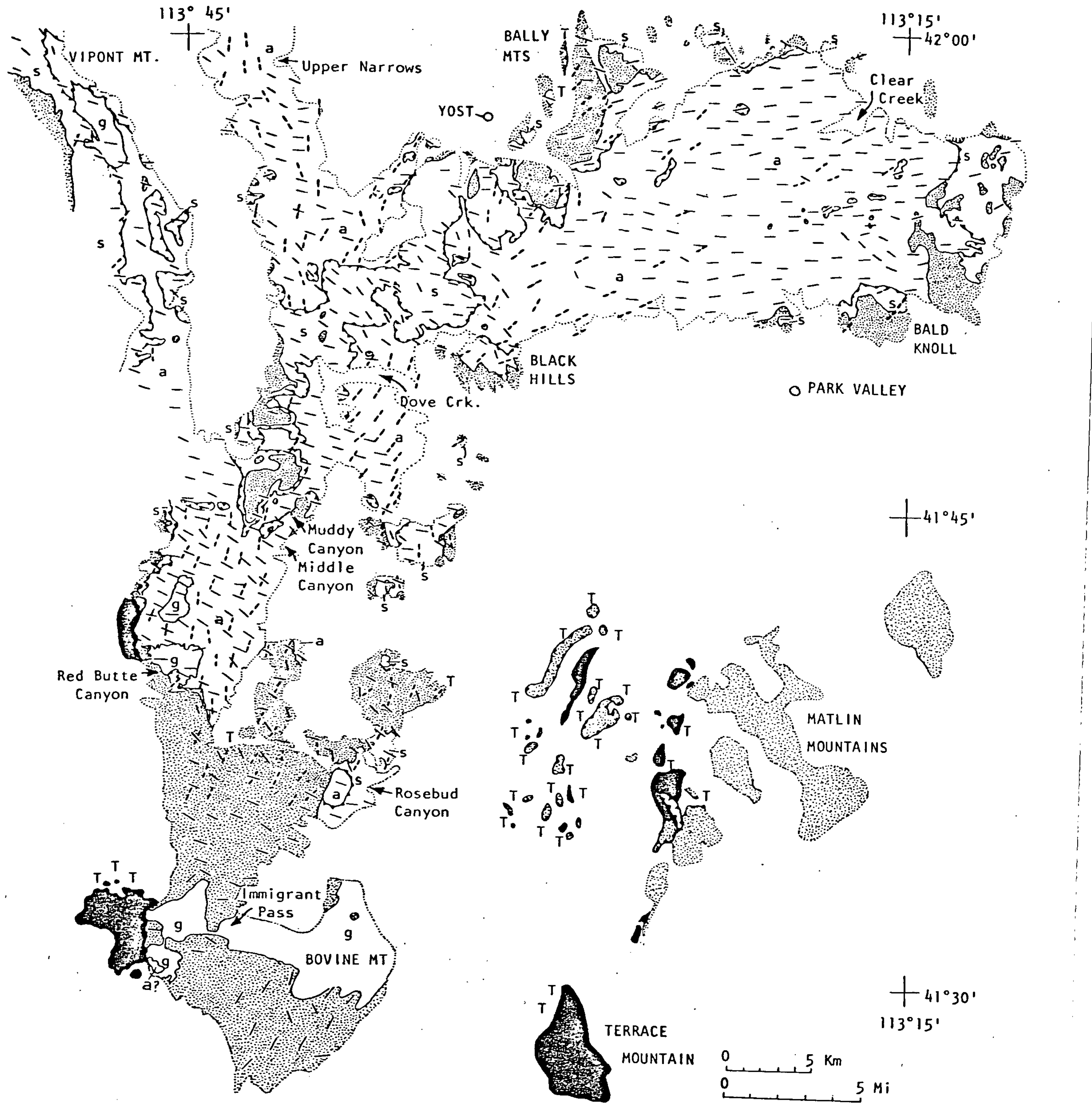

Figure 2. Structure map of Grouse Creek Mountains (north-south outcrop), Raft River Mountains (east-west outcrop), and vicinity. High-angle faults have been omitted. Black = upper allochthonous sheet; dots = middle sheet (and subsidiary sheets derived from it), s = lower sheet; a = autochthon; g = Tertiary granitic bodies. Dotted boundaries = depositional contacts with Cenozoic rocks; T = allochthonous sheets on Tertiary beds. Heavy dashes show axial trends of first metamorphic folds and lineations; thin unbroken lines show trends of second metamorphic folds and lineations.

maps and many lithologic and structural details are available (Compton, 1972, 1975; Todd, 1973).

ROCK UNITS AND LOW-ANGLE FAULTS

The Raft River Mountains expose two major allochthonous sheets that lie one above the other on an autochthon consisting mainly of Precambrian rocks. The Grouse Creek Mountains are similarly composed but include a third, still higher sheet along their western flank (Fig. 2). The Matlin Mountains and other low hills east of the Grouse Creek Mountains expose one or more north-northeast–striking, westward-dipping low-angle faults along which sheets of variably metamorphosed upper Paleozoic limestone and sandstone were carried over thick unmetamorphosed limestone and sandstone of similar age (V. R. Todd, unpub. data). In many places, these thin sheets were emplaced on upper Miocene tuffaceous sandstone and fanglomerate (Fig. 2). The faults are exposed discontinuously for a distance of at least 19 km from north to south and for 11 km from east to west. Similar sheets lie on Tertiary beds at the north end of the Bally Mountains and at several localities in the Grouse Creek Mountains (Fig. 2). Fossils collected by Stanford field students at one of the latter localities include gastropods that were studied and assigned a late Miocene age by James E. Firby (1973, written commun.).

Deformed upper Miocene beds show that the Raft River Mountains formed as a doubly plunging east-trending anticline in Pliocene time and that the Grouse Creek Mountains formed at about the same time by arching and high-angle faulting. Erosion has exposed the autochthon to depths of 900 m in both ranges but has left enough klippen and peripheral patches of the allochthonous sheets so that they can be projected confidently over most of the mapped area.

Although folded in detail, the allochthonous sheets and autochthon are rudely stratified and were more or less horizontal before the mountain ranges formed. Figure 3 shows their total stratigraphic succession as well as the typical positions of the principal low-angle faults. Recumbent folding locally inverted the sequence, and low-angle faulting attenuated it and locally repeated it, but most of the rock units in the figue are generally present in the order shown.

Figure 3, however, is not a stratigraphic column. The thicknesses shown are all maximal for the area but are probably much less than the original sedimentary thicknesses, except for units younger than Mississippian. Solid-state flow caused considerable thinning, as shown by flattened grains and schistose fabrics that generally lie parallel to the subhorizontal layers. This effect varied considerably from place to place and is locally extreme: along the eastern flank of the central Grouse Creek Mountains and the adjoining southern flank of the Raft River Mountains, the total thickness of all units between the basal adamellite and the Fish Haven (?) Dolomite is commonly only 100 m.

Another important cause of thinning was faulting along surfaces that cut across stratigraphic units at low angles, displacing strata of the hanging wall onto older rocks. This is shown on a large scale by the middle sheet, which emplaced the upper part of the Mississippian or the lower part of the Pennsylvanian on Ordovician rocks throughout the north half of the area but includes progressively older Paleozoic units as it is traced southward in the Grouse Creek Mountains (Fig. 4). The feature cannot be a moderately faulted unconformity beneath an onlapping sequence because all of the units are lithologically the same as they are elsewhere in the region. The relation thus implies many tens of kilometres of displacement of the middle sheet. The middle sheet is also subdivided by subsidiary low-angle faults that produced similar but less extreme effects.

The fault at the base of the lower sheet locally rises from the schist of Stevens Spring to the schist of Mahogany Peaks or the marble of the Pogonip Group. The lower allochthonous sheet is cut out entirely in part of the eastern Raft River Mountains, where the Oquirrh Formation lies directly on the autochthon. Subsidiary imbricate thrusts that have locally emplaced older units over younger are associated with strongly overturned folds, as described in the next section.

FOLDS AND LINEATIONS

At least three sets of folds formed during metamorphism, and a fourth, which may locally be divided into several sets, formed after metamorphism. All of the folds plunge at low angles in most places. Axes of the oldest folds define a broad arc that swings from east-northeast in the Raft River Mountaisn to north, even northwest, in the Grouse Creek Mountains (Fig. 2). Almost all the folds are overturned toward the convex (northwest) side of the arc. Exceptions are east-overturned folds at the southern end of the Grouse Creek Mountains, which may not be continuous with folds to the north.

Axes of the second set of metamorphic folds trend northwest to due west in the Grouse Creek Mountains and approximately west in the Raft River Mountains. At scattered localities in the central Grouse Creek Mountains, west-trending metamorphic folds have overprinted northwest-trending folds. Almost all folds of the second set are overturned to the north. Exceptions are northwest-trending metamorphic folds in the lower, and particularly in the middle, allochthonous sheets in the central Grouse Creek Mountains that are overturned to the southwest. Still younger, scarce metamorphic folds (not shown in Fig. 2) trend northeast and are overturned toward the southeast, and in parts of the central Raft River Mountains late metamorphic folds of this trend are overturned toward the northwest.

The metamorphic folds range from upright to recumbent, most being strongly overturned. The largest are recumbent and measure 0.5 to 1.5 km from anticlinal hinge to adjoining synclinal hinge. These large folds are typically solitary or in couplets, with rock layers extending nearly unaffected for many kilometres in front of the folds or behind them. Hinges of the most prominent folds in the Raft River Mountains can be followed for 22 km in the autochthon. Only a few folds of comparable size occur elsewhere, but the numbers of smaller folds increase exponentially with decreasing fold size, such that folds with wavelengths of about 1 m can be seen at many localities (except in the upper allochthonous sheet), and folds smaller than 5 mm are so abundant as to impart a pervasive and characteristic linear ridging or striping to surfaces of many quartzite and marble layers. Other linear elements parallel to these small folds include flattened and elongated pebbles, triaxial quartz and calcite grains, prismatic kyanite and hornblende grains, elongated mica plates, and open-space fillings (typically calcite) on two sides of pyrite crystals.

The postmetamorphic folds (not shown in Fig. 2) have a variety of forms and trends, suggesting that movements at that stage were complex and localized. The largest of these folds in the western Raft River Mountains are probably of the same age as the youngest metamorphic folds in the central Grouse Creek Mountains. Their sense of transport could be determined 14 km southwest of Yost, where a fan-shaped array of large folds that are overturned generally toward the east is cut by imbricate thrusts with the same sense of transport (Compton, 1972). Six kilometres northeast of Yost, folds of approximately the same age have strongly deformed the middle low-angle fault and subsidiary low-angle faults in the lower sheet.

Recumbent north-trending folds in the middle allochthonous sheet of the central Grouse Creek Mountains are probably of the same age as those just mentioned but formed where metamorphism was still in its waning stages. They measure as much as 0.5 km from anticlinal hinge to synclinal hinge, are overturned to the east, and are cut by imbricate thrusts displaced toward the east.

Postmetamorphic folding also affected the autochthon widely but by no means universally. The folds range from slight rolls and crimps to open chevron folds overturned to the east. None have

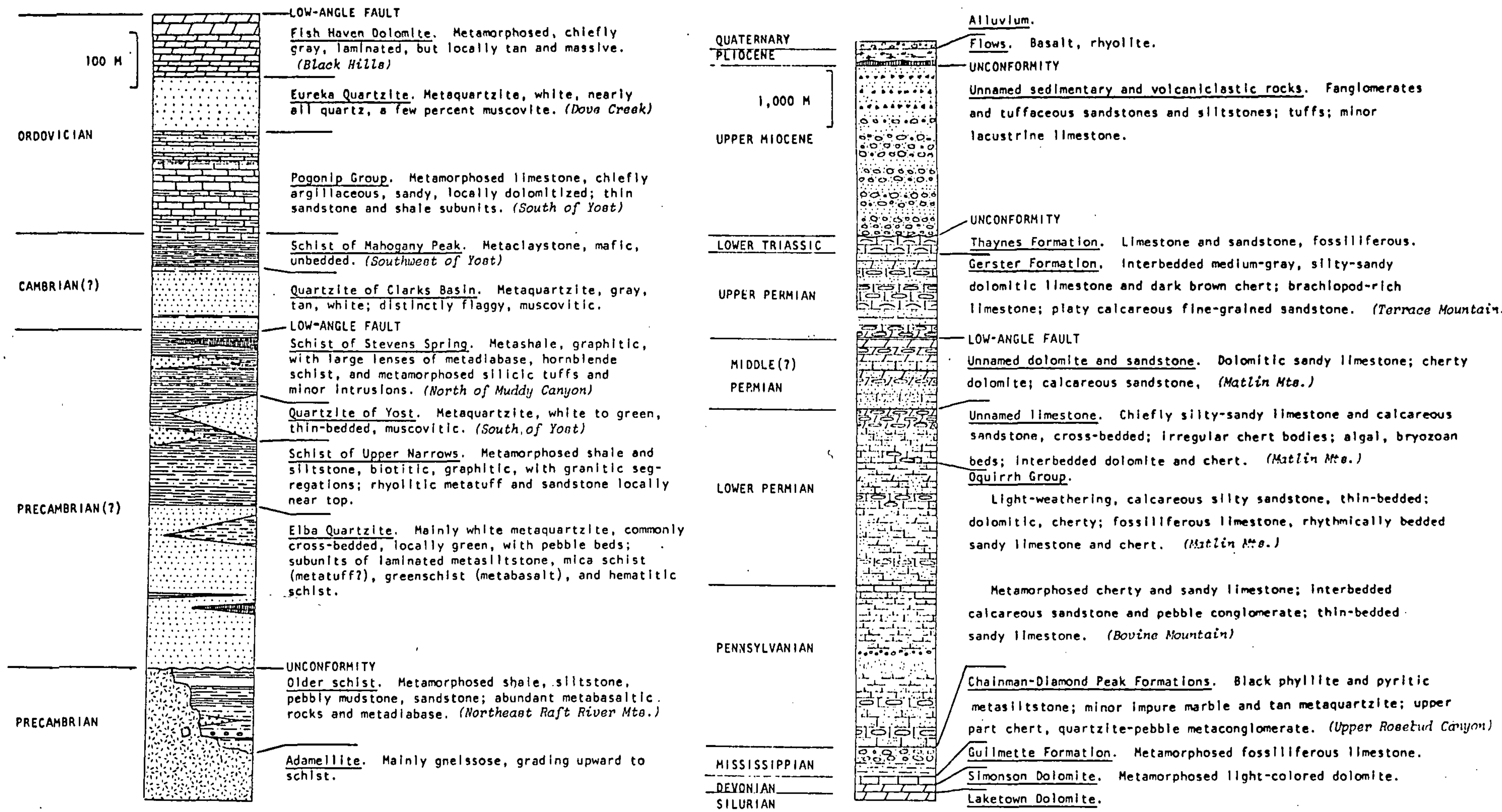

Figure 3. Sequence of rock units in area studied. Not shown are Tertiary granitic rocks, which intruded units as young as Permian. Note that scale on right-hand column is one-tenth that on left.

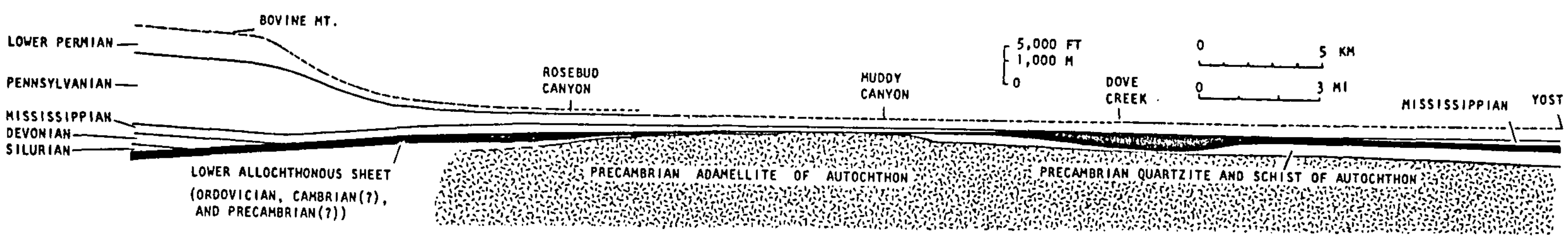

Figure 4. Partly reconstructed north-south vertical section from west end of Raft River Mountains to south end of Grouse Creek Mountains, at natural scale, showing stratigraphic composition of middle allochthonous sheet. Lower sheet and units in autochthon are shown virtually as they are now, but units in middle sheet south of Rosebud Canyon have been reconstructed from greatly folded and faulted fragments.

wavelengths of more than 1 m, and all trend between N30°W and N30°E.

METAMORPHIC VARIATIONS

Vertical and lateral variations in metamorphic grade due to temperature differences help greatly in interpreting the deformations. The general vertical variations are as follows: (1) the upper allochthonous sheet is not metamorphosed; (2) the middle sheet is not metamorphosed in some places, but in others shows an increasing degree of low-grade metamorphism downward; and (3) the lower sheet and the autochthon are metamorphosed, with metamorphic grades generally increasing downward. Table 1 lists the principal mineral assemblages for the highest grade part of each unit. Because parts of the sheets were displaced after metamorphism, the tabulated section is a reconstructed metamorphic sequence for the most heated part of the area at the peak of prograde metamorphism. Textures indicate that the minerals in each assemblage coexisted at that time, whether or not true equilibria were attained. Except for the fine-grained schists of the Oquirrh and Chainman or Diamond Peak Formations, most mineral grains are between 0.05 and 5 mm in diameter.

The lateral variations in metamorphic grade are simplest in the autochthon: the highest grade rocks are in the western part of the area and the lowest grade in the eastern part. The pre-adamellite schists have not been studied in enough places to be meaningful, but in the west the amphibolite consists of hornblende, intermediate plagioclase, and garnet and in the east of finer grained hornblende, epidote, albite, and chlorite. The Precambrian adamellite, which has been studied more extensively, has the prograde assemblage listed in Table 1 in the Grouse Creek Mountains, and it has the assemblage microcline–quartz–albite–white mica–epidote–biotite throughout the east half of the Raft River Mountains. The adamellite is distinctly gneissose in the Grouse Creek Mountains, with few igneous textural relics, but changes gradually eastward to less foliated varieties with many igneous textural relics.

TABLE 1. MINERAL ASSEMBLAGES IN HIGHEST GRADE PARTS OF ROCK UNITS IN GROUSE CREEK AND RAFT RIVER MOUNTAINS

Rock unit	Original rock	Metamorphic minerals
Oquirrh Formation	Silty limestone	Calcite, dolomite, quartz, colorless mica, relict detrital feldspars
Diamond Peak Formation	Shale	Colorless mica, quartz, biotite, chloritoid, graphite
Fish Haven(?) Dolomite	Dolomite	Dolomite, quartz, colorless mica, tremolite, relict K-feldspar
Eureka(?) Quartzite	Sandstone	Quartz, colorless mica
Pogonip Group	Sandy, clayey limestone	Calcite, dolomite, zoisite, calcic plagioclase, colorless mica, biotite, quartz
Schist of Mahogany Peaks	Mafic shale	Colorless mica, staurolite, garnet, biotite, quartz
Quartzite of Clarks Basin	Feldspathic sandstone	Quartz, colorless mica, kyanite, chloritoid (locally biotite and garnet)
Schist of Stevens Spring	Shale	Colorless mica, quartz, biotite, garnet, oligoclase, graphite
	Basalt	Green hornblende, plagioclase
	Granite porphyry	Quartz, K-feldspar, oligoclase, colorless mica, biotite
Schist of Upper Narrows	Shale	Biotite, colorless mica, quartz, K-feldspar, oligoclase
Elba Quartzite	Feldspathic sandstone	Quartz, colorless mica, biotite, K-feldspar, plagioclase
Older Precambrian units	Adamellite	Oligoclase, orthoclase, quartz, biotite
	Gabbro	Green hornblende, intermediate plagioclase, garnet, quartz
	Shale	Biotite, quartz, oligoclase, garnet (altered metasomatically during late metamorphism to assemblages with kyanite, staurolite, andalusite, sillimanite)

Note: Minerals listed in order of decreasing abundance.

Lateral changes of the Elba Quartzite have been studied in 130 thin sections. Where the rock shows its highest grade assemblage, in the central part of the Grouse Creek Mountains, quartz grains are nearly equant polyhedra, and white mica and biotite form distinct plates. Toward the east, biotite disappears, quartz grains are more flattened and irregular, and white mica is finer grained and more irregular. Near the east end of the Raft River Mountains, quartz and feldspar grains larger than 0.5 mm commonly have the shapes of relict sand grains, some even preserving diagenetic overgrowths. Quartz grains also show an increasing amount of postcrystallization strain toward the eastern part of the area.

In the schist immediately above the Elba Quartzite, biotite is coarser (0.2 to 0.7 mm) in the western part of the area than in the eastern part (where it is 0.01 to 0.05 mm), and the degree of granulation during recrystallization increases toward the east. Schist of the Upper Narrows in the eastern part of the Raft River Mountains has assemblages such as chlorite–white mica–albite–quartz and albite-quartz-biotite-epidote, which contrast with the western assemblages (Table 1).

The lower allochthonous sheet also varies laterally in metamorphic grade, being highest in grade in the western Raft River Mountains, about 12 km northeast of the highest grade part of the autochthon (Fig. 5). Especially recognizable are variations within the Pogonip Group, which is coarsely porphyroblastic marble where it

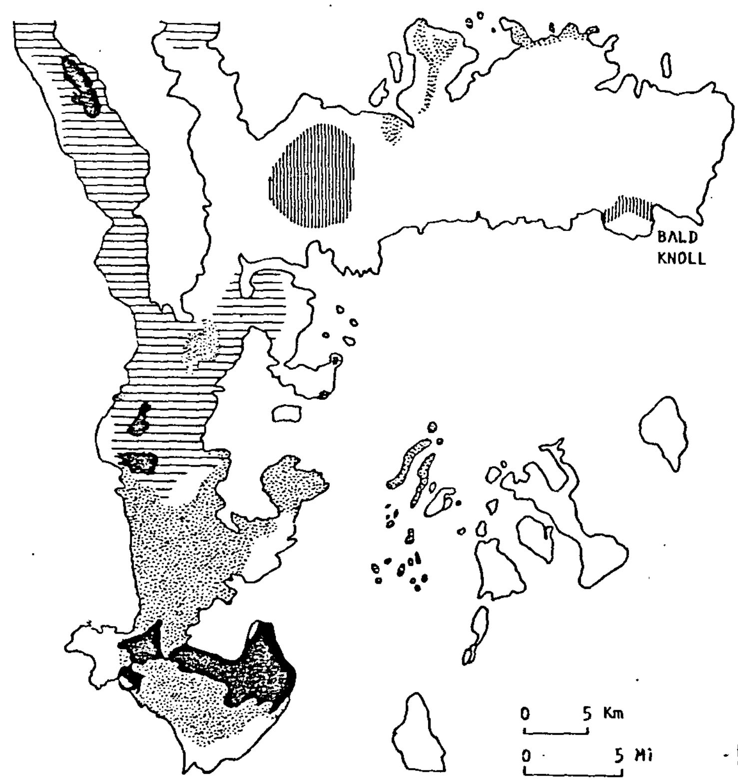

Figure 5. Locations of highest grade parts of autochthon (horizontal lines) and of lower allochthonous sheet (vertical lines). Dots show where Oquirrh Formation of middle sheet is metamorphosed. Tertiary plutons show in black. Outcrop is same as that of Figure 2.

contains high-grade minerals (Table 1) but changes to the southwest and to the east. White mica is the only new metamorphic mineral in marble of intermediate grade, and the lowest grade rocks, near the east end of the Raft River Mountains, contain abundant relics of sedimentary grains, including shredded white mica. An important exception is a high-grade outlier at Bald Knoll (Fig. 5). Variations in other Cambrian(?) and Ordovician units are consistent; the schist of Mahogany Peaks loses its large staurolite and garnet grains to the south, east, and west, and white mica grains in the Eureka(?) Quartzite and Fish Haven(?) Dolomite become smaller in the same directions, again except for the outlier at Bald Knoll.

The Mississippian rocks of the middle sheet are metamorphosed everywhere, but the Oquirrh Formation is metamorphosed only locally (Fig. 5). Gradations within the Oquirrh from metamorphosed to unmetamorphosed rocks are well exposed in the central and southern Grouse Creek Mountains.

In view of the systematic variations of metamorphic grade in the autochthon and the allochthonous sheets, and considering the thinness of the lower sheet, the distribution of high-grade rocks shown in Figure 5 is provocative. The high-grade rocks of the lower sheet at Bald Knoll are 30 km east of the high-grade part of the autochthon and lie on some of the lowest grade rocks of the autochthon. Likewise, the metamorphosed Oquirrh of the middle sheet lies on low-grade rocks of the lower sheet along the north side of the Raft River Mountains and in the central Grouse Creek Mountains. Unmetamorphosed Oquirrh rocks lie directly on the most metamorphosed part of the lower sheet, and, near Vipont Mountain, they lie only 100 m, vertically, from the highest grade rocks of the autochthon. These relations indicate major low-angle faulting after metamorphism or late in metamorphism, with a large resultant transport from west to east. The isolated occurrence of higher grade rocks in the lower sheet at Bald Knoll also indicates separate movement of a subsidiary part of the lower sheet. Separate movements of subsidiary sheets are also suggested by metamorphic relations around Tertiary stocks of the Grouse Creek Mountains, as will be discussed when the dating of the stocks is described.

DATING OF PRECAMBRIAN ADAMELLITE

Precambrian adamellite was sampled for dating near the east end of the Raft River Mountains and in the central Grouse Creek Mountains, in the lowest and highest grade parts, respectively, of the autochthon. Exposures elsewhere show that similar adamellite extends under all or most of the mapped area, and studies by Armstrong (1968a) of the Albion Range show that similar rock extends at least 38 km northward from the western part of our area.

Clear Creek Canyon

Adamellite is well exposed from its contact with older rocks, 5 km from the mouth of Clear Creek Canyon (Fig. 2), to the canyon head, 6 km to the southwest (Compton, 1975). Five samples for dating were collected at various places along the canyon, starting 1 km west of the contact with the older schist and extending 4 km southwest. Throughout the east half of the Raft River Mountains the rock is typically homogeneous and nearly granular, with a weak metamorphic foliation and lineation. Feldspar phenocrysts, as long as 3 cm, are typically sparse but locally abundant; otherwise the grain size is typically 1.5 mm. Contacts with the older rocks are sharp in most places, although metashales are feldspathized locally for as much as 10 m from the adamellite. In several places the adamellite grades outward to a porphyroaphanitic border zone against older mafic igneous rocks. The irregular boundary is apparently a chilled margin, suggesting a shallow emplacement of the adamellite in this part of the area.

The adamellite is dominantly hypidiomorphic granular, with plagioclase distinctly subhedral although altered to albite, white mica, and Fe-poor epidote. Metamorphism deformed and recrystallized quartz, recrystallized biotite into scaly aggregates, recrystallized single sphene grains into aggregates, and formed epidote in the foliated parts of the rock. Small amounts of postmetamorphic alteration are shown everywhere by minute cracks filled with very fine grained Fe-smectite(?).

The analytical data are plotted on a Rb-Sr diagram in Figure 6. The samples define only a poor linear array, and a least-squares regression line yields an age of 2,180 ± 190 m.y. The high $^{87}Sr/^{86}Sr$ intercept (0.764) may reflect either a later disturbance of the rock chemistry or a crustal contribution to the initial strontium in the magma. We cannot distinguish uniquely between these two possibilities, but the generally older ages of 2.5 b.y. or greater for basement rock throughout the Wyoming province (Condie, 1969; Reed and Zartman, 1973) and the substantial degree of alteration shown by these rocks causes us to suspect postcrystallization open-system conditions. Furthermore, the adamellite has appreciably higher Rb/Sr ratios than other analyzed Precambrian rocks in the vicinity — a factor often found to correlate with age modification during subsequent metamorphism and weathering.

Fission-track ages on the Precambrian adamellite and associated rocks of the Raft River Mountains indicate metamorphism of Tertiary age followed by exceptionally rapid cooling. Sphene and apatite from adamellite sample CC-1 (Table 2) gave annealing ages of 20 ± 10 m.y. for sphene and 20 ± 4 m.y. for apatite; (the ± values are 2σ and $\lambda_F = 6.85 \times 10^{-18}$ yr^{-1}). A second sample is from the older schist 100 m above an intrusive contact with Precambrian adamellite at lat 41°55′46″N, long 113°19′59″W, which is 2.6 km southeast of locality CC-1. This sphene gave an age of 10.2 ± 1.9 m.y., and the apatite 12.4 ± 2.4 m.y. A sample of Pogonip marble metamorphosed to schist consisting mainly of epidote, quartz, potassium feldspar, biotite, calcite, and colorless mica was collected 30 m above the base of the lower allochthonous sheet, at the northwest edge of the Black Hills (lat 41°50′18″N, long 113°33′31″W). The apatite has a very low uranium content (0.4 ppm) but gave an age of 46 ± 26 m.y. for one determination and 69 ± 32 m.y. for another.

Annealing of fission tracks in sphene takes place at temperatures of about 400 °C (Calk and Naeser, 1973) if the temperatures are sustained for geologically significant periods — greater than 10^6 yr. Apatite is annealed of fission tracks if temperatures above 100 °C are sustained for 10^6 yr or more (Naeser and Faul, 1969). The fission-track ages of the sphenes thus suggest that the rocks in and around Clear Creek Canyon were at metamorphic temperatures as recently as Miocene time. The quartzites in that part of the range have strongly preferred crystallographic fabrics that are coaxial

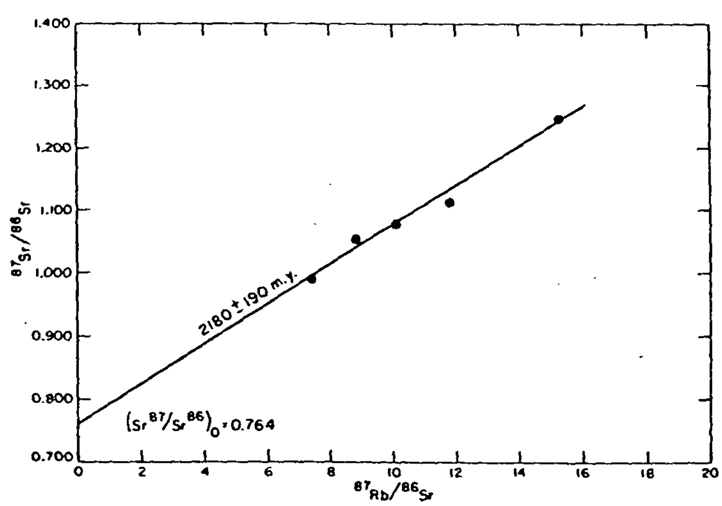

Figure 6. Plot of Rb-Sr isotopic data from adamellite of Clear Creek Canyon, Raft River Mountains. Data are listed in Table 2.

with large recumbent folds of the second metamorphic set, and they also show abundant features produced by postcrystallization strain. Evidently, the east-west-trending folds were still forming in Miocene time, and the close similarity of the sphene and apatite ages for each rock suggests that the rocks then cooled rapidly.

The older ages for the apatites from the Black Hills cannot be interpreted firmly because they are very approximate and because the sample is from an allochthonous sheet that probably moved many kilometres after metamorphism. The data show, nonetheless, that some parts of the terrain cooled well before others. This is supported by data of Armstrong and Hansen (1966, p. 123), who reported K-Ar ages of biotites from two autochthonous rocks of the Raft River Mountains. A sample of Precambrian adamellite from Clear Creek Canyon, about 2.5 km southwest of our CC-1, gave an age of 57 + 8/−3 m.y., and a sample of older schist (possibly schistose adamellite) from Big Hollow, 5 km east of the Black Hills, gave an age of 38 + 6/−2 m.y. for one biotite split and an age of 41 + 6/−2 m.y. for a second split.

Central Grouse Creek Mountains

The contact between the Precambrian adamellite and younger quartzites and schists is a metamorphosed unconformity throughout the Raft River and the northern Grouse Creek Mountains, but in the central Grouse Creek Mountains, adamellite appears to intrude quartzite and schist. In Muddy Canyon, thin sills of adamellite gneiss and schist occur between beds of Elba Quartzite, and bedded quartzite forms concordant inclusions in the upper 100 m of adamellite. The upper contact of the adamellite cuts across upper Precambrian(?) units of the autochthon into the lower allochthonous sheet at a low angle (Fig. 4). The youngest unit intruded by Precambrian adamellite is Cambrian(?) quartzite of Clarks Basin. Partly granitized, contorted schist inclusions are notably abundant in the upper part of the adamellite, suggesting that the missing section was in part downfolded and incorporated by mobilized adamellite.

The Elba Quartzite thins from 215 m about 2.5 km north of Muddy Canyon to 6 m in the north wall of the canyon (Fig. 4). Equally striking are the thinning by metamorphic flow and low-angle faulting of all metasedimentary rocks of the autochthon and of the lower allochthonous sheet above the area of mobilized adamellite.

The adamellite of the central Grouse Creek Mountains shows a systematic change in texture upward, from coarse- and medium-grained gneiss in the lowest exposures to fine-grained gneiss and schist in the upper part, about 920 m above the base of the range. Textures indicate simultaneous deformation and recrystallization. Similarly, numbers of relict igneous grains decrease upward, and phengitic white mica, quartz, albite, iron-poor epidote, and sphene increase upward, as the higher temperature oligoclase-orthoclase-quartz-biotite assemblage is replaced. Under the Elba Quartzite is a zone about 6 m thick in which medium-grained adamellite grades upward through feldspathic schist of adamellite composition to phengite-quartz-albite schist (Fig. 7). It is noteworthy that these schists contain the same accessory minerals, principally allanite and dark red-brown metamict zircon, as the less altered adamellite below. Locally, the metamict zircon in the schists bears partial jackets of colorless birefringent zircon.

Adamellite in the central Grouse Creek Mountains was folded twice during metamorphism. Recrystallized mineral aggregates form two prominent lineations oriented parallel to the two fold sets. The earlier lineation (northeast to north-northwest-trending) consists of quartzofeldspathic rods, elongate biotite aggregates, and parallel crenulations 0.5 to 1 cm wide lying in the foliation plane, in deeper lying exposures. Wavelengths of the crenulations and widths of the linear mineral aggregates decrease upward; near the top of the range they are typically only a few millimetres wide. This decrease is part of an increase in deformation and recrystallization. In deeper lying rocks, the second (northwest to west-northwest) lineation consists of subhedral biotite grains that cross the earlier coarser biotite aggregates and, in thin section, appear to have recrystallized from them. In the reconstituted upper shell of the adamellite and in rocks surrounding the two small Tertiary stocks on the west side of the range (roughly the upper 185 m of adamellite), the second lineation consists of quartz-feldspar rods, biotite aggregates, and distinct crenulation, and the first lineation is present only as faint wrinkling. These relations suggest two important points: (1) strain and recrystallization increased upward in the

TABLE 2. Rb-Sr ISOCHRON AGES OF WHOLE-ROCKS FROM PRECAMBRIAN ADAMELLITE, NORTHWESTERN UTAH

Sample no.	Lat (N)	Long (W)	Rb (ppm)	Sr_n (ppm)	$^{87}Rb/^{86}Sr$	$^{87}Sr/^{86}Sr$	Age (m.y.)*
Clear Creek Canyon							
CC-1	41°56′50″	113°21′07″	297.2	75.5	11.85	1.113	
CC-2	41°55′57″	113°22′49″	275.4	110.7	7.40	0.9908	
CC-3	41°56′00″	113°22′43″	257.6	86.9	8.87	1.055	2,180 ± 190
CC-5	41°56′31″	113°22′02″	271.1	80.3	10.12	1.077	
CC-6	41°56′43″	113°21′32″	293.7	58.5	15.30	1.248	
Central Grouse Creek Mountains							
9W-97-19A	41°41′21″	113°44′20″	83.4	144.2	1.684	0.7679	
9W-97-19B	41°41′21″	113°44′20″	111.7	138.3	2.360	0.7998	
9W-97-19C†	41°41′21″	113°44′20″	240.9	152.4	4.629	0.8263	
9W-97-21	41°41′32″	113°44′23″	166.2	98.2	4.988	0.8883	
9W-97-26	41°41′23″	113°41′22″	101.5	148.2	1.998	0.7902	
9W-97-28	41°40′18″	113°44′34″	124.9	141.3	2.582	0.8111	
10W-21-1A†	41°45′10″	113°41′19″	184.7	77.3	6.990	0.8208	2,510 ± 170
10W-21-1B†	41°45′10″	113°41′19″	150.2	28.8	15.24	0.8048	
10W-21-4A	41°45′03″	113°41′10″	126.7	109.3	3.396	0.8222	
10W-21-4B	41°45′03″	113°41′10″	141.3	121.9	3.399	0.8368	
10W-23-1	41°43′36″	113°42′04″	129.8	109.2	2.488	0.8456	
10W-23-2A	41°43′33″	113°42′23″	170.0	138.0	3.613	0.8391	
10W-23-2B	41°43′33″	113°42′23″	123.4	136.7	2.638	0.8014	

* Calculated from least-squares regression method of York (1966). See graphic representation of these data in Figures 6 and 8. Decay constant $\lambda_\beta = 1.39 \times 10^{-11} yr^{-1}$.

† Samples not included in calculation of age.

adamellite when the first folds and lineations formed, and (2) recrystallization of minerals during the second folding reached a maximum in rocks adjacent to, and lying above, the Tertiary stocks.

In the central part of the Grouse Creek Mountains, Precambrian adamellite is interlayered with lesser amounts of granodiorite, tonalite, and leucocratic gneiss. Suites of these four rocks were collected from three areas for dating. Three medium-grained gneisses representative of deeper exposures are from Middle Canyon (Fig. 2). Six fine-grained samples, typical of the upper part of the gneiss, were collected on Ingham Peak, which is 4 km southwest of Middle Canyon. Four samples of metasomatically altered gneiss and schist are from Muddy Canyon, where the intrusive-appearing contact of Precambrian adamellite with the Elba Quartzite is well exposed (Fig. 7). The samples are listed below by locality.

Middle Canyon. Sample 10W-23-1 is medium-grained tonalite gneiss, 10W-23-2a is medium- to coarse-grained adamellite gneiss (the typical adamellite of the gneiss complex), and 10W-23-2b is medium-grained muscovitized granodiorite gneiss.

Ingham Peak. Samples 9W-97-19a, b, and c were collected from a typical outcrop of interlayered adamellite and mafic gneiss from the highest peak of the central Grouse Creek Mountains. Sample 9W-97-19c is from a thin gneissic granitic pegmatite layer in fine-to medium-grained adamellite gneiss, the rock of sample 9W-97-19b. Sample 9W-97-19A is fine- to medium-grained granodiorite gneiss from an adjoining mafic layer and was collected 10 cm from 9W-97-19b. Sample 9W-97-21 is adamellite gneiss from a site about 610 m north of 9W-97-19, 9W-97-26 is muscovitized adamellite gneiss collected 92 m north of 9W-97-19, and 9W-97-28 is leucoademellite gneiss from a site about 2,200 m south of 9W-97-19. All three samples are fine to medium grained.

Muddy Canyon. Samples 10W-21-1a and 1b are phengite-quartz schists collected adjacent to an inclusion of Elba Quartzite 1.8 m below the contact between mobilized Precambrian adamellite and Elba Quartzite. The inclusion consists of several thin beds, in all 10 cm thick, that lie parallel to the foliation of the schist. Sample 10W-21-1b was 0.6 m above the quartzite inclusion, and sample 10W-21-1a lay about 0.5 m below it. Samples 10W-21-4a and 4b were collected about 7.5 m below the contact between the Elba Quartzite and Precambrian adamellite. Sample 10W-21-4b is fine- to medium-grained muscovitized adamellite gneiss, and sample 10W-21-4a is a 30-cm, concordant fine- to medium-grained leucoadamellite dike in 10W-21-4b. This series of samples is representative of the border zone of the Precambrian adamellite in which muscovitized adamellite gneiss grades upward through feldspathic schist to phengite-quartz schist (Fig. 7).

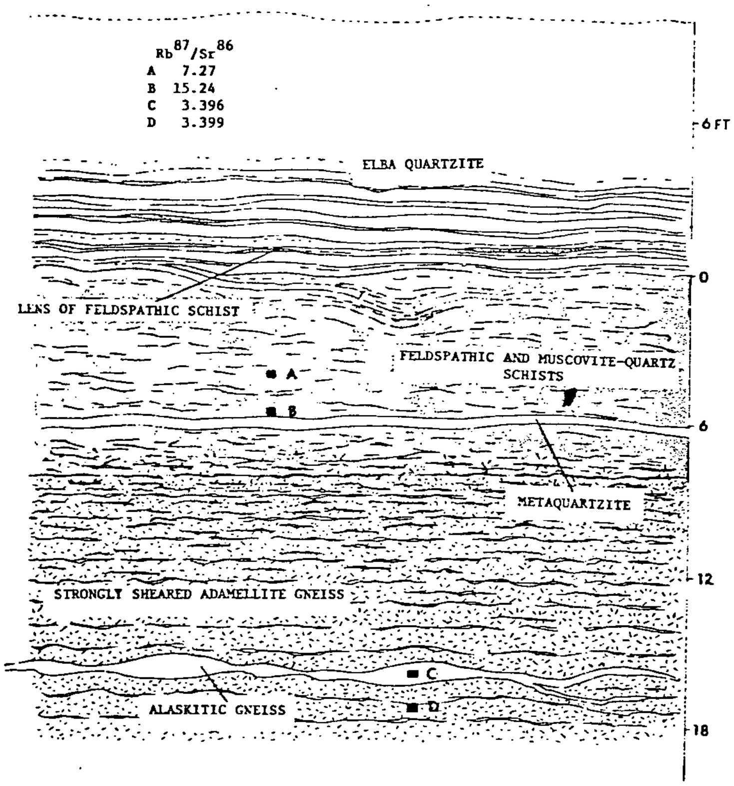

Figure 7. Diagrammatic section through upper part of Precambrian adamellite and Elba Quartzite in Muddy Canyon, showing gradation from gneiss to schist, interposition of schistose adamellite in quartzite, and isotope ratios determined from samples from positions indicated.

Although we originally interpreted the adamellite of the central Grouse Creek Mountains to be Phanerozoic, the Rb-Sr diagram (Fig. 8) reveals an old Precambrian age. A whole-rock isochron age of 2,510 ± 170 m.y. was obtained from our data, excluding the two schistose rocks (10W-21-1a and 1b) associated with the metaquartzite in Muddy Canyon and the pegmatite (9W-97-19c) from Ingham Peak. The ten remaining samples show approximately the same degree of scatter as those from the Clear Creek Canyon locality despite their being more metamorphosed. Indeed, the somewhat older age and lower $^{87}Sr/^{86}Sr$ intercept seem to suggest a more restricted isotope redistribution in these rocks. In particular, the closely adjoining adamellite gneiss (9W-97-19b) and granodiorite gneiss (9W-97-19a) gave no evidence of strontium isotope homogenization between the two layers. The granitic pegmatite layer (9W-97-19c), which intrudes the adamellite gneiss, however, either has undergone exchange or possibly is slightly younger.

The only samples that have obviously undergone major chemical reconstitution are the phengite-quartz schists (10W-21-1a and 1b) within the immediate border zone between the basement rocks and the overlying Elba Quartzite. The schistose rocks have similar strontium isotope compositions but appreciably higher Rb/Sr ratios and, consequently, younger ages than the gneiss. We do not know whether this effect arises from metamorphic differentiation in the extremely sheared rock or from a mechanical mixing with the younger mantling rocks. The other, less deformed samples (10W-21-4a and 4b) from Muddy Canyon show little disturbance of their Rb-Sr systems even though they have recrystallized. The relations between the rheomorphic and chemical responses of the basement rock have not been adequately resolved by this study; they remain an interesting and important subject for further work.

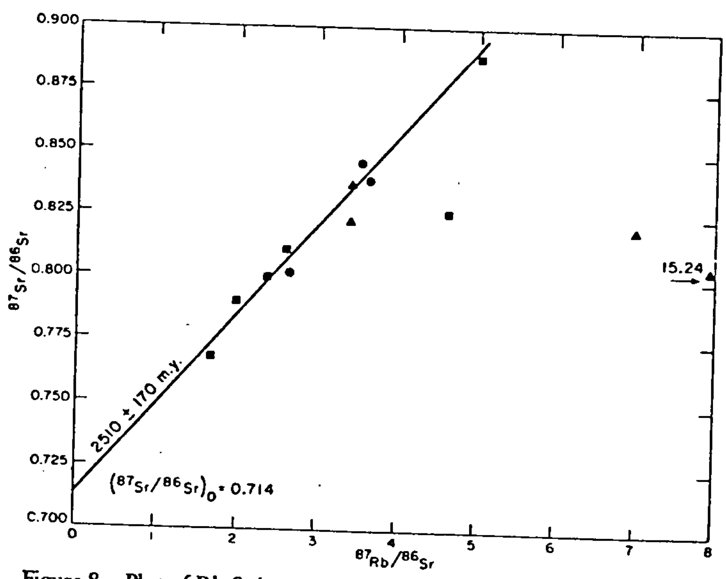

Figure 8. Plot of Rb-Sr isotope data from gneissose to schistose adamellite of central Grouse Creek Mountains. Data are listed in Table 2. Circles = Middle Canyon; squares = Ingham Peak; triangles = Muddy Canyon.

In order to determine whether the individual mineral grains had equilibrated isotopically among themselves within a hand specimen, the plagioclase, microcline, and biotite were analyzed from two of the samples (9W-97-21 and 10W-23-2a). The results, together with those of the whole-rock analyses, are given in Table 3. On this scale the minerals have rather recently attained internal homogenization of their strontium isotopes. Only the biotite with its very high Rb/Sr ratio has evolved isotopically to a significant extent after homogenization. Assuming that the biotite did indeed fully participate in the exchange, we were able to calculate biotite whole-rock ages of 11.9 and 8.0 m.y. on these samples. If our assumptions are correct, the results indicate that chemical mobility and, presumably, elevated temperatures persisted in late Miocene time in the central Grouse Creek Mountains, a situation similar to that indicated by the fission-track ages in the eastern Raft River Mountains.

DATING OF TERTIARY INTRUSIONS

The Grouse Creek Mountains expose several young granitic bodies, shown individually in Figures 2 and 5: (1) at Vipont Mountain, in the northwest corner of the mapped area, (2) two closely spaced stocks in and near Red Butte Canyon in the central part of the range, and (3) the large, probably multiple intrusion near the south end of the range at Immigrant Pass.

Vipont Mountain Intrusion

The lineated granodiorite and adamellite of Vipont Mountain intruded all of the rock units in the lower allochthonous sheet but did not intrude the middle sheet. The country rocks dip 5° to 20° west, and the upper contact of the intrusion is roughly concordant with them, being emplaced mainly below the quartzite of Clarks Basin but breaking across this unit toward the south and connecting with thick sills in marble of the Pogonip Group and the schist of Mahogany Peaks (Fig. 9). The upper part of the intrusion and the associated sills somehow engulfed and assimilated much of the stratigraphic section, especially the schist of Mahogany Peaks and the upper part of the quartzite of Clarks Basin. Possibly because of this, the upper part of the intrusion is banded by variably biotitic adamellites, many bearing garnet, whereas the main body of the intrusion is homogeneous garnet-free granodiorite.

Age relations of the intrusion to deformational features are well exposed. The first set of metamorphic folds is developed locally in the country rocks above the intrusion but nowhere in the intrusion. All of the body is lineated parallel to the second set of metamorphic folds and associated lineations in the country rocks. The country rocks are exceptionally high grade near the intrusion, the Pogonip marble bearing garnet and pyroxene, and the schist of Mahogany Peaks being converted to oligoclase-quartz-sillimanite-muscovite-biotite gneiss in which sillimanite and biotite are lineated parallel to the second metamorphic folds. The rocks of the middle allochthonous sheet lying on these high-grade rocks are metamorphosed little, if at all, so this part of the middle sheet must have been emplaced after the intrusion cooled almost completely.

The highest lying adamellite sills are converted in several places to sheets of dark blastomylonite in which rounded relics of igneous feldspar are surrounded by recrystallized, swirled trains of fine-grained quartz, biotite, and feldspar. Because these rocks are strongly lineated parallel to overturned folds of the second metamorphic set, it appears that the allochthonous sheet shown in Figure 2 rode over the intrusion during the second folding episode. This relation indicates low-angle faulting during the second metamorphic folding.

The localities of the analyzed rocks are shown in Figure 9, and their textural and structural features are as follows: sample 4,

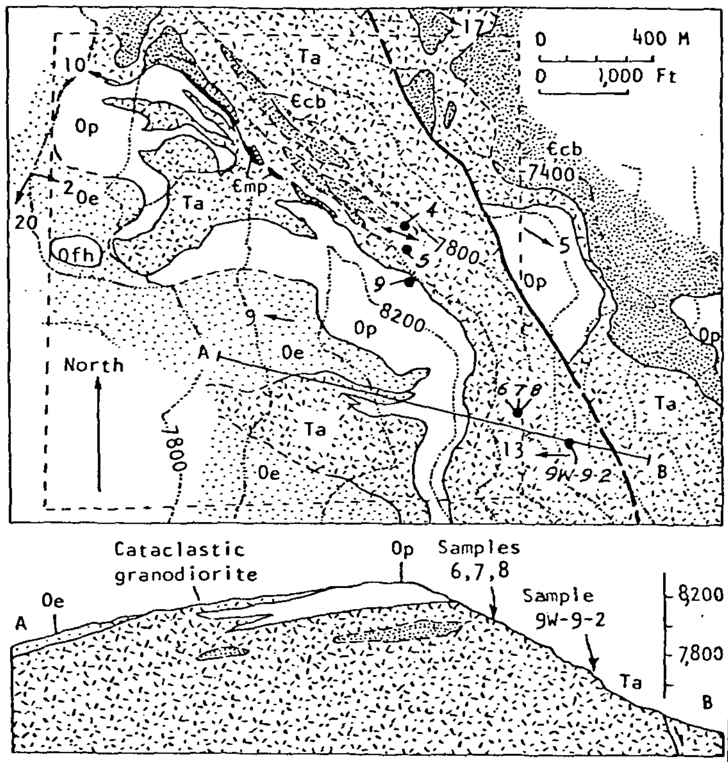

Figure 9. Geologic map and vertical section showing locations of samples used in Rb-Sr studies of Vipont Mountain intrusion. Contours (dotted) and outline of Sec. 8, T. 15 N., R. 17 W., are from the Cotton Thomas Basin 15' quadrangle. Arrows show plunges of folds and lineations. Єcb = quartzite of Clarks Basin (Cambrian?) (heavy stipple); Єmp, = schist of Mahogany Peaks (Cambrian?) (black); Op = marble of Pogonip Group (Ordovician) (unpatterned), Oe = Eureka(?) Quartzite (Ordovician) (light stipple); Ofh = Fish Haven(?) Dolomite (Ordovician) (unpatterned); and Ta = Tertiary adamellite and granodiorite (cross-tracked). Cross section, which is enlarged from map, has horizontal and vertical scales equal.

TABLE 3. Rb-Sr BIOTITE–WHOLE-ROCK AGES FROM PRECAMBRIAN ADAMELLITE, NORTHWESTERN UTAH

Sample no.	Lat (N)	Long (W)	Mineral	Rb (ppm)	Sr_n (ppm)	$^{87}Rb/^{86}Sr$	$^{87}Sr/^{86}Sr$	Age (m.y.)*
9W-97-21	41°41'32"	113°44'23"	Plagioclase	184	140	3.9	0.8880	
			K-feldspar	361	120	9.0	0.8897	
			Whole rock	166.2	98.2	4.99	0.8883	11.9 ± 0.
			Biotite	1,056	3.0	1,056	1.063	
10W-23-2A	41°43'33"	113°42'23"	Plagioclase	100	203	1.5	0.8348	
			K-feldspar	294	160	5.5	0.8426	
			Whole rock	170.0	138.0	3.61	0.8391	8.0 ± 0.
			Biotite	917.0	11.6	232.7	0.861	

* Calculated as biotite–whole-rock pairs. Decay constant: $\lambda_\beta = 1.39 \times 10^{-11} yr^{-1}$.

TABLE 4. Rb-Sr ISOCHRON AGES OF WHOLE ROCKS FROM TERTIARY INTRUSIONS, NORTHWESTERN UTAH

Sample no.	Lat (N)	Long (W)	Rb (ppm)	Sr_N (ppm)	$^{87}Rb/^{86}Sr$	$^{87}Sr/^{86}Sr$	Age (m.y.)*
Vipont Mountain							
9W-9-2	41°56'52"	113°48'46"	140	240	1.6	0.7217	
4	41°57'17"	113°49'11"	124.8	171.8	2.105	0.7235	
5	41°57'15"	113°49'10"	150.6	94.7	4.613	0.7308	
6	41°56'56"	113°48'53"	87.7	421.0	0.603	0.7123	Indeterminate
7	41°56'56"	113°48'53"	226.4	20.8	31.64	0.7306	
8	41°56'56"	113°48'53"	231.2	26.5	25.33	0.7276	
9	41°57'12"	113°49'09"	45.2	1,182	0.111	0.7104	
Red Butte Canyon							
9W-47-2A	41°39'47"	113°45'27"	193.0	93.1	6.01	0.7169	
9W-47-2B	41°39'47"	113°45'27"	235.5	5.22	131.2	0.7592	
9W-47-2C	41°39'47"	113°45'27"	240.6	2.36	298.7	0.8180	
9W-47-2D	41°39'47"	113°45'27"	235.5	7.44	92.0	0.7450	24.9 ± 0.6
9W-47-9	41°39'49"	113°45'32"	335.7	22.2	43.8	0.7294	
9W-47-10	41°39'49"	113°45'32"	265.7	8.22	93.5	0.7427	
Immigrant Pass							
9W-39-1	41°30'52"	113°44'59"	103.8	285	1.05	0.7102	
9W-39-2	41°31'01"	113°45'07"	246.2	6.34	112.3	0.7716	
9W39-3	41°30'58"	113°45'05"	362.1	7.16	146.4	0.7860	
9W-40-2	41°32'07"	113°45'58"	210.0	40.7	14.94	0.7184	38.2 ± 2.0
13W-167-3	41°31'44"	113°41'48"	205.0	15.4	38.60	0.7282	
13W-167-4	41°31'37"	113°41'57"	152.2	56.4	7.82	0.7140	

* Calculated from least-squares regression method of York (1966). See graphical representation of these data in Figures 10 and 12. Decay constant: $\lambda_\beta = 1.39 \times 10^{-11} yr^{-1}$.

lineated adamellite from a 2.5-m sill in quartzite of Clarks Basin; sample 5, lineated adamellite from a thick sill near or at the base of the marble of the Pogonip Group; sample 6, typical lineated granodiorite from the lower more homogeneous part of the intrusion; sample 7, muscovite-bearing leucoadamellite, part of a 1-m-thick vertical dike in the rock of sample 6, moderately lineated parallel to the folds of the second metamorphic set; sample 8, muscovitic leucoadamellite from another part of the same dike as sample 7; sample 9W-9-2, granodiorite much like sample 6 but more deformed; and sample 9, marble of the Pogonip Group, 30 m south of the locality of sample 5.

An attempt to define an age for the granitic body from Vipont Mountain has not been successful. Most of the analytical data given in Table 4 and shown in Figure 10 crudely mimic an ~500-m.y. isochron, but the pluton intrudes rocks younger than that. The leucoadamellite dike rock, which, from its high Rb/Sr ratio, appears to have undergone considerable differentiation relative to the main igneous mass, seemingly records a much younger age. Field and petrographic relations suggest that the ~500-m.y. age was largely inherited by the igneous rocks during assimilation of lower Paleozoic rocks of the lower allochthonous sheet. If the Rb and Sr so derived were not significantly fractionated in the process, an approximate lower Paleozoic isochron age could be transferred to the granite. The range in $^{87}Rb/^{86}Sr$ ratio so incorporated would impart a highly variable initial strontium isotope composition to the magma. Assuming, for example, a Tertiary age for the intrusion, the $^{87}Sr/^{86}Sr$ ratio would vary between 0.710 and 0.730. Because of this uncertainty in initial strontium isotope composition, we cannot precisely date even the two apparently differentiated leucoadamellite samples (7 and 8). If these rocks experienced no postcrystallization disturbance, we can only broadly establish their age as lying between 0 and 50 m.y., depending on what initial isotopic composition we choose to assume. This extreme involvement of the allochthonous and perhaps the autochthonous rocks in the generation of the magma without subsequent thorough homogenization and differentiation does not exist in the other Tertiary intrusions to be discussed.

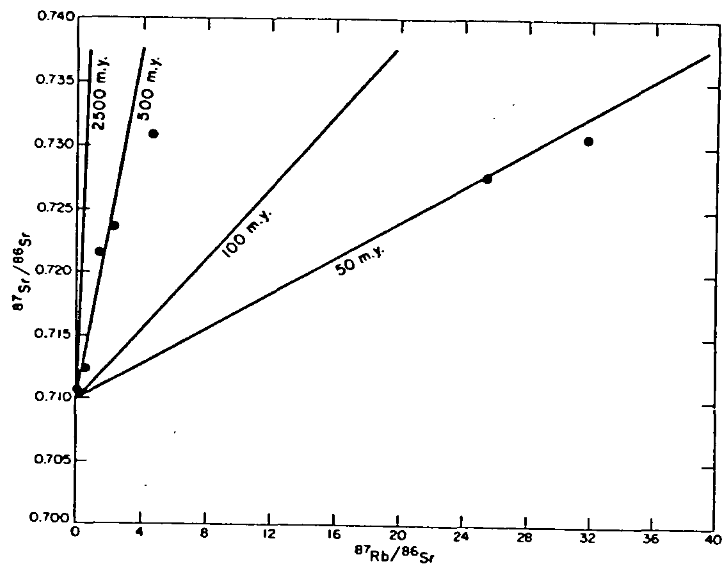

Figure 10. Plot of Rb-Sr isotope data from Vipont Mountain intrusion, northern Grouse Creek Mountains. Data are listed in Table 4.

Stocks of Red Butte Canyon

The two small Tertiary stocks on the west side of the central Grouse Creek Mountains are cupolas of an adamellite body that lies close to the surface throughout the central part of the range, judging from the distribution of dikes and metamorphism of the surrounding rocks. The upper contacts of the stocks are broadly concordant with bedding in the westward-dipping, metamorphosed lower and middle allochthonous sheets and with foliation in the Precambrian adamellite. Discordant dikes of alaskite and aplite from the stocks are abundant in the Precambrian adamellite and in the lower and middle allochthonous sheets near the stocks.

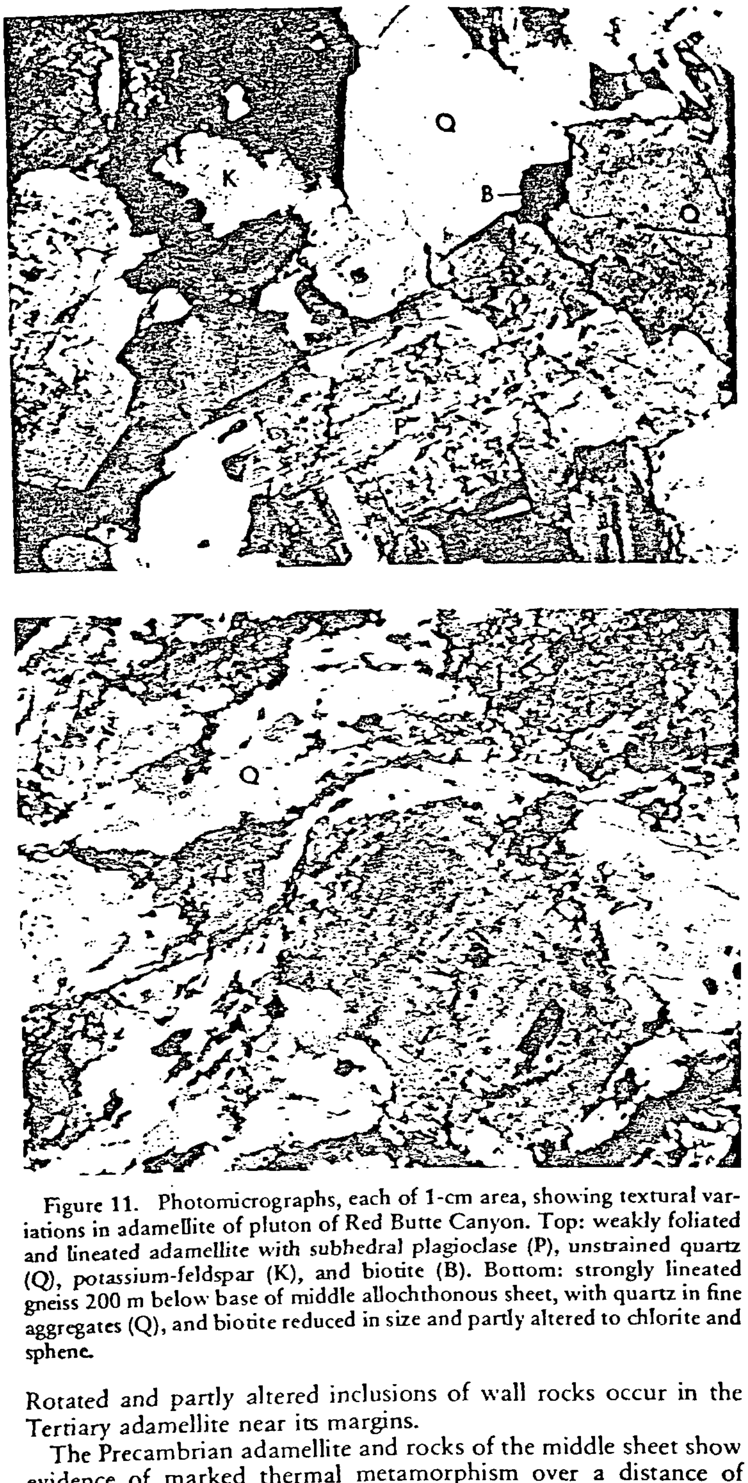

Figure 11. Photomicrographs, each of 1-cm area, showing textural variations in adamellite of pluton of Red Butte Canyon. Top: weakly foliated and lineated adamellite with subhedral plagioclase (P), unstrained quartz (Q), potassium-feldspar (K), and biotite (B). Bottom: strongly lineated gneiss 200 m below base of middle allochthonous sheet, with quartz in fine aggregates (Q), and biotite reduced in size and partly altered to chlorite and sphene.

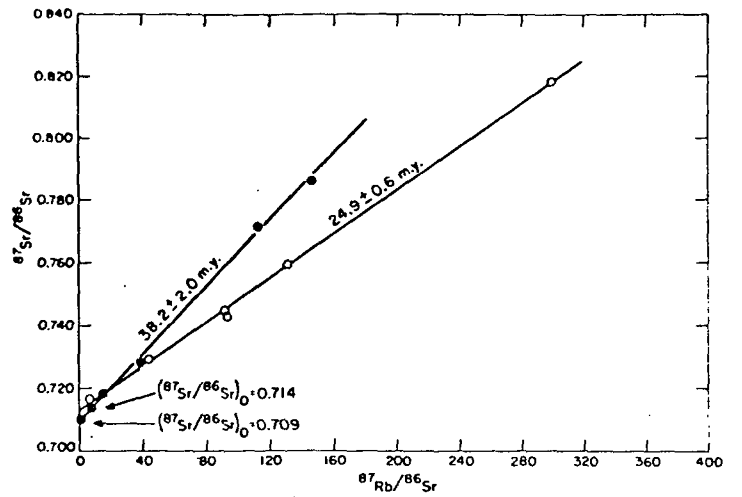

Figure 12. Plots of Rb-Sr isotope data from stocks of Red Butte Canyon and from Immigrant Pass intrusion, Grouse Creek Mountains. Data are listed in Table 4. Open circles = Red Butte Canyon; solid circles = Immigrant Pass.

Rotated and partly altered inclusions of wall rocks occur in the Tertiary adamellite near its margins.

The Precambrian adamellite and rocks of the middle sheet show evidence of marked thermal metamorphism over a distance of about 0.75 km from the stocks. Recrystallization of mineral grains in the Precambrian adamellite parallel to axes of the second metamorphic folds was most intense near the Tertiary stocks. Cherty dolomite of the middle sheet was converted to tremolite, dolomite, muscovite, and diopside(?) in a contact aureole centered approximately over the stocks, indicating that post intrusive displacement was not large on this part of the middle fault. In contrast, the upper sheet, locally only 200 m above the Tertiary body, shows no thermal metamorphism.

Aligned biotite grains define a weak foliation that disappears gradually toward the interior of the adamellite body. A faint west-northwest to east-west lineation composed of quartz and feldspar grains and biotite aggregates can be seen on foliation surfaces and in some thick dikes of alaskite and aplite. These fabric elements parallel the foliation and second metamorphic lineation in the surrounding metamorphic rocks, including the Precambrian gneiss. The biotite fabric and lineation are moderate to strong within 46 m of the Precambrian gneiss (Fig. 11). Over a horizontal distance of 460 m under the middle allochthonous sheet, Tertiary adamellite in Red Butte Canyon is strongly gneissose and markedly lineated by microfolds and mineral grains. A zone of mylonitized adamellite about 3 m thick occurs immediately beneath the middle sheet. Microfolds and strong mineral lineation in the mylonite are parallel to west-northwest–trending folds in overlying tectonitic, thermally metamorphosed dolomite of the middle sheet. Thus, the intrusion and crystallization of the Tertiary adamellite coincided with movement on the middle low-angle fault and with the second metamorphic folding, but predated emplacement of the upper allochthonous sheet.

Except for the marginal zone, the adamellite is a medium-grained, hypidiomorphic, equigranular rock consisting of oligoclase, quartz, and potassium feldspar in approximately equal volume and roughly 5% biotite. Coarse-grained adamellite with sparse, euhedral, 2- to 4-cm potassium feldspar phenocrysts occurs locally in the inner part of the body. Abundant magmatic features include euhedral feldspar phenocrysts, synneusis aggregates, and delicate euhedral oscillatory zoning in plagioclase. The core of the body appears structureless, suggesting that it solidified after deformation had ceased. Leucoadamellite, alaskite, and aplite in irregular bodies and dikes ranging from several millimetres to 100 m in thickness occur in and around the stocks.

All dated samples of the Tertiary body were collected from the southernmost part of the southern stock about 0.8 km north of upper Ingham Creek. Sample 9W-47-2A (illustrated in Fig. 11) is homogeneous, weakly foliated biotite adamellite; 9W-47-2B is fine-grained muscovitic adamellite from a 30-cm-thick, sharp-walled dike in rock of sample 9W-47-2A; 9W-47-2C is a muscovitic aplite dike, 15 cm thick, intruded into rock of sample 9W-47-2B; and 9W-47-2D is aplite from several 6-cm-thick dikes approximately 60 m from the collection site of samples 9W-47-2B and 2C. Sample 9W-47-9 is aplite from a dike 20 cm thick, and 9W-47-1D is from the center of a vertical aplite dike 1.2 m thick. Other samples of average adamellite had $^{87}Rb/^{86}Sr$ and $^{87}Sr/^{86}Sr$ ratios similar to that of 9W-47-2A.

The six samples from the southern stock define a whole-rock isochron age of 24.9 ± 0.6 m.y., with an initial $^{87}Sr/^{86}Sr$ ratio of 0.714 ± 0.002 (Table 4; Fig. 12). The ability to obtain so precise an age on a body so young is attributable to the extremely high Rb/Sr ratios present in the differentiated leucoadamellite and aplite dike rocks. Also, even if the slight scatter observed in the isochron diagram is a reflection of initial strontium isotope variability, the magma could not have been as heterogeneous as the one at Vipont Mountain. The initial $^{87}Sr/^{86}Sr$ ratio, however, does imply some crustal contribution to the magma, although the ratio is considerably lower than would be acquired solely from melting of the nearby Precambrian adamellite basement rocks.

The intimate association between the main adamellite body and the various dikes that cut it and the adjacent country rock implies a genetic and, presumably, a temporal relation. Thus, we feel confident that this late Oligocene age applies not only to the dikes but also to the entire intrusion and to the superimposed second metamorphic fabric. We further conclude from the lack of contact metamorphic effects in the upper allochthonous sheet that it had not moved into its present position at this time. This interpretation is compatible with field evidence showing allochthonous sheets resting upon upper Miocene beds (Fig. 2).

Fission-track data from the pluton strongly support the idea that even though the body was emplaced in late Oligocene time, it crystallized and cooled in Miocene time. One sample (13W-29-11) is from moderately gneissose adamellite from the northwest edge of the northern stock, about 3 m from the contact with Precambrian adamellite (lat 41°42′49″N, long 113°45′45″W). Zircon from this rock gave an age of 18.3 ± 1.9 m.y., and apatite gave an age of 13.7 ± 3.7 m.y. The second sample (9W-99-39) came from a dike of garnetiferous alaskite, 1 m thick, in the Precambrian adamellite about 25 m from the contact of the southern stock in upper Ingham Canyon (lat 41°39′50″N, long 113°44′46″W). The apatite from this rock gave an age of 18.9 ± 6.3 m.y. These data suggest that the pluton continued to be heated for many millions of years after it crystallized.

Immigrant Pass Intrusion

The largest and least known of the Tertiary granitic bodies was named the Grouse Creek pluton by Baker (1959). It consists of a large eastern lobe and two smaller western lobes (Fig. 5). All of these intruded the middle allochthonous sheet, but the upper sheet is unmetamorphosed even where it is in contact with the western lobes, so that it must have been emplaced here after they cooled. The pluton cuts north- to northeast-trending folds in the middle sheet, folds interpreted to be of the first set. We have not yet established the age relation of the pluton to the younger set of metamorphic folds. Mapping to date indicates that the granitic rocks are not distinctly lineated. The ten thin sections examined, however, show considerable low-temperature strain, including kinking of plagioclase and biotite. A large (1 by 2 km) mass of Elba Quartzite in the southwest lobe (labeled a? in Fig. 2) has also been strained at low temperature.

All three lobes of the Immigrant Pass intrusion are mainly biotite granodiorite verging on adamellite. Textures are hypidiomorphic granular, with grains averaging 3 mm in diameter, although locally with scattered 1 to 2-cm grains. Garnetiferous leucoadamellite of about the same grain size forms thick dikes in the west half of the body and a broad zone along the west margin of the two western lobes. Diorite, syenodiorite, and similar rather mafic rocks are abundant in the small southwestern lobe. Aplite and pegmatite dikes are widespread and locally abundant in all the lobes.

Samples for isotopic dating were collected from each of the three lobes. Sample 9W-39-1 is from a freshly blasted roadcut in homogeneous granodiorite typical of the central part of the southwestern lobe; 9W-39-2 is from a nearby garnetiferous leucoadamellite dike, 8 to 10 m thick, that intrudes the granodiorite; 9W-39-3 is from the finer grained part of an aplitic and pegmatitic leucoadamellite forming a 0.5- to 1-m-thick dike in typical granodiorite, 200 m northeast of the locality of 9W-39-1. Samples 13W-167-3 and 4 are dike rocks from the large eastern lobe of the pluton; 13W-167-3 is from a 0.7-m-thick dike of homogeneous aplite near the center of the lobe, and 13W-167-4 is from a 0.2-m-thick dike of porphyritic alaskite about 400 m distant from the other. The remaining sample, 9W-40-2, is from a 0.3-m-thick aplite dike in granodiorite typical of the northwestern lobe.

The six samples define a composite whole-rock isochron age of 38.2± 2.0 m.y. with an initial $^{87}Sr/^{86}Sr$ ratio of 0.709 ± 0.002 (Table 4; Fig. 12). This age, however, is controlled predominantly by the two samples of dike rock from the southwestern lobe of the pluton and should be applied strictly only to this locality. Although the other sample points lie close to the isochron, their low radiogenic enrichments and the uncertainties observed elsewhere in initial $^{87}Sr/^{86}Sr$ ratios combine to obscure an accurate interpretation. For example, the one analysis for a sample of the large eastern lobe plots equally well on the Red Butte Canyon isochron.

The present stage of the mapping also does not allow a determination of the relative ages of the three lobes. Possibly the late Eocene or early Oligocene age applies to the southwestern lobe only. Armstrong (1970) determined a K-Ar biotite age of 23.3 m.y. on granodiorite from the north end of the northwestern lobe, but it is not known whether this result reflects primary crystallization or later heating.

DISCUSSION

The fission-track and Rb-Sr data from the pluton in Red Butte Canyon set one firm date in the tectonic history: the second metamorphic deformation was still underway in late Oligocene time. A Miocene date for the end of metamorphism is suggested by the fission-track data from the autochthon in the eastern Raft River Mountains and by the Rb-Sr mineral isochrons for the Precambrian adamellite of the Grouse Creek Mountains.

The first metamorphic deformation probably ended before 38.2 ± 2.0 m.y. ago, for the intrusion at Immigrant Pass cuts through large folds that are probably of that deformation. We have no other dates on this deformation, but its metamorphic minerals, fold forms, and vertical distribution of strains are so similar to those of the second deformation as to suggest that the two followed one another closely.

Looking at the region broadly, the first deformation was directed at large angles, even 180°, to the west-to-east transport indicated by overthrusts in the late Mesozoic and early Tertiary thrust belt (Fig. 1). Activity in the thrust belt must thus have ended before the first metamorphic deformation, or else directions of transport varied greatly in the region. We have found no folds or other small-scale tectonic features older than those of the first metamorphic deformation. For example, countless pebbles and cobbles in Precambrian units are flattened and elongated into simple triaxial ellipsoids that lie parallel to the metamorphic fold axes, and these forms are otherwise only locally kinked on north-trending axes of the postmetamorphic folds.

Postmetamorphic deformation and igneous activity were widespread, variable, and locally of large magnitude. Tectonic transport during the period from about 20 to 12 m.y. ago was eastward, as shown by strongly overturned folds and by offsets of parts of the allochthonous sheets, some traveling as much as 30 km. These events led up to the deposition of the upper Miocene beds, which record voluminous volcanic activity and rapid erosion of the allochthonous sheets. Coarse detritus from unmetamorphosed Triassic, Permian, and Pennsylvanian units makes up the lower thousand or so metres of the sequence, and clasts of metamorphic rocks appear at higher levels. This clast stratigraphy is so consistent over the entire area as to suggest that the sediments accumulated in broad basins and that the allochthonous sheets were not broken by high-angle faults with large vertical displacements. The upper Miocene beds were then folded on approximately north-trending axes, and parts of the middle and upper allochthonous sheets were emplaced onto them. Finally, the present ranges formed, probably in Pliocene time, and faults of basin-and-range type developed along the eastern front of the Grouse Creek Mountains and locally elsewhere.

With that much overview of the history, we can turn to the question of what caused it. Probably the most significant facts come from the dating and structural study of the Precambrian adamellite: (1) the entire area was underlain by a nearly flat-topped body of great strength and low porosity, from about 2.5 b.y. ago onward; (2) the metamorphic fabrics in the body, like those in the rocks above it, are dominantly horizontal or nearly so; and (3) the fabrics decrease in intensity downward — so rapidly in the least metamorphosed (eastern) part of the area as to be scarcely discernible 800 m below the top of the adamellite.

These facts are difficult to reconcile with horizontally directed compression of either the adamellite or the layered rocks above it, which tends to rule out thrusting during the period of metamorphism. The vertical distribution of strain also excludes infrastructure-suprastructure models, such as that proposed by Armstrong and Hansen (1966) for this same area.

A model proposed by Kehle (1970), on the other hand, seems suitable to the distribution of deformation. His model has three rock layers: a rigid basement, a ductile intermediate layer, and a less ductile upper layer. The layers remain immobile as long as they are horizontal or nearly so, but when they are tilted to some critical slope, gravity induces shear in the ductile layer. Rocks in the ductile layer thus flow laterally over the basement and carry the upper layer with them. For the area studied, the basement was the Precambrian adamellite, and the ductile layer included all the metamorphosed rocks above it — part of the autochthon, all of the rocks of the lower allochthonous sheet, and parts of the middle sheet. Figure 13 is a simplified diagram, similar to those used by Kehle, showing the relative amounts of displacive strain at various depths. The relation between the ductile layer and the overlying rocks is poorly known because of erosion, but it is probably a gradation.

Our case differs from Kehle's simple three-layer model in that major low-angle faults have developed. The lowest fault lies mainly in the graphitic schist of Stevens Spring, or at its upper contact, and the middle fault (which is apparently the one with the largest displacement) lies mainly in the metamorphosed organic shales of the Mississippian, or at their upper contact. Water and organic fluids were unquestionably produced in these units during thermal diagenesis and metamorphism. These facts fit the general mechanism proposed by Hubbert and Rubey (1959): the expelled fluids led to separation and nearly frictionless translation of the

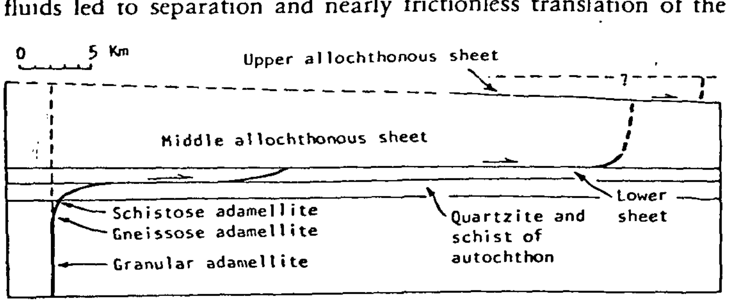

Figure 13. Vertical section showing displacements of various parts of autochthon and allochthonous sheets by flowage and low-angle faulting. Heavy line indicates positions of points originally on dashed vertical line. Strains are idealized to one movement plan. Actual slopes of surfaces are unknown. Vertical dimensions are approximate and are depicted to scale at time that deformation started.

allochthonous sheets. At the several places where we can determin the direction of translation, it is the same as the sense of shear in th ductile rocks above and below the faults.

It thus appears that both flow and faulting resulted from ther mally induced changes and were probably driven by gravity. In deed, it is plausible that the entire deformational system was causec by widespread heating and uplift. The greater degree of heatin (metamorphism) in the part of the area where granitic pluton occur suggests that more extensive, subjacent plutons caused the heating as well as the uplift, perhaps forming a broad dome. The shape of the dome could have changed with time, thus providing an explanation for the changes in direction of flow and low-angle faulting as well as for the varied overturn of folds with depth and for the unequal cooling histories from place to place. The first set of metamorphic folds would represent the west and north sides of the dome during that deformation. The crest of the dome may have shifted to a position near Muddy Canyon during the second deformation, for the folds north of the canyon are overturned to the north whereas those in the middle and lower allochthonous sheets south of the canyon are overturned to the southwest. The crest would then have shifted to the west, leading to large-scale eastward transport at the close of metamorphism and afterward. Finally, the late Miocene basins suggest that large parts of the eastward-facing surface sagged at that time. Even so, the recent cooling dates, the contemporaneous volcanism, and the emplacement of subsidiary sheets on the upper Miocene rocks suggest that heating and deformation remained closely related until they ended, about 10 m.y. ago.

ACKNOWLEDGMENTS

Mapping by Stanford field classes in 1965, 1967, 1969, and 1973 contributed to our data and ideas, and the Bureau of Land Management, the U.S. Forest Service, and many ranchers aided the field studies. We thank Max Crittenden, Jr, for visits in the field and for his suggestions and general encouragement. Todd's field studies were financed by a Geological Society of America Research Grant and by a U.S. Geological Survey Postdoctoral Fellowship, and her petrographic materials were financed by a grant from the Shell Research Fund at Stanford University. Compton's work was supported in part by the U.S. Geological Survey. We thank Max Crittenden, Jr., and Fred K. Miller for reading and criticizing this paper.

REFERENCES CITED

Ahlborn, R. C., 1973, Tectonic and plutonic events in the Kern Mountains: Geol. Soc. America Abs. with Programs, v. 5, p. 1–2.

Anderson, A. L., 1931, Geological and mineral resources of eastern Cassia County, Idaho: Idaho Bur. Mines and Geology Bull. 14, 29 p.

Armstrong, R. L., 1968a, Mantled gneiss domes in the Albion Range, southern Idaho: Geol. Soc. America Bull., v. 79, p. 1295–1314.

——1968b, Sevier orogenic belt in Nevada and Utah: Geol. Soc. America Bull., v. 79, p. 429–458.

——1970, Geochronology of Tertiary igneous rocks, eastern Basin and Range province, western Utah, eastern Nevada, and vicinity, U.S.A.: Geochim. et Cosmochim. Acta, v. 34, p. 203–232.

——1972, Low-angle (denudation) faults, hinterland of the Sevier orogenic belt, eastern Nevada and western Utah; Geol. Soc. America Bull., v. 83, p. 1729–1754.

Armstrong, R. L., and Hansen, E., 1966, Cordilleran infrastructure in the eastern Great Basin: Am. Jour. Sci., v. 264, p. 112–127.

Baker, W. H., 1959, Geologic setting and origin of the Grouse Creek pluton, Box Elder County, Utah [Ph.D. thesis]: Salt Lake City, Univ. Utah, 175 p.

Calk, L. C., and Naeser, C. W., 1973, The thermal effect of a basalt intrusion on fission-tracks in quartz monzonite: Jour. Geology, v. 81, p. 189–198.

Cebull, S. E., 1970, Bedrock geology and orogenic succession in southern Grant Range, Nye County, Nevada: Am. Assoc. Petroleum Geologists Bull., v. 54, p. 1828–1842.

Compton, R. R., 1969, Thrusting in northwest Utah: Geol. Soc. America Abs. with programs for 1969, Pt. 3 (Rocky Mountain Sec.), p. 15.

——1972, Geologic map of the Yost quadrangle, Box Elder County, Utah, and Cassia County, Idaho: U.S. Geol. Survey Misc. Geol. Inv. Map I-672.

——1975, Geologic map of the Park Valley quadrangle, Box Elder County, Utah, and Cassia County, Idaho: U.S. Geol. Survey Misc. Geol. Inv. Map I-873.

Condie, K. C., 1969, Geologic evolution of the Precambrian rocks in northern Utah and adjacent areas: Utah Geol. and Mineralog. Survey Bull., v. 82, p. 71–95.

Dover, J. H., 1969, Bedrock geology of the Pioneer Mountains, Blaine and Custer Counties, central Idaho: Idaho Bur. Mines and Geology Pamph. 152, 61 p.

Drewes, Harald, 1967, Geology of the Connors Pass quadrangle, Schell Creek Range, east-central Nevada: U.S. Geol. Survey Prof. Paper 557, 93 p.

Fagan, J. J., 1962, Carboniferous cherts, turbidites, and volcanic rocks in northern Independence Range, Nevada: Geol. Soc. America Bull., v. 73, p. 595–612.

Hazzard, J. C., and Turner, F. E., 1957, Décollement-type overthrusting in south-central Idaho, northwestern Utah and northeastern Nevada: Geol. Soc. America Bull., v. 68, p. 1829.

Hose, R. K., and Blake, M. C., Jr., 1976, Geology and mineral resources of White Pine County, Nevada; Part 1, Geology: Nevada Bur. Mines and Geology Bull. 85, p. 1–35.

Hose, R. K., and Danes, Z. F., 1973, Development of the late Mesozoic to early Cenozoic structures in the eastern Great Basin, *in* DeJong, K. A., and Scholten, Robert, eds., Gravity and tectonics: New York, John Wiley & Sons, p. 429–441.

Howard, K. A., 1966, Structure of the metamorphic rocks of the northern Ruby Mountains, Nevada [Ph.D. thesis]: New Haven, Conn., Yale Univ., 170 p.

Hubbert, M. K., and Rubey, W. W., 1959, Mechanics of fluid-filled porous solids and its application to overthrust faulting: Geol. Soc. America Bull., v. 70, p. 115–166.

Kehle, R. O., 1970, Analysis of gravity sliding and orogenic translation: Geol. Soc. America Bull., v. 81, p. 1641–1664.

Kerr, J. W., 1962, Paleozoic sequences and thrust slices of the Seetoya Mountains, Independence Range, Elko County, Nevada: Geol. Soc. America Bull., v. 73, p. 439–460.

King, P. B., 1969, Tectonic map of North America: U.S. Geol. Survey, scale 1:5,000,000, 1 sheet.

Kistler, R. W., and Willden, R., 1969, Age of thrusting in the Ruby Mountains, Nevada: Geol. Soc. America Abs. with Programs for 1969, pt. 3 (Rocky Mountains Sec.) p. 40.

Lee, Donald E., Marvin, Richard F., Stern, T. W., and Peterman, Zell E., 1970, Modification of potassium-argon ages by Tertiary Thrusting in the Snake Range, White Pine County, Nevada: U.S. Geol. Survey Prof. Paper 700-D, p. D92–D102.

Misch, P., 1960, Regional structural reconnaissance in central-northeast Nevada and some adjacent areas — Observations and interpretations, *in* Inter. Assoc. Petroleum Geologists Guidebook 11th Ann. Field Conf. Geology of east-central Nevada: p. 17–42.

Misch, P., and Hazzard, J. C., 1962, Stratigraphy and metamorphism of late Precambrian rocks in central-northeast Nevada and adjacent Utah: Am. Assoc. Petroleum Geologists Bull., v. 46, p. 289–344.

Moores, E. M., Scott, R. B., and Lumsden, W. W., 1968, Tertiary tectonics of the White Pine–Grant Range region, east-central Nevada, and some regional implications: Geol. Soc. America Bull., v. 79, p. 1703–1726.

Naeser, C. W., and Faul, H., 1969, Fission-track annealing in apatite and sphene: Jour. Geophys. Research, v. 74, p. 705–710.

Nelson, R. B., 1966, Structural development of northernmost Snake Range, Kern Mountains, and Deep Creek Range, Nevada-Utah: Am. Assoc. Petroleum Geologists Bull., v. 50, p. 921–951.

——1969, Relation and history of structures in a sedimentary succession with deeper metamorphic structures, eastern Great Basin: Am. Assoc. Petroleum Geologists Bull., v. 53, p. 307–339.

Nolan, T. B., 1935, The Gold Hill mining district, Utah: U.S. Geol. Survey Prof. Paper 177, 172 p.

Olson, Richard H., 1956, Geology of Promontory Range, *in* Guidebook to the geology of Utah, no. 11: Utah Geol. and Mineralog. Survey, p. 41–75.

O'Neill, J. M., 1969, Structural geology of the southern Pilot Range, Elko County, Nevada, and Box Elder and Tooele Counties, Utah: Geol. Soc. America, Abs. with Programs for 1969, Pt. 3 (Rocky Mountain Sec.), p. 61.

Oversby, B., 1972, Thrust sequences in the Windermere Hills, northeastern Elko County, Nevada: Geol. Soc. America Bull., v. 83, p. 2677–2688.

Peace, F. S., 1956, History of exploration for oil and gas in Box Elder County, Utah and vicinity, *in* Guidebook to the geology of Utah, no. 11: Utah Geol. and Mineralog. Survey p. 17–31.

Reed, J. C., Jr., and Zartman, R. E., 1973, Geochronology of Precambrian rocks of the Teton Range, Wyoming: Geol. Soc. America Bull., v. 84, p. 561–582.

Riva, J., 1970, Thrusted Paleozoic rocks in the northern and central HD Range, northeastern Nevada: Geol. Soc. America Bull., v. 81, p. 2689–2716.

Roberts, R. J., 1968, Tectonic framework of the Great Basin: Missouri Univ. Rolla Tech. Ser., no. 1, p. 101–119.

Roberts, R. J., and Crittenden, M. D., Jr., 1973, Orogenic mechanisms, Sevier orogenic belt, Nevada and Utah, *in* DeJong, K. A., and Scholten, Robert, eds., Gravity and tectonics: New York, John Wiley & Sons, p. 409–428.

Roberts, R. J., Crittenden, M. D., Jr., Tooker, E. W., Morris, H. T., Hose, R. K., and Cheney, T. M., 1965, Pennsylvanian and Permian basins in northwestern Utah, northeastern Nevada and south-central Idaho: Am. Assoc. Petroleum Geologists Bull., v. 49, p. 1926–1956.

Schaeffer, F. E., and Anderson, W. L., 1960, Geology of the Silver Island Mountains, Box Elder and Tooele Counties,Utah, and Elko County, Nevada, *in* Guidebook to the geology of Utah, no. 15: Utah Geol. Soc., 185 p.

Slack, J. F., 1974, Jurassic suprastructure in the Delano Mountains, northeastern Elko County, Nevada: Geol. Soc. America Bull., v. 85, p. 269–272.

Thorman, C. H., 1970, Metamorphosed and nonmetamorphosed Paleozoic rocks in the Wood Hills and Pequop Mountains, northeast Nevada: Geol. Soc. America Bull., v. 81, p. 2417–2448.

Todd, V. R., 1973, Structure and petrology of metamorphosed rocks in central Grouse Creek Mountains, Box Elder County, Utah [Ph.D. thesis]: Stanford, Calif., Stanford Univ., 316 p.

Tschanz, L. M., and Pampeyan, E. H., 1970, Geology and mineral deposits of Lincoln County, Nevada: Nevada Bur. Mines Bull., v. 73, 188 p.

Whitebread, D. H., 1966, Snake Range décollement and related structures in the southern Snake Range, eastern Nevada [abs.]: Geol. Soc. America Spec. Paper 101, p. 345.

Willden, R., Thomas, H. H., and Stern, T. W., 1967, Oligocene or younger thrust faulting in the Ruby Mountains, northeastern Nevada: Geol. Soc. America Bull., v. 78, p. 1345–1358.

Woodward, L. A., 1964, Structural geology of central northern Egan Range, Nevada: Am. Assoc. Petroleum Geologists Bull., v. 48, p. 22–39.

Woodward, L. A., 1967, Stratigraphy and correlation of late Precambrian rocks of Pilot Range, Elko County, Nevada, and Box Elder County, Utah: Am. Assoc. Petroleum Geologists Bull., v. 51, p. 235–243.

York, Derek, 1966, Least-squares fitting of a straight line: Canadian Jour. Physics, v. 44, p. 1079–1086.

Young, J. C., 1960, Structure and stratigraphy in north-central Schell Creek Range, *in* Intermn. Assoc. Petroleum Geologists Guidebook, 11th Ann. Field Conf., Geology of east-central Nevada: p. 158–172.

Manuscript Received by the Society March 29, 1976
Revised Manuscript Received November 10, 1976
Manuscript Accepted December 11, 1976

AREA
UT
Cenoz
Ages

A LIST OF AGE DETERMINATIONS OF CENOZOIC IGNEOUS ROCKS OF UTAH

by J. B. Noblett, *Department of Geology, Stanford Univ.,*
W. S. Snyder, *and* M. L. Rappaport, *Department of Applied Earth Sciences, Stanford Univ., Stanford, CA 94305*

This report presents a list of the available radiometric age dates of igneous rocks of Utah for the time interval 80 m.y. to the present. These data were used by Snyder, Dickinson, and Silberman in their paper, "Tectonic Implications of Space-Time Patterns of Cenozoic Magmatism in the Western United States" (Earth and Planetary Science Letters, 1976, v. 32, p. 91-106).

The list is arranged by age from the present to 80 m.y. The range of error is shown in the column "+/-". Latitude and longitude follow. Rock types are listed in the next column. These rock type names are general descriptions and should be loosely interpreted. The type of analysis is given under the heading "Method" and this is followed by a column that lists the mineral analyzed. The reference for each date is cited in the final column. The second part of this report consists of a more detailed bibliography of each of these references.

This list of age dates was compiled up through mid-1975 from available published sources. It should be noted that the dates presented here represent a selected set of data.

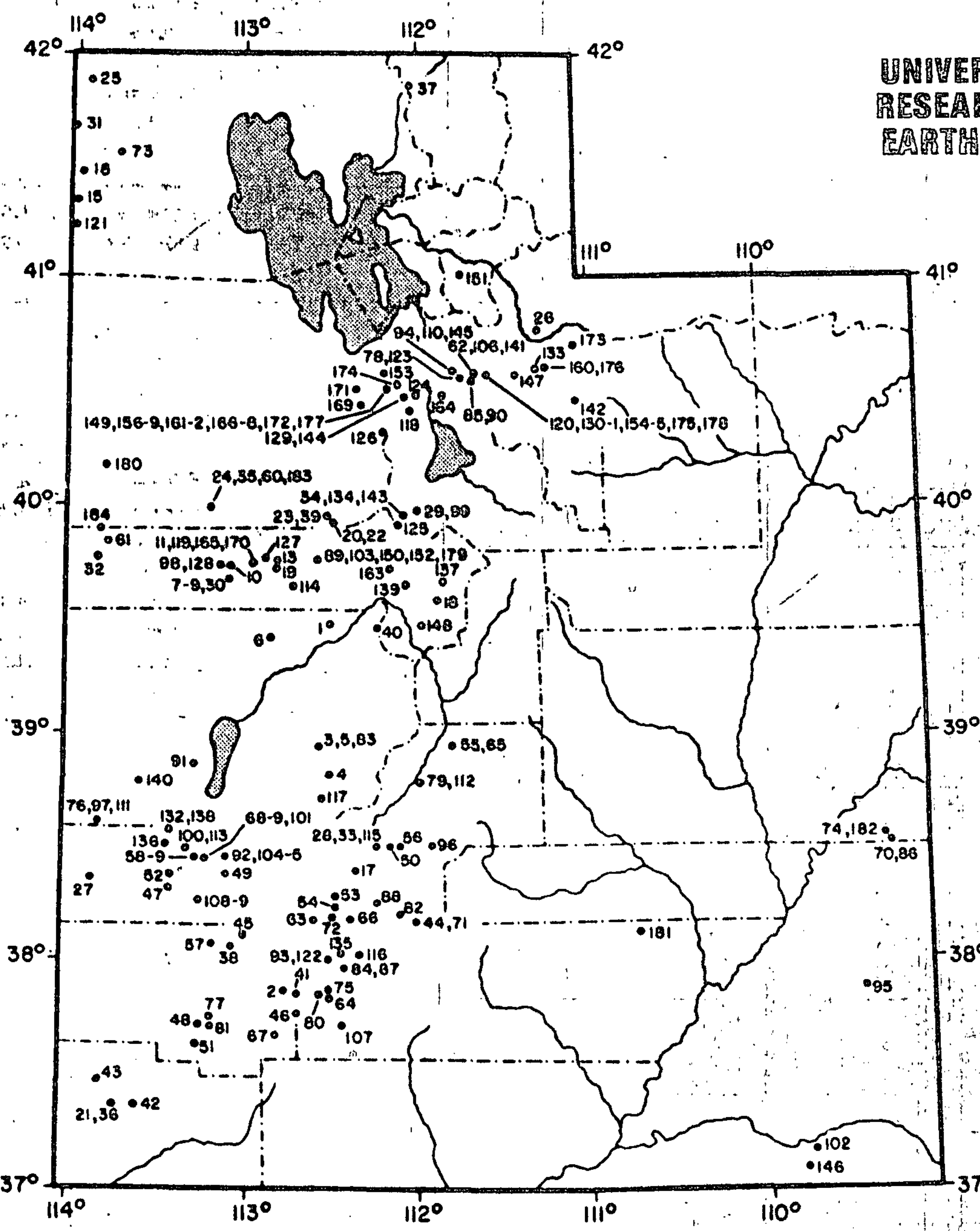

Discordant dates were not used, although a few borderline cases are reported. Concordant dates based on the same mineral were averaged and are indicated by an asterisk (*) following the date. Concordant dates based on two or more different minerals were also averaged for use in the summary by Snyder and others (1976), but here the dates for each mineral are reported separately. Interested readers should consult the individual references for more complete information about specific dates.

A list of abbreviations used in the table follows:

- ap – apatite
- bio – biotite
- feld – feldspar
- FT – fission track
- gl – glass
- hbl – hornblende
- KA – potassium-argon
- kf – potassium-feldspar
- LA – lead-alpha
- mus – muscovite
- plag – plagioclase
- pyx – pyroxene
- san – sanidine
- sp – sphene
- WR – whole rock
- zir – zircon

Map no.	Age	+/-	Latitude	Longitude	Rock type	Method	Mineral	Reference
1	0.003 0.128	min max	39.50N	112.50W	basalt	KA	WR	Hoover (1974)
2	0.4		37.87N	112.77W	basalt	KA	WR	Fleck & others (1975)
3	0.536*		38.97N	112.60W	basalt	KA	WR	Hoover (1974)
4	0.667*		38.80N	112.48W	basalt	KA	WR	Hoover (1974)
5	0.918*		38.87N	112.58W	basalt	KA	WR	Hoover (1974)
6	3.4	0.2	39.44N	112.85W	rhyolite	KA	san	Armstrong (1970)
7	6.0	0.2	39.69N	113.11W	rhyolite	KA	san	Armstrong (1970)
8	6.1	0.3	39.70N	113.08W	alkali rhyolite	FT	zir	Lindsey & others (1975)
9	6.2	0.4	39.68N	113.08W	alkali rhyolite	FT	zir	Lindsey & others (1975)
10	6.6	0.3	39.75N	113.08W	alkali rhyolite	FT	zir	Lindsey & others (1975)
11	7.8	0.6	39.77N	112.94W	alkali rhyolite	FT	sp	Lindsey & others (1975)
12†	7.9	0.5	42.00N	115.42W	basalt	KA	WR	Mark & others (1975)
13	8.2	0.5	39.77N	112.81W	alkali rhyolite	FT	zir	Lindsey & others (1975)
14†	8.2	0.6	41.95N	114.60W	basalt	KA	WR	Mark & others (1975)
15	8.4	0.2	41.34N	114.03W	quartz latite	KA	san	Armstrong (1970)
16	8.4*	0.2	41.48N	113.98W	rhyolite	KA	feld	Armstrong & others (1976)
17	9.2	0.3	38.39N	112.36W	granite	KA	bio	Armstrong (1970)
18	10.0		39.59N	111.89W	tuff, pumice, ash flow	KA		Evernden & James (1964)
19	10.0	0.9	39.75N	112.81W	rhyolite	FT	zir	Lindsey & others (1975)
20	12.0		39.94N	112.50W	rhyolite	LA	zir	Whelan (1970)
21	12.3	0.3	37.37N	113.75W	tuff, pumice, ash flow	KA	san	Noble & McKee (1972)
22	13.0		39.94N	112.50W	granite	LA	zir	Whelan (1970)
23	13.0		39.95N	112.53W	granite	KA		Odekirk (1963)
24	13.0	5	40.00N	113.21W	tuff, pumice, ash flow	KA	kf	Edwards & McLaughlin (1972)
25	13.1*	0.3	41.88N	113.92W	rhyolite	KA	feld	Armstrong & others (1976)
26	13.3		40.78N	111.29W	trachyte	KA	mus	Best & others (1968)
27	15.5	1.5	38.37N	113.88W	skarn	KA	bio & mus	Whelan (1970)
28	15.6*		38.50N	112.23W	obsidian	KA	WR	Bassett & others (1963)
29	15.6 18.3	2.6 0.5	39.98N	112.01W	latite	KA	san	Damon (1968)
30	16.2	1.5	39.70N	113.10W	rhyolite	KA	san	Whelan (1970)
31	16.3	2.0	41.65N	114.10W	basalt	KA	WR	Armstrong & others (19
32	17.7	0.9	39.78N	113.87W	granite	KA	mus	Whelan (1970)
33	17.8		38.49N	112.23W	obsidian	KA	WR	Bassett & others (196
34	17.9	0.5	39.96N	112.07W	latite	KA	bio	Damon (1968)
35	18.0	1	40.00N	113.21W	trachyte	KA	kf	Edwards & McLaug
36	18.2	0.5	37.37N	113.75W	tuff, pumice, ash flow	KA	bio	Noble & McKee (1
37	18.9	1.6	41.86N	112.06W	tuff, pumice, ash flow	KA		Williams (1964)
38	19.0	0.6	38.07N	113.07W	intermediate volcanic	KA	WR	Fleck & others (
39	19.0	3	39.94N	112.53W	adamellite	KA	bio	Armstrong (19
40	19.7*		39.48N	112.26W	obsidian	KA	WR	Bassett & other
41	19.7	0.5	37.85N	112.70W	diabasic gabbro	KA	WR	Fleck & other
42	19.9	0.5	37.37N	113.63W	tuff, pumice, ash flow	KA	bio	Noble & McK
43	20.3	0.5	37.47N	113.83W	tuff, pumice, ash flow	KA	bio	Noble & Mc
44	20.3	0.5	38.17N	112.03W	tuff, pumice, ash flow	KA	san	Damon (19

Map no.	Age	+/-	Latitude	Longitude	Rock type	Method	Mineral	Reference
45	20.6	0.4	38.11N	113.00W	intermediate volcanic	KA	WR	Fleck & others (1975)
46	20.7	0.5	37.76N	112.68W	andesite	KA	WR	Fleck & others (1975)
47	20.8	0.9	38.32N	113.44W	rhyodacite	KA	plag	Lemmon & others (1973)
48	22.4	0.9	37.71N	113.25W	granodiorite	KA	bio	Armstrong (1970)
49	20.9	0.4	38.40N	113.12W	adamellite	KA	bio	Marvin (1968)
50	20.9	0.6	38.53N	112.19W	plutonic	KA	bio	Bassett & others (1963)
51	21.0	0.5	37.64N	113.29W	tuff, pumice, ash flow	KA	bio	Armstrong (1970)
52	21.3	0.5	38.37N	113.44W	dacite	KA	gl	Lemmon & others (1973)
53	23.3	0.7	38.28N	112.47W	rhyodacite	KA	bio	Fleck & ohters (1975)
54	24.7	0.9	38.23N	112.48W	basalt	KA	plag	Fleck & others (1975)
55	21.6	0.4	38.96N	111.80W	rhyodacite	KA	kf	Fleck & others (1975)
56	21.8	0.4	38.61N	112.11W	adamellite	KA	bio	McDowell (1971)
57	21.8	0.4	38.08N	113.18W	intermediate volcanic	KA	WR	Fleck & others (1975)
58	21.8	0.7	38.45N	113.27W	tuff, pumice, ash flow	KA	bio	Marvin (1968)
59	21.8	0.4	38.45N	113.26W	latite tuff	KA	bio	Lemmon & others (1973)
60	21.9	0.7	40.00N	113.21W	granite	KA	bio	Edwards & McLaughlin (1972)
61	21.9	0.9	39.85N	113.81W	adamellite	KA	kf	Armstrong (1966)
62	21.9	1	40.58N	111.66W	granodiorite	KA	san	Armstrong (1966)
63	22.0	3	38.19N	112.60W	tuff	KA	kf	Fleck & others (1975)
64	22.0	3	37.83N	112.52W	rhyolite tuff	KA	bio	Fleck & others (1975)
65	22.0	0.4	38.96N	111.80W	tuff	KA	bio	Fleck & others (1975)
66	22.1	0.6	38.20N	112.39W	basalt	KA	bio	Fleck & others (1975)
67	22.1	0.4	37.68N	112.83W	tuff, pumice, ash flow	KA	plag	Armstrong (1970)
68	22.3	0.4	38.45N	113.23W	tuff, pumice, ash flow	KA	bio	Marvin (1968)
69	22.3	0.5	38.45N	113.24W	latite tuff	KA	WR	Lemmon & others (1973)
70	22.3	0.5	38.53N	109.27W	monzonite	KA	san	Stern & others (1965)
71	24.0	0.7	38.15N	112.03W	tuff	KA	bio	Fleck & others (1975)
72	22.4	0.9	38.19N	112.50W	andesite dike	KA	bio	Fleck & others (1975)
73	22.4	3.3	41.56N	113.74W	adamellite	KA	bio	Armstrong (1970)
74	22.5	0.4	38.57N	109.29W	diorite	KA	pyx	Armstrong (1969)
5	22.8	0.4	37.87N	112.53W	tuff	KA	bio	Fleck & others (1975)
6	22.9	0.5	38.62N	113.84W	tuff	KA	WR	Armstrong (1966)
	23.3	0.5	37.75N	113.21W	granodiorite	KA	bio	Armstrong (1966)
	23.5	0.4	40.57N	111.75W	qtz monzonite	FT	pyx-hbl	Crittenden & others (1973)
	24.0	3	38.79N	111.98W	latite	KA	bio	Armstrong (1970)
	24.0	3	37.85N	112.57W	tuff	KA	bio-hbl	Fleck & others (1975)
	24.0	0.6	37.71N	113.20W	tuff, pumice, ash flow	KA	bio	Armstrong (1970)
	24.1	0.6	38.20N	112.10W	tuff	KA	sp	Fleck & others (1975)
	24.5	0.8	38.95N	112.58W	andesite	KA	zir	Fleck & others (1975)
	25.1	0.5	37.97N	112.43W	tuff	KA	bio	Fleck & others (1975)
	24.5	0.4	40.56N	111.68W	ore, greisen	KA	WR	Crittenden & others (1973)
	25.0	0.5	38.53N	109.25W	syenite	KA	plag	Stern & others (1965)
	25.0	0.4	37.97N	112.44W	mylonite	KA	WR	Armstrong (1970)
	25.1	0.7	38.25N	112.26W	andesite	KA	bio	Fleck & others (1975)
	25.1	0.4	39.78N	112.59W	granite	KA	WR	Armstrong (1970)
	25.2	0.8	40.57N	111.70W	adamellite	KA	plag	McDowell (1971)
	5.5	2.5	38.88N	113.30W	tuff	KA	mus	Armstrong & others (1976)
	5.5	0.5	38.46N	113.10W	qtz monzonite	KA	pyx	Lemmon & others (1973)
	.8	0.8	38.00N	112.51W	mylonite	KA	bio	Armstrong (1970)
	0	0.5	40.58N	111.79W	schist	KA	hbl	Hashad (1964)
	5	0.6				KA	bio	
		0.8					kf	
		0.4					bio	
		1.0					bio	
		0.6					hbl	
							bio	

Map no.	Age	+/–	Latitude	Longitude	Rock type	Method	Mineral	Reference
95	27.4	0.6	37.87N	109.45W	diorite	KA	alt. mafic	Armstrong (1969)
	28.2	0.6					WR	
96	27.5	0.4	38.50N	112.42W	tuff	KA	bio	Caskey & Shuey (1975)
97	27.7	0.6	38.62N	113.84W	tuff	KA	gl	Armstrong (1970)
	29.2	0.6					bio	
98	27.8		39.76N	113.16W	rhyolite tuff	FT	sp	Lindsey & others (1975)
	29.9	3.0					zir	
	31.9	0.9					ap	
99	27.8	0.8	39.98N	112.04W	quartz latite	KA	san	Laughlin & others (1969)
100	28.0	0.8	38.48N	113.32W	granodiorite	KA	bio	Marvin (1968)
101	28.0	1.2	38.48N	113.21W	granodiorite	KA	bio	Lemmon & others (1973)
102	28.0	3	37.17N	109.73W	granite	FT	ap	Naeser (1971)
	30.3	2.7						
103	28.2	2.3	39.78N	112.58W	qtz monzonite	FT	sp	Lindsey & others (1975)
	32.4	1.2					zir	
104	28.4	0.9	38.48N	113.12W	granodiorite	KA	hbl	Marvin (1968)
105	28.4	1.2	38.48N	113.13W	granodiorite	KA	hbl	Lemmon & others (1973)
106	28.4	1.4	40.58N	111.66W	qtz monzonite	KA	bio	Crittenden & others (1973)
107	28.9	1.2	37.71N	112.43W	dacite tuff	KA	bio	Fleck & others (1975)
108	29.0	0.9	38.28N	113.27W	tuff, pumice, ash flow	KA	bio	Marvin (1968)
	29.2	0.9					hbl	
109	29.2	1.2	38.29N	113.28W	dacite tuff	KA	hbl	Lemmon & others (1973)
	29.3	1.2					bio	
110	29.5		40.68N	111.70W	pegmatite	KA	mus	Whelan (1970)
111	29.6	0.6	38.62N	113.84W	tuff, pumice, ash flow	KA	bio	Armstrong (1970)
112	29.6	0.6	38.79N	111.98W	tuff, pumice, ash flow	KA	bio	Armstrong (1970)
113	29.7	0.6	38.49N	113.31W	adamellite	KA	bio	Armstrong (1970)
114	30.0	2	39.67N	112.71W	pegmatite	KA	mus	Whelan (1970)
115	30.0	3.0	38.53N	112.26W	monzonite	KA	hbl	McDowell (1971)
116	30.4	1.5	38.03N	112.33W	plutonic	KA	hbl	Damon (1968)
117	30.6	0.3	38.72N	112.55W	tuff	KA	bio	Caskey & Shuey (1975)
118	30.7	0.9	40.43N	112.04W	tuff	KA	bio	Moore (1973)
119	30.8	1.8	39.77N	112.92W	qtz latite intrusive	FT	zir.	Lindsey & others (1975)
120	30.9	1.5	40.58N	111.59W	granite	KA	hbl	Crittenden & others (1973)
	32.6	1.0					bio	
121	31.0	1.5	41.21N	114.03W	granodiorite	KA	bio	Coats & others (1965)
122	31.1	0.5	38.01N	112.54W	tuff	KA	bio	Fleck & others (1975)
123	31.1	0.9	40.57N	111.75W	qtz monzonite	KA	hbl	Crittenden & others (1973)
124	31.2	0.9	40.42N	112.02W	rhyolite	KA	bio	Moore (1973)
125	31.5	0.9	39.92N	112.12W	monzonite	KA	bio	Laughlin & others (1969)
126	31.6	1.1	40.31N	112.20W	rhyolite	KA	bio	Moore (1973)
127	31.6	2.5	39.78N	112.88W	rhyolite tuff	FT	sp	Lindsey & others (1975)
	32.2	1.6					zir	
	32.5	2.5					ap	
	31.7	2.1	39.73N	113.16W	rhyolite tuff	FT	sp	Lindsey & others (1975)
	32.5	1.2					zir	
	32.0	0.9	40.49N	112.08W	rhyolite	KA	bio	Moore & others (1968)
	32.1	1.0	40.58N	111.61W	granite	KA	bio	Crittenden & others (1973)
	32.8	0.7						
	32.1	1.0	40.60N	111.58W	granite	KA	bio	Crittenden & others (1973)
	32.7•	0.9				FT	sp	
	33.5	1.0				KA	hbl	
	33.7•	0.9				FT	zir.	
	32.3	1.2	38.57N	113.43W	andesite	KA	hbl	Lemmon & others (1973)
	2.7	1.0	40.60N	111.29W	andesite-rhyodacite	KA	bio	Crittenden & others (1969)
	.7	1.0	39.98N	112.06W	quartz latite	KA	san	Laughlin & others (1969)
	.8	1.0					bio	
	8	0.5	38.02N	112.44W	andesite	KA	WR	Fleck & others (1975)
		1.5	38.51N	113.47W	rhyodacite	KA	plag	Lemmon & others (1973)
			39.66N	111.86W	tuff	KA		Evernden & James (1964)

Map no.	Age	+/-	Latitude	Longitude	Rock type	Method	Mineral	Reference
138	33.6	1.5	38.59N	113.43W	dacite	KA	bio	Lemmon & others (1973)
139	33.8	0.7	39.66N	112.07W	tuff, pumice, ash flow	KA	bio	Armstrong (1970)
140	33.9 39.0	0.5 1.0	38.80N	113.60W	tuff	KA	bio hbl	Armstrong & others (1976)
141	34.0		40.58N	111.67W	monzonite	KA		Hashad (1964)
142	34.0	1.0	40.47N	111.06W	andesite-rhyodacite	KA	bio	Crittenden & others (1973)
143	34.1	1.0	39.96N	112.07W	monzonite	KA	bio	Damon (1968)
144	34.1	1.0	40.50N	112.07W	obsidian	KA	bio	Moore & others (1968)
145	34.5		40.58N	111.79W	adamellite	LA	zir	Whelan (1970)
146	35.0	4	37.10N	109.78W	greenschist, blueschist	FT	ap	Naeser (1971)
147	35.1	1.1	40.58N	111.43W	andesite-rhyodacite	KA	bio	Crittenden & others (1973)
148	35.8	0.7	39.48N	111.97W	tuff, pumice, ash flow	KA	bio	Armstrong (1970)
149	35.9	1.6	40.52N	112.16W	latite	KA	bio	Moore & others (1968)
150	36.0		39.79N	112.58W	granite	KA		Odekirk (1963)
151	36.0 37.4 37.5		41.03N	111.75W	tuff	KA	gl san bio	Evernden & others (1964)
152	36.0 41.0		39.78N	112.55W	granite	LA	zir	Whelan (1970)
153	36.5	1.1	40.58N	112.20W	latite	KA	bio	Moore (1973)
154	36.7	1.5	40.60N	111.54W	quartz diorite	KA	bio	Crittenden & others (1973)
155	36.8	1.1	40.61N	111.53W	granodiorite	KA	bio	Crittenden & others (1973)
156	36.9	1.0	40.52N	112.16W	quartz latite	KA	bio	Moore & others (1968)
157	36.9	1.0	40.52N	112.13W	quartz latite	KA	bio	Moore & others (1968)
158	36.9	1.1	40.52N	112.16W	latite	KA	bio	McDowell (1971)
159	36.9	1.1	40.52N	112.15W	quartz latite	KA	bio	McDowell (1971)
160	37.0		40.62N	111.26W	potassic rock	KA	mus	Best & others (1968)
161	37.1	1.1	40.49N	112.21W	quartz latite	KA	bio	Moore (1973)
162	37.2 37.5	1.2 1.2	40.52N	112.16W	syenite	KA	bio mus	Moore & others (1968)
163	37.2 39.7	1.6	39.71N	112.16W	andesite	FT	zir ap	Lindsey & others (1975)
164	37.3	1.1	40.49N	111.83W	andesite(?)	KA	bio	Crittenden & others (1973)
165	37.5 39.0	2.2	39.81N	112.96W	rhyolite tuff	FT	sp ap	Lindsey & others (1975)
166	37.6	1.2	40.52N	112.14W	monzonite	KA	bio	Moore & others (1968)
67	37.8	1.4	40.52N	112.16W	latite	KA	bio	Moore & others (1968)
68	37.9	1.0	40.51N	112.16W	pegmatite	KA	bio	Moore & others (1968)
69	38.0	1.1	40.45N	112.33W	monzonite	KA	bio	Moore (1973)
0	38.3	1.5	39.78N	112.95W	andesite	FT	zir	Lindsey & others (1975)
	38.6	1.1	40.50N	112.32W	qtz monzonite	KA	bio	Moore (1973)
	38.6*	1.3	40.51N	112.16W	monzonite	KA	bio	Moore & others (1968)
	38.7		40.70N	111.08W	peridotite	KA	WR	Best & others (1968)
	38.8	0.9	40.53N	112.11W	andesite, trachyandesite	KA	bio	Armstrong (1970)
	39.0	4	40.58N	111.62W	granodiorite	KA	bio	Armstrong (1966)
	39.9		40.62N	111.26W	trachyte	KA	mus	Best & others (1968)
	40.5	1.3	40.51N	112.17W	adamellite	KA	bio	McDowell (1971)
	40.9 41.2	2.2 3.0	40.60N	111.54W	quartz diorite	FT	zir ap	Crittenden & others (1973)
	41.0		39.79N	112.58W	granite	KA		Odekirk (1963)
	42.5	0.8	40.17N	113.83W	adamellite	KA	bio & hbl	Armstrong (1970)
	3.7 8.0		38.14N	110.73W	porphyry	KA	hbl WR	Armstrong (1969)
	.8	1.5	38.57N	109.29W	diorite	KA	hbl	Stern & others (1965)
	0	2	40.00N	113.21W	granodiorite	KA	bio	Edwards & McLaughlin (1972)
	[illegible]		39.81N	113.84W	granite	LA	zir	Whelan (1970)

in Nevada

REFERENCES

Armstrong, R. L. (1966) K-Ar dating using neutron activation for Ar analysis—granitic plutons of the eastern Great Basin, Nevada and Utah: Geochim. et Cosmochim. Acta, v. 30, p. 565-600

_____ (1969) K-Ar dating of laccolithic centers of the Colorado plateau and vicinity: Geol. Soc. America Bull., v. 80, p. 2081-2086

_____ (1970) Geochronology of Tertiary igneous rocks, eastern Basin and Range province, western Utah, eastern Nevada and vicinity, U. S. A.: Geochim. et Cosmochim. Acta, v. 34, p. 203-232

Armstrong, R. L., Speed, R. C., Graustein, W. C., and Young, A. Y. (1976) K-Ar dates from Arizona, Montana, Nevada, Utah and Wyoming: Isochron/West, no. 16, p. 1-6

Bassett, W. A., Kerr, P. F., Schaeffer, O. A., and Stoenner, R. W. (1963) K-Ar dating of the late Tertiary volcanic rocks and mineralization of Marysvale, Utah: Geol. Soc. America Bull., v. 74, p. 213-220

Best, M. G., Henage, L. F., and Adams, J. A. S. (1968) Mica peridotite, wyomingite, and associated potassic igneous rocks in northeastern Utah: Am. Mineralogist, v. 53, p. 1041-1048

Caskey, C. F., and Shuey, R. T. (1975) Mid-Tertiary volcanic stratigraphy, Sevier-Cove Fort area, central Utah: Utah Geol., v. 2, no. 1, p. 27-48

Coats, R. R., Marvin, R. F., and Stern, T. W. (1965) Reconnaissance of mineral ages of plutons in Elko County, Nevada and vicinity: U. S. Geol. Survey Prof. Paper 525-D, p. D11-D15

Crittenden, M. D., Jr., Stuckless, J. S., Kistler, R. W., and Stern, T. W. (1973) Radiometric dating of intrusive rocks in the Cottonwood area, Utah: Jour. Research, U. S. Geol. Survey, v. 1, p. 173-178

Damon, P. E. (1968) Correlation and chronology of ore deposits and volcanic rocks: Annual Progress Report No. C00-689-100, Contract AT(11-1)-689 to Research Division, U. S. Atomic Energy Commission, Geochronology Lab., Univ. of Arizona, Tucson, Arizona

Edwards, G., and McLaughlin, W. A. (1972) Shell list No. 1-K-Ar and Rb-Sr age determinations of California, Nevada, and Utah rocks and minerals: Isochron/West, no. 3, p. 1-7

Evernden, J. F., and James, G. T. (1964) Potassium-argon dates and Tertiary floras of North America: Am. Jour. Sci., v. 262, p. 945-974

Evernden, J. F., Savage, D. E., Curtis, G. H., and James, G. T. (1964) Potassium-argon dates and the Cenozoic mammalian chronology of North America: Am. Jour. Sci., v. 262, p. 145-198

Fleck, R. J., Anderson, J. J., and Rowley, P. D. (1975) Chronology of mid-Tertiary volcanism in high plateaus region of Utah: Geol. Soc. America Special Paper 160, p. 53-61

Hashad, A. H. (1964) Geochronological studies in the central Wasatch Mountains, Utah: unpubl. Ph.D. thesis, Univ. of Utah

Hoover, J. D. (1974) Periodic Quaternary volcanism in the Black Rock Desert, Utah: Brigham Young Univ. Geology Studies, v. 21, Part 1, p. 3-72

Laughlin, A. W., Lovering, T. S., and Mauger, R. L. (1969) Age of some Tertiary igneous rocks from the East Tintic district, Utah: Econ. Geol., v. 64, p. 915-918

Lemmon, D. M., Silberman, M. L., and Kistler, R. W. (1973) Some K-Ar ages of extrusive and intrusive rocks of the San Francisco and Wah Wah Mountains, Utah: Utah Geol. Assoc. Pub., no. 3, p. 23-26

Lindsey, D. A., Naeser, C. W., and Shawe, D. R. (1975) Age of volcanism, intrusion, and mineralization in the Thomas Range, Keg Mountain and Desert Mountain, western Utah: Jour. Research, U. S. Geol. Survey, v. 3, p. 597-604

Mark, R. K., Lee-Hu, C., Bowman, H. R., Asaro, F., McKee, E. H., and Coats, R. R. (1975) A high 87 Sr/86 Sr mantle source for low alkali tholeiite, northern Great Basin: Geochim. et Cosmochim. Acta, v. 39, p. 1671-1678

Marvin, R. F. (1968) Transcontinental geophysical survey (35°-39° N), radiometric age determinations of rocks: U. S. Geol. Survey Misc. Geol. Inv. Map I-537

McDowell, F. W. (1971) K-Ar ages of igneous rocks from the western United States: Isochron/West, no. 2, p. 1-16

Moore, W. J. (1973) A summary of radiometric ages of igneous rocks in the Oquirrh Mountains, north central Utah: Econ. Geol., v. 68, p. 97-101

Moore, W. J., Lanphere, M. A., and Obradovich, J. D. (1968) Chronology of intrusion, volcanism, and ore deposition at Bingham, Utah: Econ. Geol., v. 63, no. 6, p. 612-621

Naeser, C. W. (1971) Geochronology of the Navajo-Hopi diatremes, Four Corners area: Jour. Geophys. Research, v. 76, p. 4978-4985

Noble, D. C., and McKee, E. H. (1972) Description and K-Ar ages of volcanic units of the Caliente volcanic field, Lincoln County, Nevada, and Washington County, Utah: Isochron/West, no. 5, p. 17-24

Odekirk, J. R. (1963) Lead alpha age determinations of five Utah rocks: unpubl. M. S. thesis, Univ. of Utah

Stern, T. W., Newell, M. F., Kistler, R. W., and Shawe, D. R. (1965) Zircon, uranium-lead and thorium-lead ages and mineral potassium-argon ages of La Sal Mountain rocks, Utah: Jour. Geophys. Research, v. 70, p. 1503-1507

Whelan, J. A. (1970) Radioactive and isotopic data determinations of Utah rocks: Utah Geol. and Mineral Survey Bull. 81, Univ. of Utah, Salt Lake City, 75 pp.

Williams, J. S. (1964) The age of the Salt Lake Group in Cache Valley, Utah-Idaho: Utah Acad. Sci., Arts, and Letters Proc., v. 41, pt. 2, p. 269-277

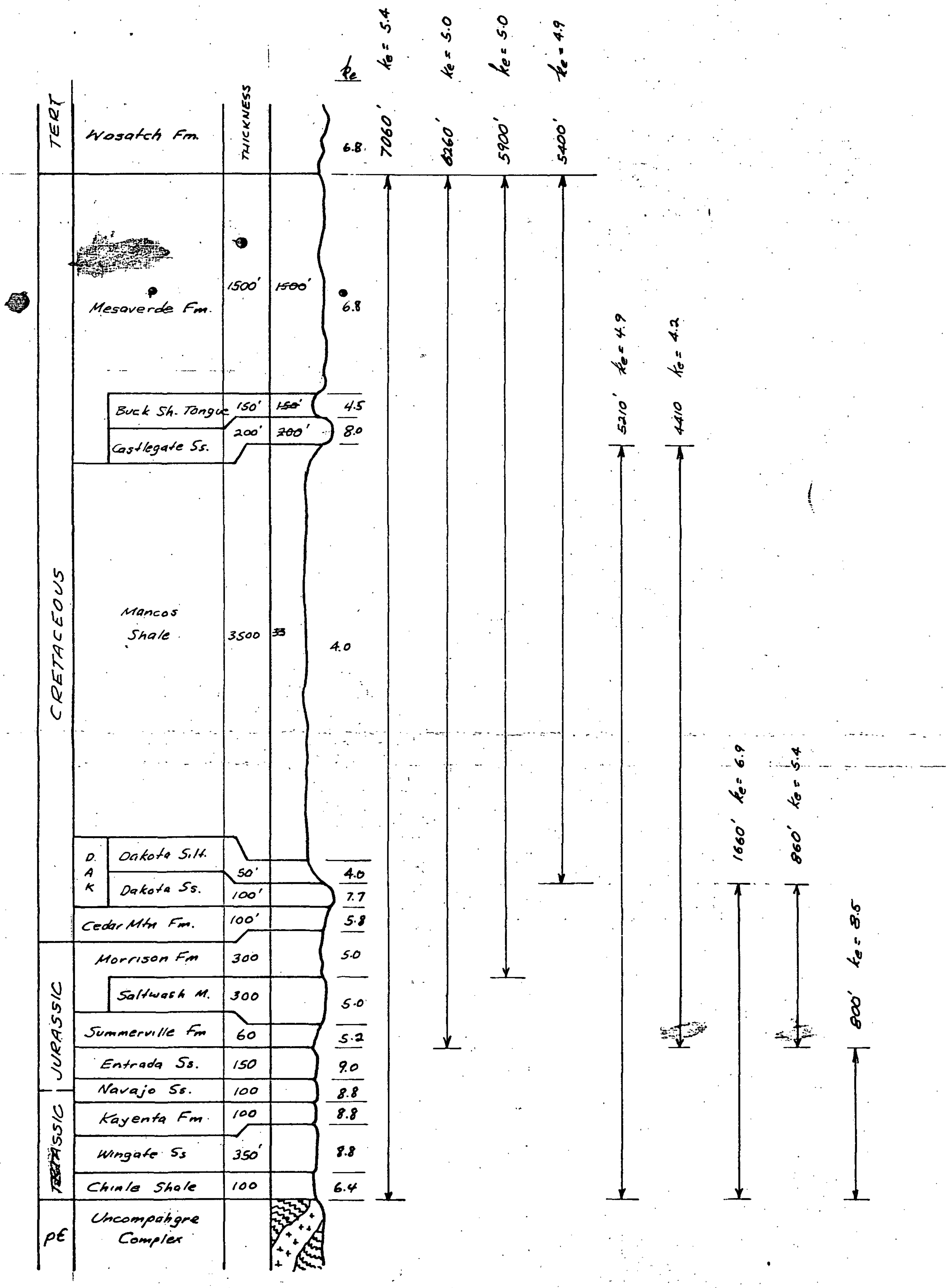

CISCO - BAR-X AREA, GRAND CO.

SECTION AS TYPICALLY RECORDED IN WELLS AND ESTIMATED THERMAL CONDUCTIVITIES IN $\frac{mCal}{cm\ sec\ °C}$

Ke's weighted avs. 6-14-79

GLEN CANYON TO PARADOX	7.6 $\frac{mcal}{cm\ sec\ ^\circ C}$	
PARADOX	9.0	
PRE PARADOX CARBONATES	7.0	
		GREEN RIVER AREA (Cisco - Bar-X ONLY)
GREEN RIVER	7.0	
WASATCH	5.8	
MESAVERDE (incl Kcg)	6.5	6.8
CASTLEGATE	8.0	
MANCOS	4.1	4.1
DAKOTA SILT	4.0	4.0
DAKOTA (Not incl. Silt or Cedar Mtn)	7.7	7.0
CEDAR MTN	5.8	5.8
MORRISON (Not incl Salt wash)	5.0	4.9
SALT WASH	5.1	5.2
SUMMERVILLE	5.2	5.2
CURTIS	8.1	
ENTRADA	9.0	9.3
CARMEL	7.6 (ONE VALUE)	

CISCO-BAR-X ONLY

NAVAJO	9.5	8.8
KAYENTA	8.9	8.8
WINGATE	9.2	8.8
CHINLE (Not incl. Shinarump)	6.1	6.4
SHINARUMP	4.6	(ONE VALUE)
MOENKOPI	5.3	
KAIBAB	6.9	(ONE VALUE)
WHITE RIM	9.5	
CUTLER (NOT INCL WHITE RIM)	?	5.6 – 7.0 (2 VAL)
ELEPHANT CANYON	7.2	(ONE VALUE)
HONAKER TRAIL	6.8	(ONE VALUE)
PARADOX	9.0	
PRE SALT CARBONATES	7.0	
pЄ UNCOMPAHGRE COMPLX.	7.0	(?)

CISCO DOME AREA

MANCOS 4.1
DAKOTA THRU SUMMERVILLE 6.6
ENTRADA 9

T17S, COLO BORDER BAR X

DAKOTA THRU SUMMERVILLE 5.2

T17S NEAR COLO BORDER

MANCOS 3660'
DAK SILT 90'
DAKOTA 84'
$\}$ 150
CEDAR MTN 30
MORRISON ~~SALTWASH~~ 322
SALTWASH 209
SUMMERVILLE 115
ENTRADA

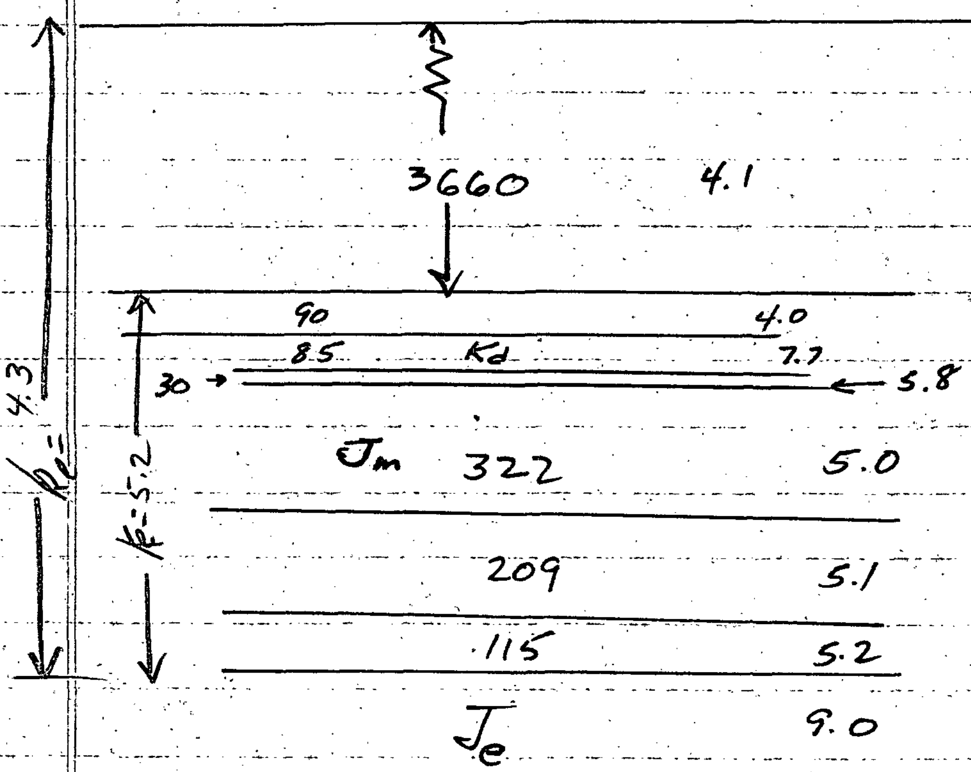

3660	4.1	15006
90	4.0	360
85	7.7	654
30	5.8	174
320	5.0	1600
209	5.1	1066
115	5.2	598
4509		19458
849		4452

av 4.3
incl Km

av 5.2
Dakota
Entrada

71 487 CISCO DOME TO BAR-X 163

fm tops only - no litho logs

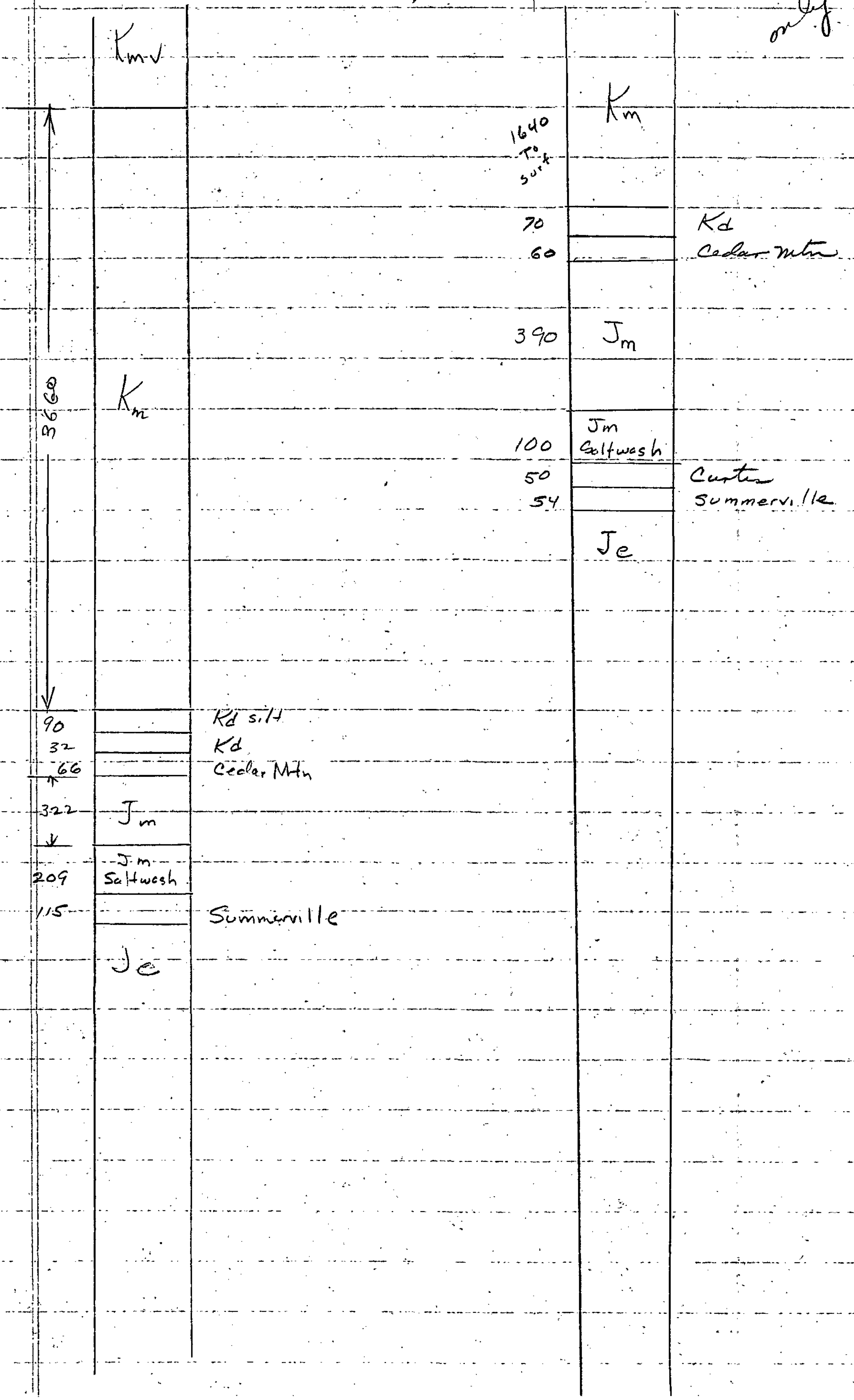

150

Thickness	Unit	Name	Value
	Kmv		
72		Castlegate	
3326	Km		4.0
50		Kd silt	4.0
102	Kd		NES
82		Cedar Mtn	5.5
103	Jm	[illegible]	4.6
315	Jm Salt Wash	[illegible]	5.0
60		Summerville	4.6
	Je		10.0

93

Thickness	Unit	Name	Value
	Tw		6.8
1890?	Kmv		7.0
(?) 300	Kcg	Castlegate	7.6
3490	Km		4.1
190	Kd		7.0
325	Jm		5.2
307	Jm Saltwash		5.2
58		Summerville	6.4
130	Je		8.2
90	Jn		8.8
118	$\bar{R}$k	Kayenta	8.8
465		Wingate	8.8
95		Chinle	6.4
	pЄ		

			k_e
	Kmv		6.7
122		Buck Tongue	5.3
286	Kcg	Castlegate	8.3
3259	K_m		4.1
30		Dakota silt	4.0
104		Kd	7.1
19		Cedar Mtn	6.2
152	Jm		4.6
404	Jm Saltwash		5.4
72		Sommerville	4.7
	Je		9.7

234

GREEN RIVER AREA

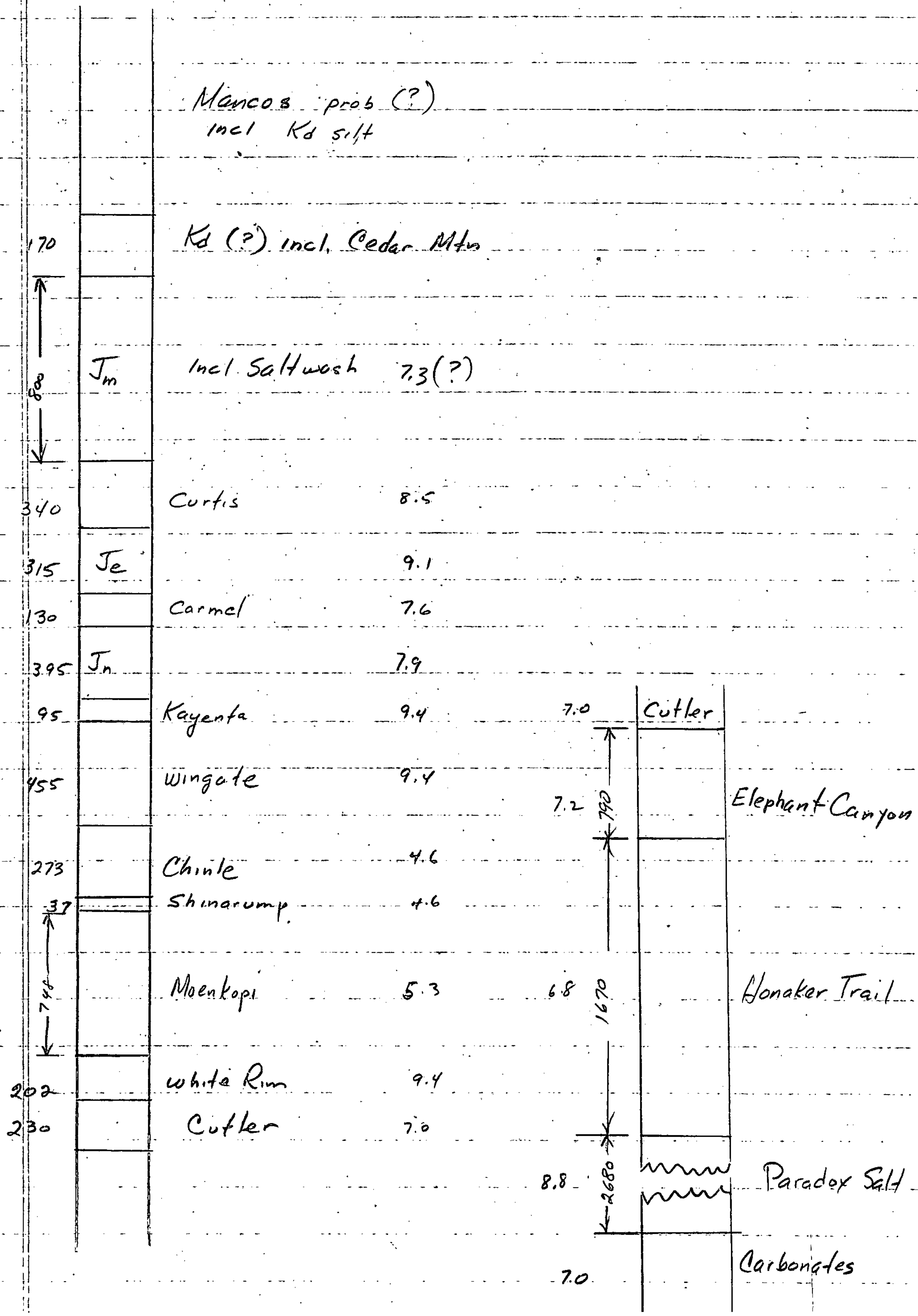

394 by G.S. CAMPBELL

Jm 5.2

TOP SALT WASH

1200 5.8 Incl. most of Jurassic (seems low though)

TOP NAVAJO

920 9.4 Incl all Glen Canyon

260 Chinle 4.6

TOP SHINARUMP

1020 4.3 All Moenkopi

TOP KAIBAB

130 Kaibab 6.9

415 Coconino 9.7

130 Elephant Can 4.0 ? (do not use) (for Eleph. Can.)

1987

Probably Honaker Tr (7.0)
(4535 - 6522, TD)

← BHT 130°F @ 6522 (Ke to surface 6.6)

297

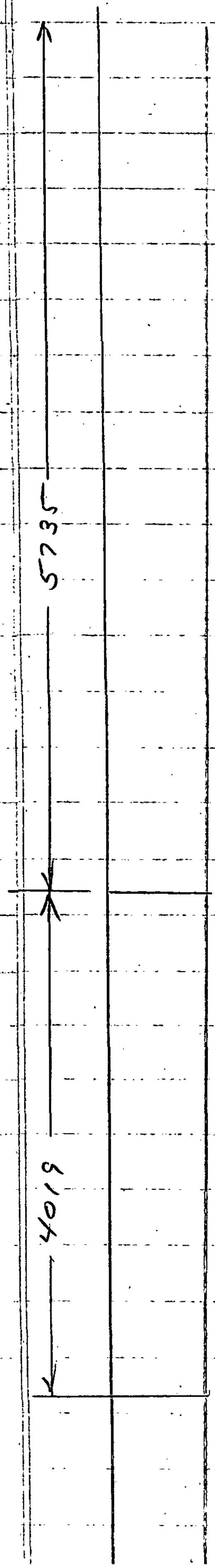

Surface prob. Morrison

$k_e = 7.1$

← BHT 130° @ 5734 k_e to Surface 7.1

Paradox Salt 9.1

Perm(?) Carbonates 7.0

← BHT @ 10330 k_e to surface 7.9

377

PETER'S POINT AREA

	Surface Tgr	
1260	Tgr	8.2
390	Green River Marker	6.7
952	Wasatch Tongue	5.6
488	Upper Wasatch	6.1
	132°F at 4982' kc to surface = 6.2	
3968	Middle Wasatch	5.5
1494	Mesaverde	5.5
	Km	4.0 for 100'
	162 @ 9121 TD, kc to Surfc 6.0	

SW GRAND CO.

ke's

316 317 318 319

Thickness	Formation		319	316	317	318
	surface Glen Canyon Gr.	7.6	7.6	8.7 (?)	7.6	7.6
228	Wingate				10.0	
310	Chinle				5.2	
10	Shinarump				10.0	
552	Moenkopi				5.2	
210	White Rim				9.7	
1226	Cutler				5.6 6.6	
1260	Hermosa	7.0			7.0	
4020	Paradox Salt	8.6	9.0	9.7	8.6	9.0
	Carbonates		7.0	7.3		7.0

WELLS WITH LITHO LOGS

WELL	°F	Depth	°F/1000	°C/km	k_e $\frac{mcal}{cm\,sec\,°C}$ surface to BHT	
✓ 93	110	4713	12.5	22.8	6.9 ✓ ✓	6.4
93	110	5447	10.8	19.7	6.8 ✓	
93	173	9869	12.4	22.6	5.8 ✓	
93	176	10787	11.6	21.1	6.0 ✓	
✓ 96	183	7023	18.8	34.3	5.5 ✓ ✓	
✓ 121	135	5398	15.6	28.4	5.0 ✓ ✓	
✓ 150	120	4323	16.0	29.1	4.4 ✓ ✓	
✓ 234	61	1770	5.6	10.2	5.0 ✓	6.9 ✓
"	146	7559	12.6	22.9	7.2 ✓	
	153	8268	12.3	22.4	7.2 ✓	
	161	8468	13.0	23.7	7.3 ✓ ✓	
	165	10786	10.6	19.3	7.7 ✓	
✓ 297	130	5734	13.8	25.2	7.1 ✓ ✓	7.8 ✓
"	164	10330	10.9	19.9	7.9 ✓	
✓ 307	95	1474	29.8	54.3	8.4 ✓ ✓	7.9 ✓
"	119	5218	13.0	23.7	7.0 ✓	
	143	9125	10.1	18.4	7.7 ✓	
✓ 311	90	4785	8.2	14.9	6.6 ✓	
	94	4964	8.7	15.8	6.6 ✓ ✓	

Cont

WELL	°F	Depth	°F/1000		ke	
✓ 316	86	2081	16.8	30.6	8.5 ✓ ✓	8.0
	102	4059	12.6	23.0	7.6 ✓	
	116	6165	10.5	19.1	8.1 ✓	
	120	7850	8.8	16.0	8.0 ✓	
✓ 317	148	6912	14.0	25.5	7.4 ✓ ✓	
✓ 318	102	4078	12.5	22.8	7.7 ✓	7.7 ✓
	130	4916	16.0	29.2	7.5 ✓ ✓	
	122	6775	10.4	19.0	7.8 ✓	
	115	6850	9.3	17.0	7.8 ✓	
319	85	2375	14.3	26.1	8.2 ✓ ✓	8.0 ✓
	103	4209	12.4	22.6	7.7 ✓	
	125	8126	9.1	16.6	8.1 ✓	
✓ 372 no temps						
✓ 377	132	4982	16.2	29.5	6.2 ✓ ✓	
	162	9121	12.2	22.2	6.0 ✓ ✓	
✓ 380	105	4840	11.2	20.4	6.7 ✓ ✓	
✓ 394	130	6522	12.1	22.0	6.6 ✓ ✓	
✓ 428	139	6550	13.4	24.4	5.9 ✓ ✓	
	172	9812	12.3	22.4	6.0 ✓ ✓	

✓ 7.5
7.4

7.8

Continued

WELL	°F	Depth	°F/1000		ke
453	140	5196	17.1	31.2	6.2
	123	5984	12.0	21.9	6.2
	140	7792	11.4	20.8	6.4
	148	8516	11.3	20.6	6.9
513	173	9601	12.7	23.1	5.2
	182	10017	13.1	23.9	5.3
515	208	9600	16.4	29.9	5.8
365	134	5288	15.7	28.6	6.1
	115	5520	11.6	21.1	6.1

ECU WELLS WITHOUT LITHO-LOGS

* Compl. Repts

#	LOC	BHT	DEPTH	°C/km	ke
158	22-20-21	121	3230	39.5	5.0
163	26-20-21	109	2763	38.3	4.9
176	2-20-23	112	2700	41.2	4.9
71*	4-17-25	169	4607	46.7	4.4
87*	19-17-26	100	3281	27.2	4.3